Analysis of mitochondrial transcription and replication on the single nucleoid level

Dissertation

for the award of the degree

"*Doctor rerum naturalium*"

Division of Mathematics and Natural Sciences
of the Georg-August-Universität Göttingen

within the doctoral program *Molecular Biology of Cells*

of the Georg-August University School of Science (GAUSS)

submitted by

Christian Brüser

from Düsseldorf

Göttingen, 2018

Thesis Committee:

Prof. Dr. Stefan Jakobs
Department of NanoBiophotonics
Mitochondrial Structure and Dynamics Group
Max Planck Institute for Biophysical Chemistry, Göttingen

Prof. Dr. Peter Rehling
Department of Cellular Biochemistry
University Medical Center Göttingen

Prof. Dr. Ahmed Mansouri
Department Molecular Developmental Biology
Molecular Cell Differentiation Group
Max Planck Institute for Biophysical Chemistry, Göttingen

Members of the Examination Board:

Prof. Dr. Stefan Jakobs (Referee)

Prof. Dr. Peter Rehling (2nd Referee)

Prof. Dr. Ahmed Mansouri

Prof. Dr. Patrick Cramer
Department of Molecular Biology
Max Planck Institute for Biophysical Chemistry, Göttingen

PD Dr. Wilfried Kramer
Institute for Microbiology and Genetics
University of Göttingen

PD Dr. Thomas Teichmann
Department of Plant Cell Biology
University of Göttingen

Date of oral examination:

17.05.2018

„Richtiges Auffassen einer Sache und Missverstehen der gleichen Sache schließen einander nicht vollständig aus.“

Franz Kafka, Der Prozeß

Table of contents

Summary

Human mitochondrial DNA (mtDNA) is a circular molecule encoding for 13 subunits of the respiratory chain that are essential for its maintenance. Inside the mitochondria, mtDNA is associated with various proteins, forming a nucleoprotein complex termed a nucleoid. Mutations of the mtDNA as well as deviations in the composition of the associated proteins are implicated in a variety of diseases in humans. However, the regulation of the basic nucleoid functions, i.e. replication and transcription on the single nucleoid level is poorly understood.

Human cells contain up to several hundreds of nucleoids, each with an average diameter of about 80 nm. Since nucleoids cluster together within mitochondria, the resolution and analysis of single nucleoids is impaired in diffraction-limited microscopy methods. In this work, nanoscopy is used to visualize single nucleoids and to address fundamental questions about the transcription and replication of mtDNA.

For this purpose, a robust staining protocol to identify nucleoids engaged in replication or transcription, was established based on the incorporation of synthetic nucleosides. Three-color STED nanoscopy revealed the organization of nucleoids into at least two subpopulations within single cells. The results of this study indicate that nucleoids can either be active with a tendency to be engaged in both processes or seemingly totally inactive. This finding provides new explanations for the high copy number of the mitochondrial genome.

In addition, the approach developed here was used to analyze knockdown cells of important key players of mitochondrial regulation, namely, the mitochondrial RNA Polymerase POLRMT and mitochondrial elongation factor TEFM. POLRMT is required for functional transcription and synthesis of the replication primer, while the switch between mitochondrial transcription and replication is mediated by TEFM.

The present work demonstrates that POLRMT and TEFM together coordinate whether the mtDNA is used as a template for transcription or replication. Upon POLRMT reduction, transcription is favored over replication of mtDNA, whereas a decrease in the expression of TEFM leads to increased replication. This provides fundamental insights into the reciprocal regulation of mitochondrial transcription and replication.

1. Introduction

In the early 1960, more than 70 years after the discovery of mitochondria in eukaryotic cells, DNA-containing structures within this organelle were described for the first time (Nass and Nass, 1963). This finding required a "modification and extension of some generally accepted hypotheses of cell function which consider the nucleus to be the exclusive site of cellular DNA and genetic information." (Nass and Nass, 1963). Mitochondrial DNA became a very popular field of research since its mutations are key factors in many age-related diseases (Ernster and Schatz, 1981). Although some cultivated cell types can live without mitochondrial DNA, this does not hold true for a single free-living multicellular organism (Holt et al., 2012). The present work centers the transcription and replication of mitochondrial DNA and its regulatory mechanisms.

1.1 Mitochondria

1.1.1 Structure and function of mitochondria

Mitochondria are cell organelles, which represent the predominant energy-generating system in eukaryotic cells by providing a very efficient pathway to regenerate the universal energy-carrier adenosine triphosphate (ATP) through a process termed as oxidative phosphorylation (OXPHOS) (Wallace et al., 2005). Mitochondria are also essential for a variety of different cellular functions like heme biogenesis, regulation of apoptosis and the assembly of iron-sulfur clusters. The versatile function of mitochondria in different biochemical pathways and cellular processes makes them indispensable for multicellular life (Wallace, 2005, Lill et al., 2005). Malfunctions of mitochondria are accompanied with age-related metabolic and degenerative diseases like type-II diabetes and Parkinson (van den Ouweland et al, 1994; Wallace, 2005).

Apart from the nucleus, mitochondria are in most organisms the only organelle separated from the cytoplasm by two membranes, defining an intermembrane-space, a mitochondrial matrix and a cristae lumen (Fig. 1.1 A). Both membranes contribute to the function of mitochondria differently and show therefore a very different structure and composition (Chan, 2006). Import of nuclear encoded proteins into the mitochondria is mediated by the translocase of the outer membrane (TOM) complex that reveals strong interaction with the translocase of the inner membrane (TIM) complex (Neupert and Herrmann, 2007). The proper transport of proteins into the different mitochondrial membranes and compartments needs additional proteins and protein complexes like

the sorting and assembly machinery (SAM) complex in the outer membrane or small TIM proteins in the intermembrane-space (Neupert and Herrmann, 2007).

In contrast to the outer membrane, the inner membrane represents a tight diffusion barrier to ions and molecules. Due to this impermeability, an electrochemical membrane potential can be formed across the inner membrane (Kühlbrandt, 2015). This potential is created by proteins of the respiratory chain, which are assembled into five complexes and are exclusively located in the cristae membrane. These complexes are also termed OXPHOS complexes and required for ATP regeneration by oxidizing nutrients. During oxidative phosphorylation by respiratory chain proteins, protons are pumped from the mitochondrial matrix into the cristae lumen by complex I, III and IV. Backflow of these protons into the mitochondrial matrix is realized by a proton channel in the fifth OXPHOS complex also termed the ATP synthase complex. This backflow of protons provides the energy for the regeneration of ATP using ADP and inorganic phosphate (Wallace, 2005).

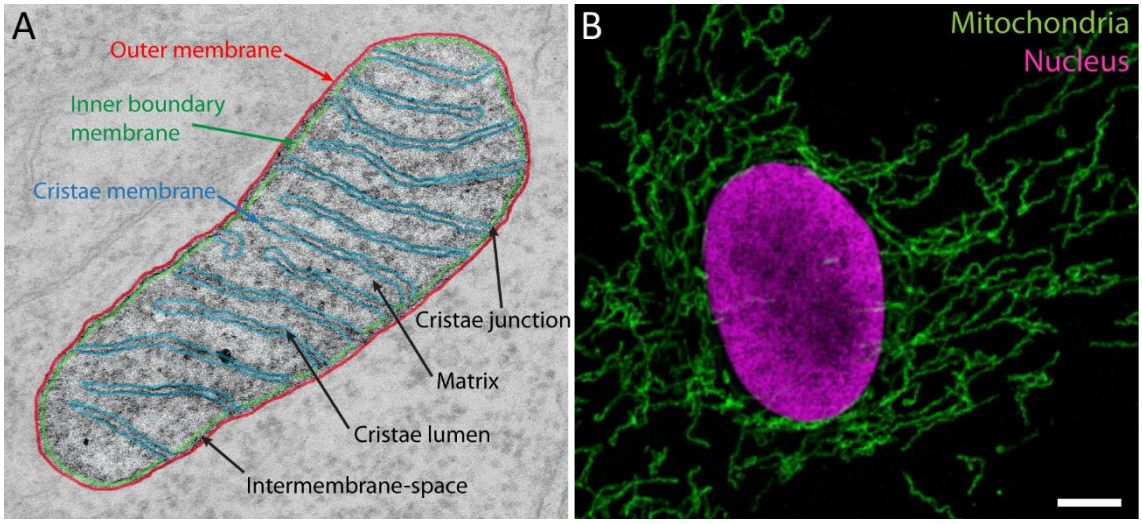

Figure 1.1 Structure of mitochondria: A) Membranes and compartments of mitochondria: Image of a mitochondrion in a cervical cancer cell (HeLa) recorded with transmission electron microscopy. Different membranes are highlighted: *Outer membrane* (red), *inner boundary membrane* (green) and *cristae membrane* (blue). The inner boundary membrane and the cristae membrane are separated by a structure termed *cristae junctions*. The mitochondrial membranes define the *intermembrane-space* between outer and inner boundary membrane and the *cristae lumen* within the cristae membrane. Furthermore, the cristae membrane and inner boundary membrane enclose an additional compartment termed the mitochondrial *matrix*. **B) Morphology of the mitochondrial network:** Mitochondria within adult human dermal fibroblasts (HDFa) were labeled with antibodies against Mic60 (green), which is located at the cristae junctions. The nucleus was stained with DAPI (magenta). Scale bar: 2 µm

Within most human cells, mitochondria appear as tubular structures, forming a highly dynamic network that is constantly undergoing fusion and fission (Scott and Youle, 2010). Remodeling of the mitochondrial network and changes of mitochondria's size are

associated with its environment and physiological needs (Scott and Youle, 2010). The dynamic of the mitochondrial network ensures an even distribution of mitochondrial proteins and an impairment of fusion and fission can be linked to several diseases (Scott and Youle, 2010, Nunarri et al., 2012). In mammals, identified proteins for fusion of the outer membrane are the GTPases mitofusin 1 and 2, whereas fission of the outer membrane is mediated by dynamin related protein 1 (drp1) (Chen et al., 2003; Smirnova et al. 2001). Optic Atrophy 1 (OPA1) is a dynamin-like GTPase involved in the fusion of the inner mitochondrial membrane (Chan, 2006).

The different composition of both mitochondrial membranes represents like the mitochondrial genome and the mitochondrial rRNAs a remnant of mitochondria's endosymbiotic origin.

1.1.2 Origin and evolution of mitochondria

According to the endosymbiotic theory, mitochondria in eukaryotic cells originated from an α-proteobacterium, which was ingested by an archeabacterium (Sagan, 1967; Williams et al., 2007; Gray et al, 2012). Until today there is no consensus whether endocytosis of the α-proteobacterium was a very early or quite late step during the evolution of eukaryotic cells (Embley and Martin, 2006). However, this process established the bioenergetic basis for the large variability of eukaryotic cells and the creation of multicellular organisms (Martin et al., 2015). The discovery of an independent mitochondrial genome constitutes strong evidence for the endosymbiotic theory (Nass and Nass, 1968, Gray et al., 1999). Analysis of the gene sequence of mitochondrial DNA (mtDNA) in different organisms revealed that the variety of mitochondria can be reduced to a single ancestor (Yang et al., 1985). The genetic code of mitochondria differs from the universal genetic code due to its endosymbiotic origin (Anderson et al., 1981). Although most of the primal mitochondrial genome was transferred into the nucleus during evolution, mtDNA is still essential for mitochondrial function in every eukaryotic cell (Gray, 1999; Sickmann et al., 2003).

1.2 Mitochondrial DNA – the Nucleoid

1.2.1 Structure of the nucleoid

Mammalian mtDNA is a circular, intron-free and GC-rich DNA-molecule of approximately 16.6 kilobases encoding for 13 polypeptides, 2 ribosomal RNAs and 22 transfer RNAs. As a result, mtDNA is one of the most gene-dense DNA-molecules (Gustafsson et al., 2016). All 13 polypeptides are part of the OXPHOS complexes (Fig

1.2). The remaining OXPHOS-proteins are encoded in the nucleus and are imported into the mitochondria. Although mtDNA encodes only for a minority of OXPHOS complex proteins, it is essential for its maintenance (Larsson et al., 1998). The rRNAs encoded on the mtDNA form the 12S and 16S rRNAs of the mitochondrial 55S ribosome which shares properties with the prokaryotic 70S ribosome and the eukaryotic 80S ribosome, as well (De Silva et al., 2015). This, together with the mtDNA-encoded tRNAs, explains the importance of mtDNA for the mitochondrial expression system. Since one strand of the mtDNA contains significantly more guanine, the two strands can be separated into a light and a heavy strand due to their sedimentation behavior upon density centrifugation in $CsCl_2$ gradients (Berk et al., 1974). The gene-dense mtDNA possess one major noncoding region (NCR) between the $tRNA^{Phe}$ and $tRNA^{Pro}$ gene (Nicholls et al., 2014). The NCR contain most of mtDNAs regulatory elements, like promotors for transcription, origin of replication and the regulatory D-loop region (See sections: 1.3 and 1.4; Montoya et al., 1982; Clayton et al., 1991).

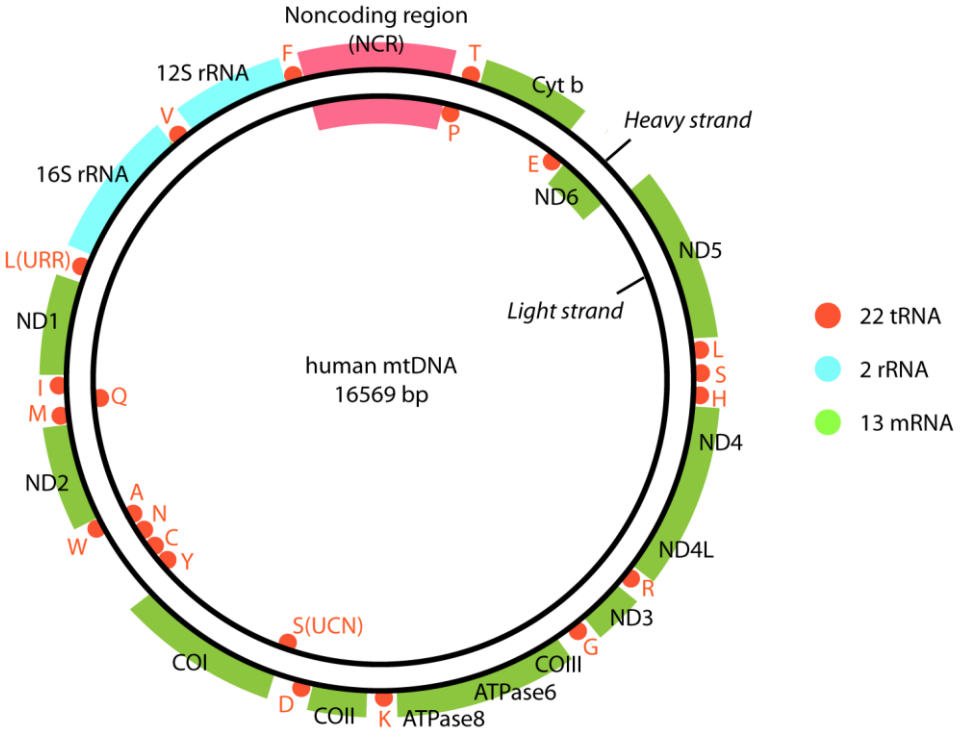

Figure 1.2 Human mitochondrial DNA: Mitochondrial DNA (mtDNA) in humans has a size of approximately 16.6 kb. The mtDNA contains a heavy and a light strand due to its uneven distribution of guanine. Heavy strand encodes for both rRNAs (blue), 14 tRNAs (orange) and 12 proteins of OXPHOS (green). Light strand encodes for 8 tRNAS (orange) and only one protein of OXPHOS (green). The mtDNA contains only one major noncoding region (red) with a size of 1.1 kb.

Furthermore, the NCR contains most of the variations among human mtDNA sequences which are concentrated in three hypervariable areas outside of the regulatory elements. Although many mtDNA with different deletions can be found in nature, the NCR is still present in all of them, showing its critical importance (Behar et al., 2008; Ingman et al 2000).

The mtDNA-molecules are located in the mitochondrial matrix and are found to be associated with the inner mitochondrial membrane, but are also observed to be mobile within the mitochondrial network (Albring et al.; 1977; Brown et al., 2011). Within cells, mtDNA is not a naked molecule but decorated with DNA-binding proteins. This nucleoprotein complex is called nucleoid. Thus, the mtDNA with a contour length of 5 µm in mammals is compacted into a structure which appears as an ellipsoid of 100-120 nm when decorated with antibodies by using nanoscopy (Nass and Nass, 1963; Brown et al. 2011; Kukat and Wurm et al., 2011). Due to its enhanced optical resolution in comparison to conventional diffraction-limited microscopy, nanoscopy revealed that nucleoids tend to cluster, making it an essential method to analyze the distinct number and distribution of nucleoids within a cell. The application of Stimulated Emission Depletion (STED) nanoscopy revealed a 60 % higher number of distinguishable nucleoids in mammalian cells compared to conventional light microscopy (Kukat and Wurm et al., 2011). A single nucleoid can contain more than one mtDNA. Nanoscopy together with qPCR revealed that single cells can contain up to approximately 2000 nucleoids with about 1.1 -1.5 mtDNA molecules per identified nucleoid (Kukat and Wurm et al., 2011; Kukat et al., 2015). This high number of mtDNA-molecules leads to rather complex mechanism of manifestation and inheritance of mtDNA-related diseases.

1.2.2 Inheritance mtDNA-related diseases

The Kearns-Sayre syndrome and Leber's hereditary optic neuropathy were the first disorders which could be linked to mtDNA mutations in 1988 (Holt et al., 1988; Wallace et al., 1988). Since it has become easy to analyze mtDNA-sequences, a huge amount of mtDNA mutations could be identified and linked to specific diseases. Today, identified mtDNA associated diseases range from neurological, gastrointestinal and cardiac diseases to respiratory failures as well as endocrinal defects (Taylor and Turnbull, 2005).

The previously described huge polyploidy of mtDNA leads to an important aspect of mitochondrial genetics which differs from mendelian genetics. All copies of mtDNA within a cell can be identical in their sequence, which is then termed homoplasmy. Besides that, different mitochondrial genotypes can occur in the same cell, a situation

denoted as heteroplasmy (Taylor and Turnbull, 2005). The mutations of mtDNA have to reach a specific threshold within a cell to cause a biochemical effect and thereby a clinical expression. Since mtDNA is permanently undergoing mutations, different populations of mutated mtDNAs are present in individuals at a low level. However, these populations often do not reach the required threshold for a clinical expression (Taylor and Turnbull, 2005, Wallace et al. 2005).

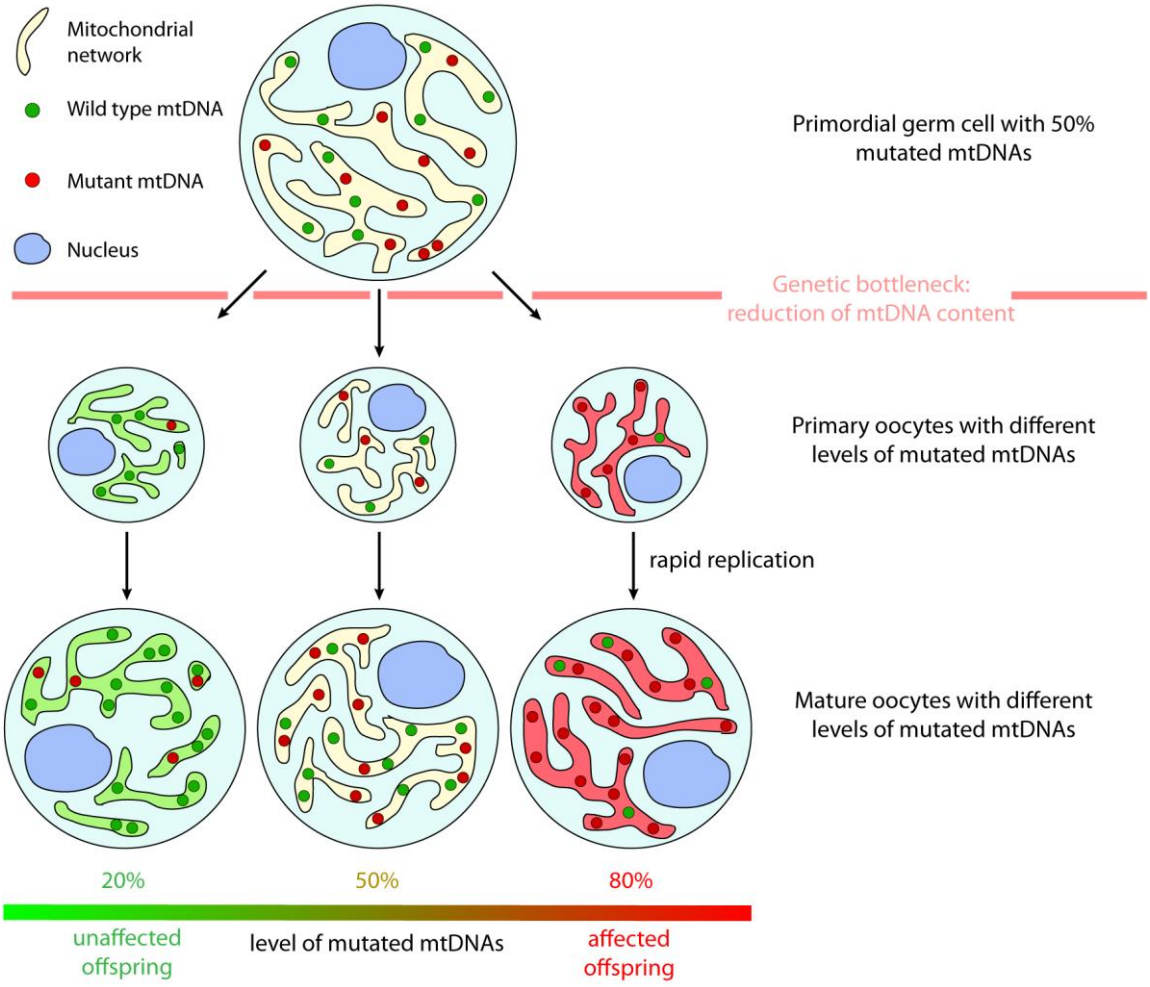

Figure 1.3 Genetic bottleneck during oogenesis: During early oogenesis the content of mtDNA of the primary germline cells is reduced and uneven distributed among the daughter cells. This leads to primary oocytes whose proportion of mutant to wild type mtDNA molecules can totally differ from that of the primary germ line cells. Maturation of oocytes is coupled with rapid replication of mtDNA to reach a normal amount of mtDNA molecules again. After fertilization, the level of mutant mtDNAs determine if the offspring is affected or not. This genetic bottleneck explains how affected mothers with a heteroplasmic mutation of mtDNA can get unaffected offspring. Mutant mtDNAs and impaired mitochondria in red; wild type mtDNAs and functional mitochondria in green.

Despite a constant mutation rate of mtDNA, mutated DNA-molecules do not accumulate at the level of a population. mtDNA is exclusively inherited maternally as the amount of

mtDNA is downregulated during spermatogenesis and moreover sperm mitochondria are degraded after fertilization (Larsson et al., 1995; Larsson et al., 1996).

Studies show that the chance of the inheritance of heteroplasmic mutations from affected mothers to the offspring is below 5% (Chinnery et al., 2004). The basis for this is the mitochondrial genetic bottleneck during oogenesis (Fig 1.3). A strong reduction of the amount of mtDNA-molecules and an uneven distribution of them during oogenesis is observed, leading to primary oocytes with a different level of mutated mtDNAs than the primordial germ cell. After this reduction of mtDNA, rapid replication is induced during maturation to normalize the DNA content. Hence, the mtDNA content of the offspring can differ from the DNA content of the mother (Hauswirth et al., 1982; Cree et al., 2008). Furthermore, a selection mechanism against the transmission of mutant mtDNA exists, as well as regulatory mechanisms within the developing embryo and decreased fertility of women with a high level of mutated mtDNA molecules. As a result, the inheritance of mutated mtDNA from the mother to the offspring is strongly reduced (Stewart et al., 2008). However, homoplasmic mutations are transmitted to every offspring. Interestingly, not only mtDNA mutations, but changes in the composition of the nucleoid can cause mtDNA related diseases (Lee and Han, 2017).

1.2.3 Nucleoid composition

As mentioned, mtDNA is decorated with proteins, forming a structure termed nucleoid. These proteins can be divided into proteins of the inner and outer layer (Fig 1.4). The proteins of the inner layer can be found in native nucleoids and bind strong enough to the mtDNA such that they can be cross linked with formaldehyde. The proteins of the outer layer which are associated with native mtDNA, fail to crosslink (Bogenhagen et al., 2008). The main structural protein of the inner layer of mammalian nucleoids is the mitochondrial transcription factor A (TFAM), present at a ratio of one molecule per 16-17 base pairs (Bogenhagen, 2012). Whereas TFAM binds to the whole mtDNA content, some other proteins of the inner layer only bind to a subset of mtDNA molecules. An example for these proteins are components of the replication and transcription machinery (Fig. 1.4; Bogenhagen, 2012). The components of both machineries are discussed in the sections 1.3.1 and 1.4.1.

Proteins of the outer layer are often also involved in mtDNA unrelated mitochondrial processes but show additionally an association with the mtDNA. Examples for proteins of the outer layer in humans are prohibitins (PHB1 and PHB2), which are important for nucleoid morphology and regulation of copy number, as well as the Mic60, most likely

linking mtDNA and the inner mitochondrial membrane and organizing its proper distribution (Fig 1.4; Gilkerson et al., 2013; Li et al., 2016). Studies that do not distinguish between the core and the peripheral nucleoid proteins claim that nucleoids from most organisms contain over 50 nuclear-encoded proteins, most of them with unknown functions (Bogenhagen, 2012). As mentioned, some of the identified nucleoid proteins are components of the mitochondrial transcription or replication machinery. As the present study focusses on both processes, they are discussed in detail in the following sections.

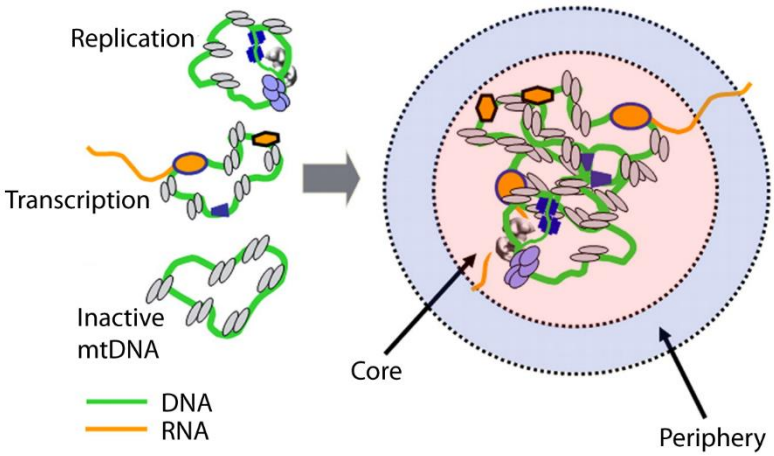

Core proteins					
TFAM	TFB1M	DHX30	HADHB	SLC25A5	LRRC59
mtSSBP	mTERF	DDX28	SHMT2	VDAC1	PDIP38
POLγ	Twinkle	HSDHA	TOP1MT	VDAC2	DNAJ3
POLγ2	SUPV3L1	LONP1	TUFM	CPS1	LRPPRC
POLRMT	ATB5β	CLPX	HSP1A	DBT	ACADVL
TFB2M					

Peripheral proteins	
HSPD1	CPT1A
PHB1	NDUFS1
PHB2	NDUFA9
ATAD3A	KTN1
MGC5352	MIC60

Figure 1.4 MtDNA associated proteins: The mtDNA is associated with proteins. Core proteins can be cross linked with formaldehyde to the mtDNA. Among these proteins is TFAM, which bind to active and inactive mtDNA molecules and proteins of the replication and transcription machinery. Peripheral proteins are found in native nucleoids but fail to crosslink (Modified after Bogenhagen et al., 2008).

1.3 Transcription of mitochondrial DNA

Each strand of the mtDNA has its own promotor for transcription initiation termed heavy strand promotor (HSP) and light strand promotor (LSP), respectively, located in the NCR. In mammals, the heavy strand encodes for both rRNAs (12S and 16S rRNA), 12 mRNAs (ND1, ND2, COI, COII, ATPase8, ATPase6, COIII, ND3, ND4L, ND4, ND5, Cytb) and 14 tRNAs. The light strand encodes for only one mRNA (ND6) and 8 tRNAs (Taanman, 1999; Fig. 1.2). However, it is still unclear whether there is only one HSP or two promotors

HSP1 and HSP2 for transcription initiation of the heavy strand. The model of two HSPs is based on the observation that cells possess an increased level of both rRNAs in comparison to mRNAs and gives a hint for the occurrence of different HSP-transcripts. According to this model, transcription from HSP2 produces complete transcripts and the favored transcripts from HSP1 only cover both rRNAS, $tRNA^{Phe}$ and $tRNA^{Val}$. However, transcription from a second HSP could not be observed so far (Montoya et al., 1982).

Complete transcription from HSP and LSP results in near-genome-length polycistronic RNAs that are processed afterwards. Genes for tRNAs often flank rRNA and protein coding genes. According to the "tRNA punctuation model", tRNA genes are specifically cropped to release single tRNAs, mRNAs and rRNAs. In mammals, this process is catalyzed in different organisms by their respective versions of RNAse P for the 5'-ends and by RNAse Z for the 3'-ends of tRNA genes (Anderson et al., 1981; Bibb et al., 1981; Ojala et al., 1981; Hallberg et al., 2014). Although, it is still very unclear how the mitochondrial transcription is regulated, the involved components have been identified.

1.3.1 Transcription machinery

The enzymatic machinery involved in mitochondrial transcription is encoded in the nucleus, but is different from the apparatus of eukaryotes. However, some of the involved proteins show also differences to the corresponding α-proteobacterial components and are instead similar to factors of the transcription machinery of the T7 bacteriophage. The proper initiation of transcription in mammals requires only three components: The Mitochondrial RNA Polymerase (POLRMT) as well as the mitochondrial transcription factors A (TFAM) and B2 (TFB2M) (Gray, 1999; Falkenberg et al., 2002, Shutt et al., 2006). Functional elongation of the transcription needs a fourth factor which is the mitochondrial transcription elongation factor (TEFM) (Minczuk et al., 2011; Agaronyan et al., 2015; Posse et al., 2015).

POLRMT consists of only one subunit and shows similarities to the RNA polymerase of bacteriophage T7 (T7 RNAP). Both polymerases belong to the polymerase A family (Hedke et al., 1997; Jeruzalmi and Steitz 1998; Cheetham et al., 1999). POLRMT has a mitochondrial targeting sequence, a catalytic C-terminal domain (CTD) and an N-terminal domain (NTD) with similarities to the promotor binding domain of T7 RNAP (Cheetham et al., 1999; Temiakov et al., 2004; Ringel et al., 2011). The crystal structure of POLRMT and cross-linking methods show that the structure of both CTDs are well conserved between T7 RNAP and POLRMT. CTDs of both polymerases contain a β-hairpin termed the specificity loop which is important for promotor specificity in the T7

RNAP (Cheetham et al., 1999; Ringel et al., 2011). Although many structures are conserved between the NTDs of both polymerases like the recognition loop and the intercalating hairpin, the NTD of POLRMT shows some differences in its function compared to T7 RNAP. In T7 RNAP, the NTD undergoes refolding as it turns from an initiation complex with functions in promotor binding and opening to an elongation complex (Temiakov et al., 2004). POLRMTs NTD seems to lack functions in promotor binding and promotor opening.

The specificity-loop as well as the AT rich recognition loop of T7 RNAP are responsible for sequence specific promotor recognition. (Cheetham et al., 1999; Hillen et al., 2017 (2)). In contrast, interactions between POLRMT and the promotor region are barely observed (Hillen et al., 2017 (1)). The intercalating hairpin in the NTD of T7 RNAP is required for the opening of the promotor region whereas the same structure in POLRMT seems to lack this function. Both, promotor binding and promotor opening, are mediated by the two transcription factors TFAM and TFB2M in mammalian mitochondria (Ringel et al 2011; Hillen et al., 2017(2)). In contrast to T7 RNAP, the mitochondrial RNA polymerase possess an N-terminal extension (NTE) containing a pentatricopeptide repeat (PPR) domain, which might be important to prevent reannealing of RNA and DNA. (Ringel et al., 2011; Schwinghammer et al., 2013).

TFAM is the core structural protein of nucleoids. Next to TFAMs roles in shaping and stabilizing the nucleoid, it is essential for transcription initiation in mammals. (Bogenhagen, 2012; Shi et al., 2012). TFAM is a high mobility group (HMG) box protein that binds to HSP and LSP, respectively. TFAM binding results in an unwinding of the DNA, creating a stable U-turn in the promotor regions and is necessary to recruit POLRMT (Dairaghi et al., 1995; Gaspari et al., 2004 (1); Yakubovskaya et al., 2014; Morozov et al., 2014). Therefore, TFAM compensates the lack of POLRMT to specifically bind both promotors (Hillen et al., 2017 (2)).

Cells contain two TFBMs, termed TFB1M and TFB2M. Both show similarities to rRNA methyltransferases of prokaryotes. TFB1M shows still methyltransferase activity, whereas TFB2M interacts with POLRMT and is essential for transcription initiation (Falkenberg et al., 2002; Guja et al., 2013). TFB2M stabilizes the key elements of POLRMT for promotor opening like the intercalating hairpin and thereby mediates promotor opening. In vitro, POLRMT, TFAM and TFB2M are sufficient to initiate transcription from HSP and LSP (Falkenberg et al., 2002). Two further proteins are directly involved in transcription: TEFM and the mitochondrial transcription termination factor 1 (MTERF1).

The role of both proteins is explained during the description of the transcription mechanism.

1.3.2 Initiation of transcription

The initiation of transcription in mammalian mitochondria can be separated into two steps. The formation of a pre-initiation complex (pre-IC) and the following formation of the initiation complex (IC) (Fig 1.5; Morozov et al., 2014, Morozov et al., 2015). On both strands, the heavy and the light strand, these initiation complexes reveal the same structure (Morozov and Temiakov 2016; Hillen et al., 2017 (2)). Formation of the pre-IC at HSP and LSP starts with binding of TFAM 10-15 base pairs (bp) upstream of transcription start. Afterwards, TFAM unwinds the DNA and introduces a 180° turn (Kukat et al., 2013). Protein-protein- and protein-DNA-crosslinking experiments show that POLRMT is recruited to the promotor region by interaction with TFAM and DNA (Gaspari et al., 2004 (2); Morizov et al., 2014, Hillen et al., 2017 (2)). The NTE of POLRMT binds with the C-terminus of TFAM due to hydrophobic and electrostatic effects. This interaction between TFAM and POLRMT requires the presence of DNA, but not the presence of TFB2M. Furthermore, POLRMT binds not only a DNA-sequences 5 and 10 bp upstream of the promotor, but also a sequences upstream of the TFAM binding site which is 49 bp upstream of the promotor. The formation of the DNAs 180° turn mediated by TFAM is essential to bring upstream DNA and POLRMT in close proximity. In this pre-IC, specificity to the promotor regions is mediated by TFAM. Hence, the affinity of TFAM to HSP and LSP could represent a mechanism to regulate transcription. (Yakubovskaya et al., 2014; Morozov et al., 2014; Morozov et al., 2015). An example for such a mechanism is the phosphorylation of TFAM since this leads to a decreased promotor affinity (Lu et al., 2013). Furthermore, studies claim another mechanism for how TFAM could be responsible for regulating transcription when full length transcription from HSP depends on the level of TFAM. A model was proposed in which low levels of TFAM trigger transcription from LSP and “HSP1” leading to a shortened HSP-transcript, whereas high levels of TFAM trigger transcription from ”HSP2” leading to the full-length product. However, no in vivo data are available to prove that model (Lodeiro et al., 2012).

After the recruitment of POLRMT to the DNA by TFAM, structural changes within the polymerase occur, enabling binding of TFB2M. The pre-ICs are likely transient and are not stable until binding of TFB2M which leads to the formation of a stable IC followed by promotor melting (Morozov et al., 2015). Crosslinking experiments show that TFB2M

strengthens the interaction between POLRMT and the DNA. Without TFAM, TFB2M does not bind to POLRMT. Hence, the pre-IC has to form first, confirming an initiation model of two separate steps (Morozov et al., 2014; Mororov et al 2015).

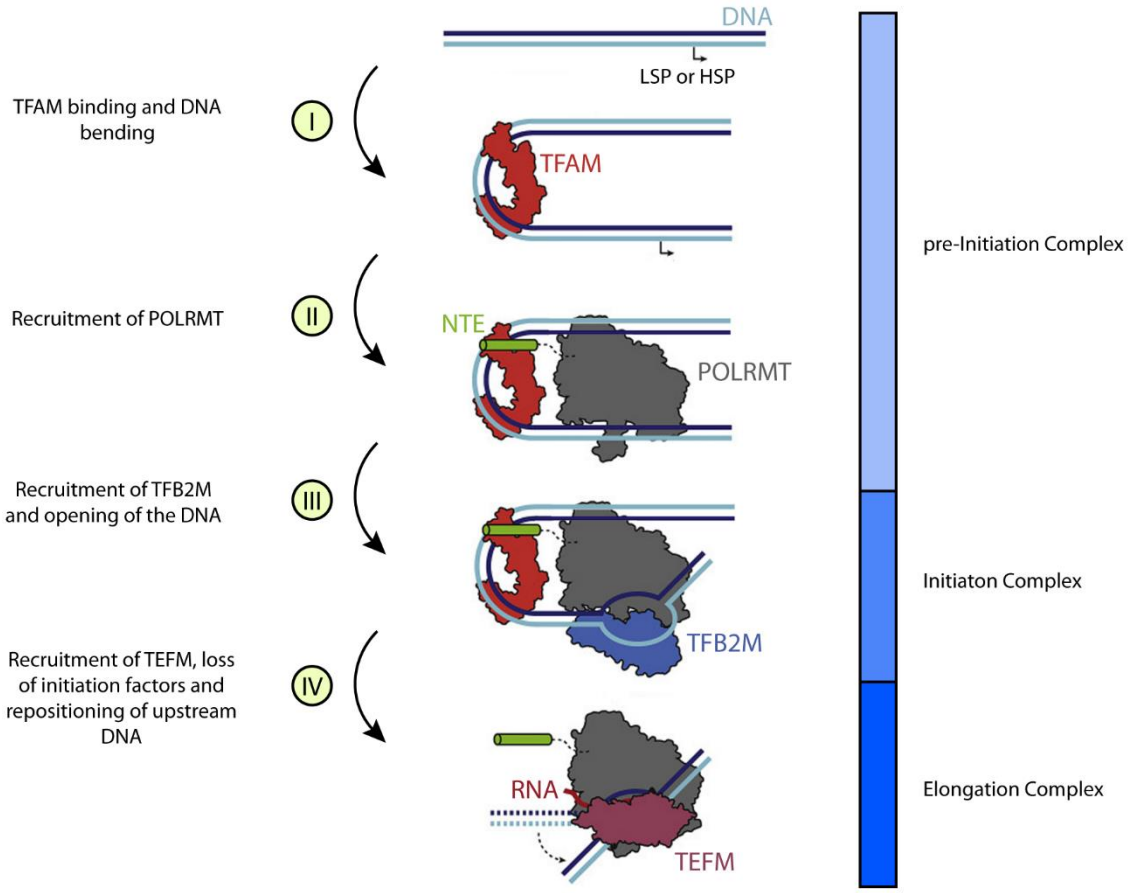

Fvi

Figure 1.5 Initiation and elongation of mitochondrial transcription in mammals: TFAM (red) binds 10-15 bp before LSP and HSP to mediate unwinding and creates a 180° turn of the promotor region. Then POLRMT (gray) is recruited and interacts with TFAM and the DNA, leading to the formation of the pre-initiation complex (pre-IC). Binding of TFB2M (blue) to the DNA and POLRMT mediates promotor melting and creation of the first phosphodiester bond. After TFB2M binding the initiation complex (IC) is complete; transition to the elongation complex (EC) is characterized by dissociation of initiation factors, binding of TEFM (dusky pink) and a conformational change of the upstream DNA. (Modified after Hillen et al., 2017 (2))

Structural changes of POLRMT leading to TFB2M binding could involve the opening of a nucleic acid binding cavity, which enables a movement of the N-terminus of TFB2M into the active site of POLRMT where it interacts with the priming ATP and the +1 base of the promotor and contacts POLRMT's intercalating hairpin. After its recruitment, TFB2M leads to an opening of the promotor DNA (Gaspari et al., 2004 (2), Schwinghammer et

al, 2013; Morozov et al., 2014; Mororov et al 2015, Hillen et al., 2017 (2)). Furthermore, TFB2M binding leads to conformational changes in POLRMT stabilizing the open promotor DNA. These changes include a movement of the intercalating hairpin between both DNA strands (Hillen et al., 2017 (2)). As a result the complete IC is formed.

1.3.3 Transcription products of the elongation complex

After initiation of transcription, TFAM and TFB2M dissociate from POLRMT. The transition from the initiation to the elongation complex is not characterized by a conformational change of POLRMT, but a structural change of the upstream DNA. After dissociation of TFB2M, the upstream DNA occupies the former binding site of TFB2M. The dissociation of TFB2M also enables the recruitment of the mitochondrial elongation factor TEFM (Fig. 1.5; Hillen et al., 2017 (2))

The interaction between POLRMT and TEFM is mediated by the exposure of the intercalating hairpin and the specificity loop of POLRMT during formation of the elongation complex (Hillen et al., 2017 (1); Hillen et al., 2017 (2)). TEFM contains two functional domains fused by an unstructured linker. The CTD shows structural similarities to Holiday junction resolvases, but has lost its nuclease activity. However, it still contains a DNA-binding activity, which is important for stability of the elongation complex. The NTD shows a helix-hairpin-helix structure with unknown function (Hillen et al., 2017(1)). TEFM shows interaction with about 19 nt of the 5’ end of the nascent RNA and the downstream DNA. TEFM binds POLRMT as a dimer and is necessary for proper interaction of POLRMT with the downstream DNA enhancing the stability of the elongation complex. Furthermore, TEFM interacts with the single stranded non template DNA to stabilize the transcription bubble. The interaction of TEFM with RNA stimulates elongation through regions generating highly structured RNA and, in general, stabilizes the POLRMT elongation complex (Hillen et al., 2017 (1)). The knockout of TEFM leads to an impairment of the transcription elongation on both strands. Interestingly, TEFM is present at the promotor regions before the transcription is initiated, leading to the hypothesis that TEFM could be a second subunit of POLRMT (Sologub et al., 2009 Minczuk et al., 2011; Posse et al., 2015; Agaronyan et al., 2015). The influence of reduced TEFM level on mitochondrial transcription was also an essential part of the current study.

The transcription from LSP produces different products. This is due to three conserved sequence blocks (CSB I-III) located upstream of LSP, from which CSBI is very well conserved among species, CSB II is only partially present in different species and CSB III

is often missing. In mammals, processes at CSB I and CSB II can lead to premature termination of transcription. This leads, together with complete functional transcription, to three possible LSP-transcripts (Walberg and Clayton, 1981; Saccone et al., 1991; Sbisa et al, 1997). CSBs are G-rich regions and during transcription, formation of G-quadruplex-structure of the nascent RNA leads to a termination of transcription (Wanrooij et al., 2012 (2), Hillen et al., 2017(1)). Since termination at CSB II is crucial for formation of a replication primer (section 1.4.2.1), its structure is well analyzed. CSB II consists of a GC-rich sequence followed by an 8 bp linker and a 9 bp AT-rich region (Fig 1.6 A).

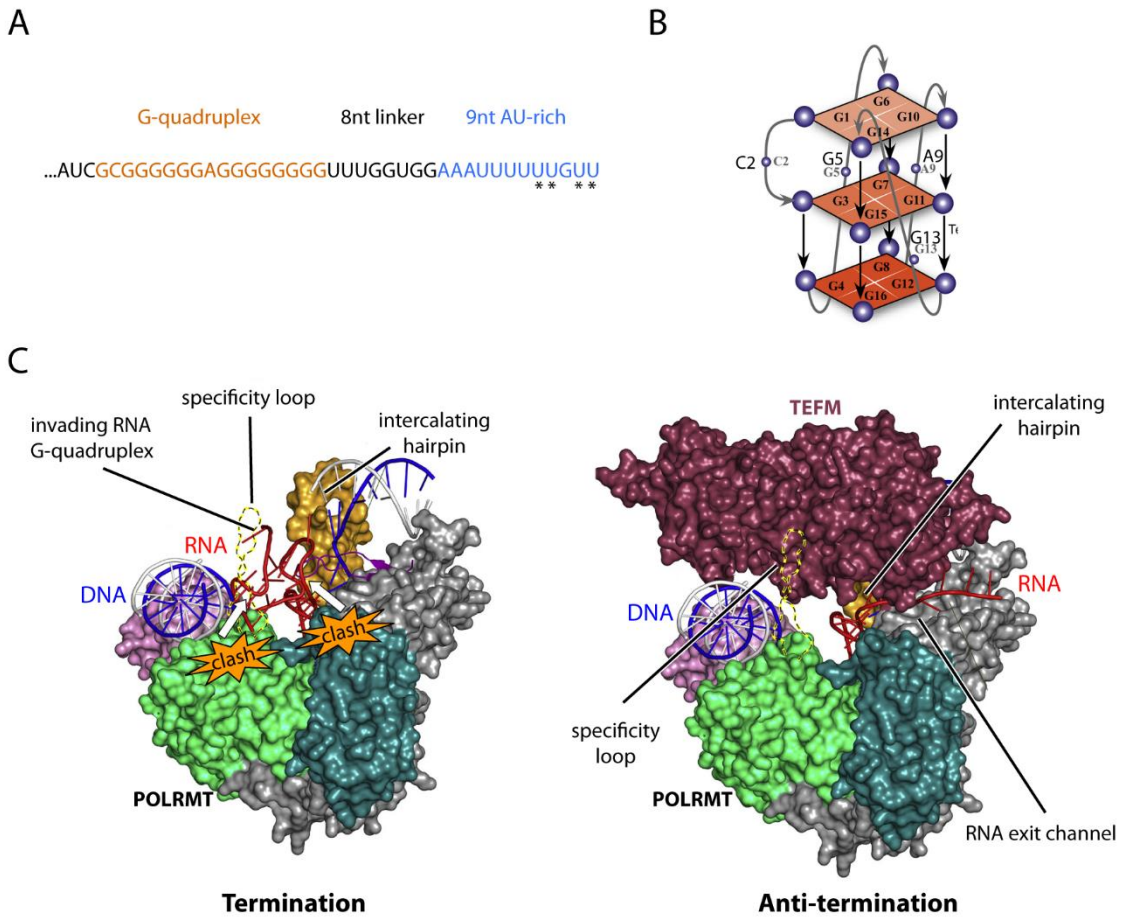

Figure 1.6 G-quadruplex structure leads to termination of transcription: A) Sequence of the nascent RNA at CSBII in human mtDNA. Nucleotides involved in G-quadruplex formation are highlighted in orange. Asterisks in the AU-rich region (blue) indicate the positions of termination. **B)** Depiction of one possibility how the G-quadruplex structure at CSBII can be organized. **C)** Without TEFM the G-quadruplex structure clashed with the specificity loop and the intercalating hairpin of the mitochondrial RNA polymerase leading to premature termination. When TEFM is present, the nascent RNA is guided through an RNA exit channel and no G-quadruplex structure can be formed. Therefore, transcription continues. (Modified after Hillen et al., 2017(1))

During transcription the nascent RNA forms a G-quadruplex structure which is a highly complex formation based on a quadratic arrangement of guanine molecules interacting via hydrogen bond. A depiction of a possible G-quadruplex structure based on the sequence of human CSBII is illustrated in Fig 1.6 B. This G-quadruplex structure destabilizes the elongation complex by clashing with POLRMTs intercalating hairpin and specificity loop (Fig 1.6 C). During G-quadruplex formation, the 9bp RNA-DNA hybrid in the elongation complex consists only of A-U and T-A pairs, therefore providing very weak RNA-DNA interaction (Wanrooij et al., 2012 (2); Agaronyan et al., 2015, Hillen et al., 2017 (1)). About two thirds of the transcription from LSP is terminated at CSB II leading to a product of about 100 nt. This short transcript works as a primer for mitochondrial replication. (Fig. 1.7 A; section 1.4.2). Transcribing through CSBs requires the presence of TEFM, which binds POLRMT and the nascent RNA. TEFM binding prevents the formation of a G-quadruplex structure by forming an RNA exit channel (Fig. 1.6 C; Falkenberg et al., 2007; Agaronyan et al., 2015, Hillen et al., 2017(1)).

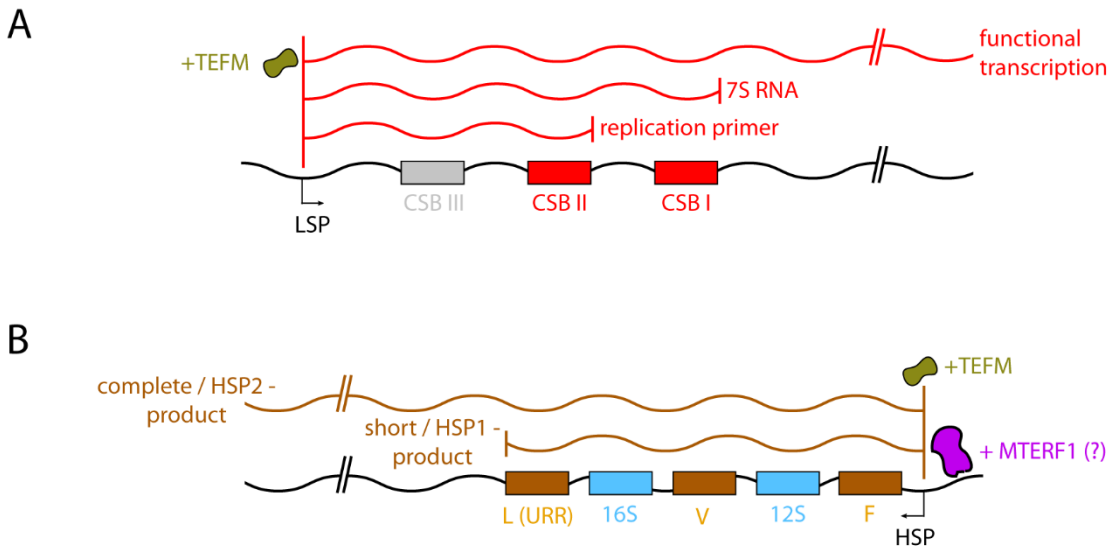

Figure 1.7 Products of mitochondrial transcription: A) Products of LSP-transcription: Downstream of LSP, mtDNA contains up to three conserved sequence blocks (CSBs). Premature termination at CSB II results in a primer for replication and termination at CSB I results in the 7S RNA. For functional near-genome length transcription TEFM is required. **B) Products of HSP-transcription:** TEFM is required for proper processivi

ty of the elongation complex. A short transcript is terminated after $tRNA_{Leu(URR)}$ possibly due to the action of MTERF1. A longer transcript covers the whole strand.

The termination of transcription at CSB I results in the 7S RNA with a size of approximately 200 nt (Fig 1.7 A). The function of 7S RNA has not been understood so far. The 7S RNA is also believed to be involved in primer formation for replication, but

studies show that it is polyadenylated at its 3'-end and is not found to be associated with the DNA. Therefore it is unlikely that it is involved in primer formation for replication (Falkenberg et al., 2007, Jemt et al., 2015). Finally, without premature termination, LSP produces a near-genome length transcript.

As mentioned above, two different promotors on the heavy strand HSP1 and HSP2 are proposed, matching two different transcripts which can be observed (Fig 1.7 B). The transcription of the heavy strand can be actively terminated after the 16S rRNA gene, leading to a shortened transcript (Shutt et al., 2010). TEFM is also important for HSP transcription due its positive effect on the processivity of the elongation complex.

1.3.4 Termination of transcription

The termination of transcription in mitochondria is not well understood. Premature termination of HSP was believed to be mediated by the protein MTERF1 (Fig 1.7 B). It was found to bind with high affinity within the $tRNA^{Leu(UUR)}$ gene, shortly after the termination point of the premature HSP-product. MTERF1 was also found to interact with POLRMT at the initiation site. It was therefore suggested that it has a role in forming a DNA-loop in which POLRMT is recycled after premature termination. However, MTERF1 knockouts do not create a clear phenotype. The relation between short and long HSP-transcripts remains unaffected during MTERF1 loss in mice (Kruse et al., 1989; Fernandez-Silva et al., 1997; Terzioglu et al., 2013). MTERF1 is not only described to be involved in terminating the HSP-transcription, but studies show that MTERF1 might be responsible for the LSP-transcription termination. MTERF1s binding site is upstream of $tRNA^{Glu}$ which represents the last gene of the light strand. The knockout of MTERF1 leads to a decrease of LSP-products. It is believed that in MTERF1 knockouts, LSP-transcription continues till it reaches LSP again, causing promotor interference (Terzioglu et al., 2013). Further studies showed that MTERF1 causes pausing but not termination of transcription and that it has multiple binding sites at the mtDNA (Hyvärinen et al., 2007). Hence, there is no consensus whether MTERF1 is involved in transcription termination.

Three further proteins of the MTERF-family exist, MTERF2-4. MTERF2 is a part of the nucleoid but knockouts lead to no phenotypes in mice (Gustafsson et al., 2016). MTERF3 was identified as a negative regulator of transcription. MTERF3 can bind to the regulatory NCR of the mtDNA and its loss leads to upregulation of transcription and impaired function of OXPHOS. MTERF3 might be important to stop transcription from elongating into the NCR but this is not clarified until today. Furthermore, studies predict a role for MTERF3 in mitochondrial ribosome biogenesis and the coupling of

transcription and translation (Park et al., 2007; Wredenberg at al., 2013). Finally, MTERF4 was also identified as a negative regulator of transcription and MTERF4 knockouts causes an increase of transcripts. However, it is unclear how MTERF4 affects mitochondrial transcription. Hence, the mechanism of transcription termination in mitochondria has not been clearly identified so far. In contrast, the link between transcription and replication of mtDNA is well understood and also discussed in the present study.

1.4 Replication of mitochondrial DNA

The replication of mitochondrial mtDNA is a very crucial process. Whether an mtDNA mutation causes a biochemical effect depends on the level of mutant DNA-molecules in heteroplasmic cells. Therefore, minimal differences in the balance between mutated and wild type mtDNA can result in a clinical expression. Different replication rates of both mtDNA populations, the mutant molecules and the wild type mtDNAs, respectively, are essential for this balance. Hence, replication is a pharmacological target to shift the heteroplasmy towards the wild type mtDNA and cure mtDNA related diseases (Taylor et al., 1997). Several studies show the importance of replication regarding the clinical expression of mtDNA related diseases. MtDNA molecules with deletions have a significant higher replication rate than wild type molecules due to the shorter length of one round of replication. Furthermore, mtDNAs with a duplication of regions including the origin of replication are also enriched in cells because of a higher replication rate (Wallace, 1989; Wallace, 1992). Finally, not only deletions and duplications but also single point mutations can lead to a higher replication rate. According to the “sick mitochondrion hypothesis”, impaired OXPHOS of mitochondria due to mutated mtDNAs lead to a higher replication rate in these areas of the mitochondrial network. Therefore, the cell amplifies and enriches the mutant mtDNAs in the impaired areas, aggravating the initial problem. This hypothesis is based on the observation that mitochondria with an impaired OXPHOS activity show a higher replication rate. However, other studies explain this observations with genetic drift. (Wallace, 1992; Yoneda et al., 1992; Elson et al., 2001). Although replication of mtDNA seems to be essential for the outbreak of diseases, the underlying regulatory processes of replication are poorly understood.

1.4.1 Replisome of mitochondrial DNA

The minimal replisome of mtDNA-replication consists of the DNA Polymerase-γ (POLγ), the helicase TWINKLE and the mitochondrial single strand DNA binding protein (mtSSBP), all together encoded in the nucleus (Fig. 1.8; Tyynismaa et al., 2004; Hance et al., 2005). This minimal replisome is sufficient to catalyze DNA-synthesis in vitro. Additional proteins like ligases or topoisomerases are not highlighted in this section. As a result of its endosymbiotic origin, the mitochondrial replication machinery shows low similarities to the nuclear machinery. However, like the transcription machinery, it shares properties with components of T7 bacteriophage (Shutt et al., 2006).

The only identified replicative polymerase in mitochondria is POLγ consisting of two subunits termed POLγA and POLγB in vertebrates, whereas yeast just possess POLγA. Human POLγ is built up of one subunit of POLγA and two subunits of POLγB. POLγA is the catalytic subunit and resembles the T7 DNA polymerase. It contains a 3'-5' exonuclease and a 5'-desoxyribosephosphate lyase activity which is important for proof reading and excision base repair, respectively (Beese et al., 1993; Pinz et al., 2000; Longley et al., 2001; Ravichandran et al., 2004). POLγB is the accessory subunit of POLγ containing a binding activity to dsDNA. Thereby it contributes to the catalytic activity and the processivity of POLγA. POLγ is unable to unwind the dsDNA, therefore it needs the helicase TWINKLE to use dsDNA as a template (Carrodeguas et al., 2002; Korhonen et al., 2004; Farge et al., 2007).

TWINKLE is similar to T7 bacteriophages gene 4 protein and mediates unwinding of the dsDNA in the 5'-3'-direction, consuming nucleotide triphosphates. In its active form, TWINKLE forms a hexamer and requires a fork-like structure to mediate the unwinding of mtDNA. TWINKLE's helicase activity is strengthened by the third protein of mtDNAs replisome, namely mtSSBP (Spelbrink et al., 2001; Korhonen et al., 2003; Korhonen et al., 2004).

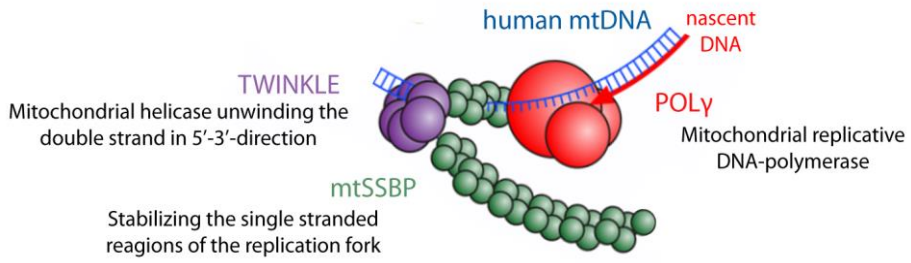

Figure 1.8 Mammalian mitochondrial replisome: The minimal mitochondrial replisome consists of the DNA-polymerase POLγ, the helicase TWINKLE and mtSSBP (Modified after Young and Copeland, 2015).

MtSSBP is essential for stabilizing single stranded sections of the replication fork. It also enhances the primer recognition of POLγ and its processivity. In its active form mtSSBP forms a tetramer. There is no consensus if mtSSBP is the only protein involved in stabilizing the replication fork, which is discussed later (see 1.4.4) (Kaguni, 2004).

Although the components required for mtDNA replication are identified, its mechanism is still a topic of ongoing discussion.

1.4.2 Primer formation

Like promotors for initiation of transcription which are HSP and LSP, the initiation site for mtDNA-replication is located within the NCR. This initiation site is termed heavy-strand origin (O_H). There is a second origin located within the coding region of mtDNA, the light-strand origin (O_L). However, the initiation of replication only occurs at O_H (Gustafsson et al., 2016).

Initiation of replication is located at position 191, termed the O_H, of mtDNA because the 5'-ends of nascent DNA could be mapped at this position (Crews et al., 1979). However, studies showed that primer formation starts at LSP, about 200 nt upstream of O_H. As described above, transcription from LSP creates close to a near-genome-length transcript, the 7S RNA and another transcript of about 100 nt length due to premature termination at CSB I and CSB II, respectively. The transcription termination at CSB II (section 1.3.2.2) results in primer formation linking transcription and replication (Elements for primer formation: Fig 1.9 A, and mechanism: Fig 1.9 B; Agaronyan et al., 2015). The switch between functional transcription and primer formation at CSB II as an essential part of the current study.

After release of POLRMT, POLγ starts creating phosphodiester bonds at CSB II, which is located approximately 100 nt upstream of O_H (Clayton, 1991; Falkenberg et al., 2007). During ongoing replication, the RNA-primer between LSP and CSB II is removed, likely by ribonuclease H1 (RNASEH1). Embryonic fibroblasts lacking RNASEH1 show a continuance of the RNA-primer. Afterwards, the DNA-part between CSB II and the O_H is removed, likely by the mitochondrial genome maintenance exonuclease 1 (MGME1). Patients with impaired MGME1 function show 5'-ends of replication at CSB II. Loss of either RNASEH1 or MGMEM1 lead to an impaired ligation after replication. (Trifunovic et al., 2004; Holmes et al., 2015). There is no consensus why the 5'- end of the nascent DNA is shifted from CSB II to O_H. The region between LSP and CSB II is highly involved in transcription. One hypothesis is that the position of ligation has to be shifted to the O_H to avoid interference between transcription and ligation (Gustafsson et al., 2016).

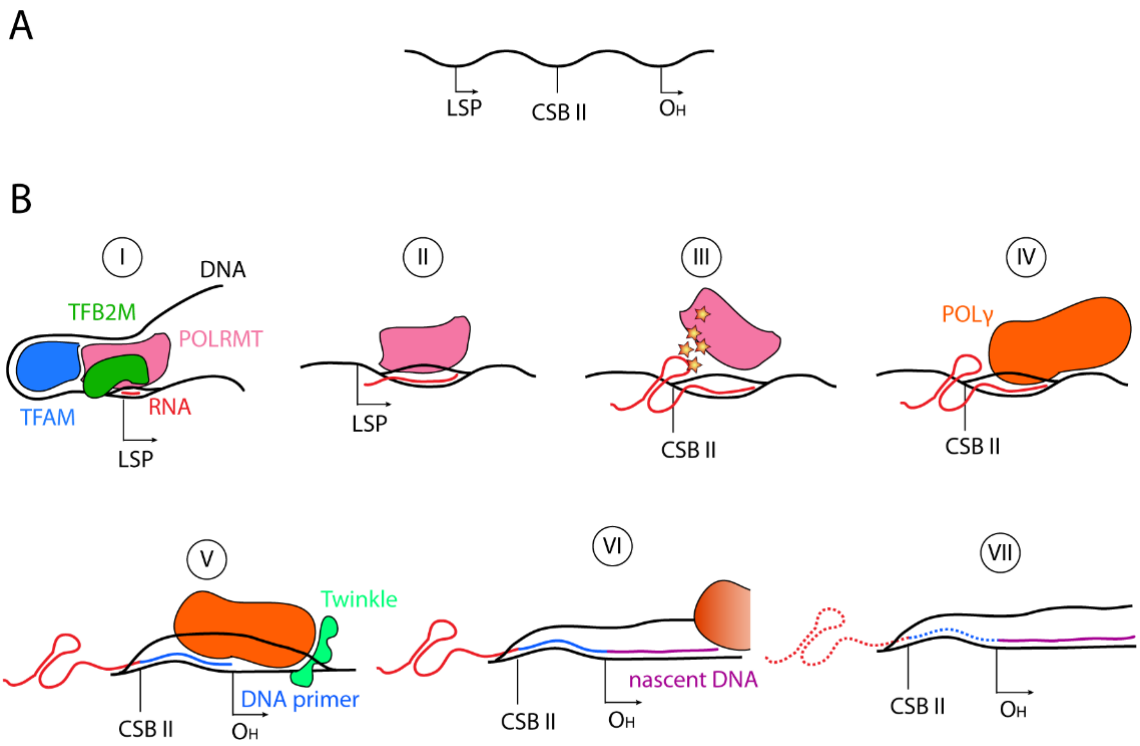

Figure 1.9 Primer formation in mammalian mitochondria: A) Important elements for primer formation on mtDNA: LSP is the transcription start. Downstream of LSP, CSB II is located, where DNA-synthesis starts. 5'-ends of nascent DNAs are mapped at O_H, downstream of CSB II. **B) Mechanism of primer formation:** (I) Transcription is initiated at LSP. (II) Transcription elongation occurs only with POLRMT (light red) without TEFM (not shown). (III) At CSB II the nascent RNA (red) forms a G-quadruplex structure which clashes with POLRMT, causing its dissociation from mtDNA. (IV) POLγ (orange) binds and starts synthesizing DNA originated from the 3' end of the RNA. (V) POLγ synthesizes the DNA part of the primer (blue) from CSB II to O_H. TWINKLE (green) is necessary for unwinding and melting of the DNA. (VI) At O_H synthesis of the daughter strand (purple) starts. (VII) The primer is removed before the replication is finished. The RNA-part is likely removed by RNASEH1 (not shown) and the DNA-part likely by MGME1 (not shown).

1.4.3 Models of mtDNA replication

Three different models describe the mechanisms of mitochondrial replication: (1) The strand coupled DNA replication model, (2) the strand displacement model (SDM) and (3) the ribonucleotide incorporation throughout the lagging strand (RITOLS) model (Clayton et al., 1991; Holt et al., 2000; Yang et al., 2002).

(1) Strand coupled replication is similar to the classical replication model of the nucleus with a leading and lagging strand. Replication was proposed to be unidirectional, starting at several origins of replications (Bowmaker et al., 2003). Using 2D agarose gel electrophoresis (2D-AGE), replication intermediates fitting to that model could be observed. However, these intermediates represent only a minority, relative to intermediates fitting to RITOLS or SDM (see below) (Holt et al., 2000; Holt et al., 2012).

In support with strand coupled replication, the whole machinery for maturation of Okazaki fragments can be found in mitochondria (Futami et al., 2007; Liu et al., 2008; Duxin et al., 2009; Holt et al., 2009). However, early EM images of mouse mtDNA support a different model in which replication occurs not simultaneously on both strands (Kasamatsu and Vinograd, 1972). This observation can be explained with both, the RITOLS and SDM, but not with strand coupled replication.

(2) SDM and (3) RITOLS have in common that replication of the heavy and light strand is uncoupled and do not involve a lagging strand or Okazaki fragments (Fig 1.10 A, Berk et al., 1974; Berk and Clayton, 1976). After initiation of replication at O_H, the daughter H-strand is synthesized by POLγ in 5'-3'-direction. After POLγ has synthesized two thirds of the new H-strand, it reaches the O_L. The origin of light strand replication is located in a cluster of five tRNAs and is exposed in its single stranded conformation by the elongation complex. Upon exposure, O_L forms a loop structure which triggers POLRMT to initiate the synthesis of a 25 nt primer. This primer works as substrate for POLγ to initiate L-strand replication in 5'-3'-direction. TWINKLE is not necessary for L-strand synthesis since it is already unwinded and single stranded. Finally, H- and L-strand replication proceeds continuously until both reach a full circle (Clayton et al., 1991; Wanrooij et al., 2012 (1)). In this model it is very important to explain how the displaced H-strand is stabilized, avoiding the exposure of direct repeats which can cause deletions, at least in bacterial plasmids (Born et al., 1991). RITOLS and SDM differ in the mechanism which stabilizes the single stranded displaced H-strand during synthesis of the daughter H-strand.

According to RITOLS the displaced H-strand is stabilized by processed RNAs. This model is also based on 2D-AGE analysis in combination with the use of endonucleases. This study together with analysis of its mass show that the displaced H-strand is double stranded (Yasukawa et al., 2006). Since the displaced H-strand cannot be cut by endonucleases, it can be ruled out that the H-strand is dsDNA. In contrast, RNAse H is able to cut DNA:RNA hybrids and removes the double stranded parts of the H-strand, revealing that the DNA is covered with RNA (Yang et al., 2002). Studies show that stabilizing RNA-fragments have a length of about 200-600 nt. However, the source of this RNA is not clarified. Most likely the RNA is derived from preformed and matured transcripts which are hybridized with the displaced strand, termed as the "bootlace model" (Yasukawa et al., 2006). Critics of RITOLS argue that the proteins involved in that hybridization process are not identified so far and that it is unclear how highly structured tRNA and rRNA can be melted to enable DNA binding (Holt et al., 2014).

The SDM prefers mtSSBP as the important molecule stabilizing the displaced H-strand during replication. Chromatin immunoprecipitation (ChIP) experiments show that mtSSBP cover the displaced strand and show exclusive affinity to the H-stand and nearly no binding at the L-strand. Furthermore, mtSSBP shows its strongest density near the O_H and is decreasing towards the O_L and another strong peak upstream of O_L. This fits to SDM since the areas in which mtDNA will be present as ssDNA for a longer period show higher levels of mtSSBP (Fuste et al., 2014).

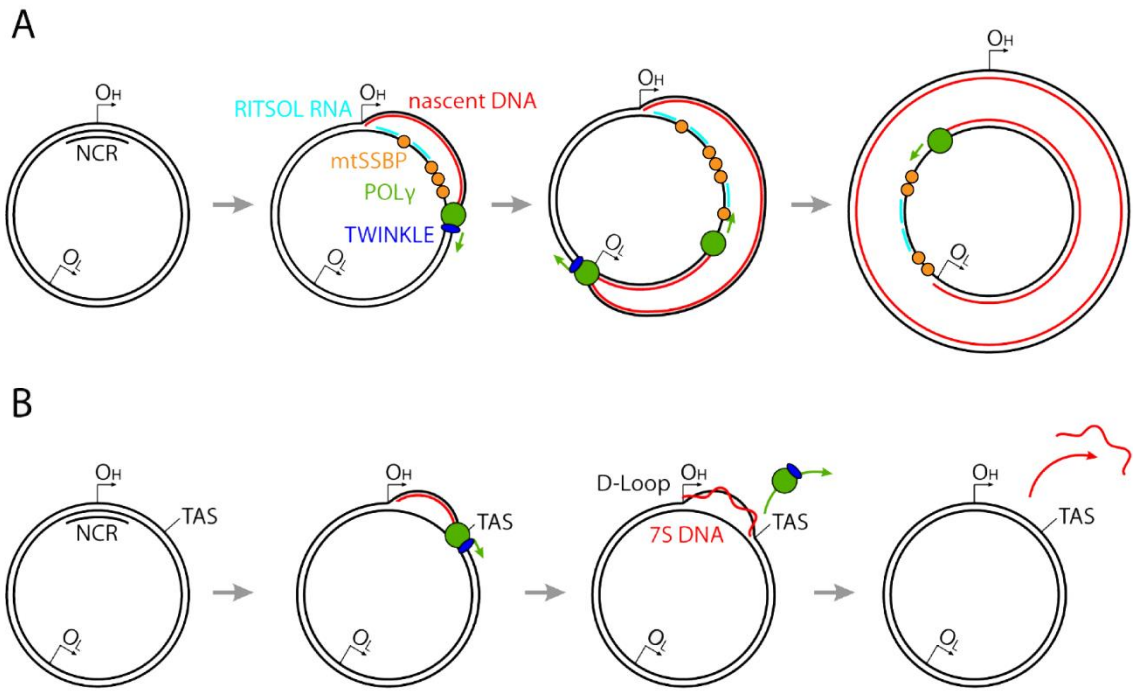

Figure 1.10 Replication of mtDNA: A) Principle of SDM and RITOLS: Replication of mtDNA is initiated at O_H within the NCR and the daughter H-strand is synthesized by the action of POLγ and TWINKLE. The parental H-strand is displaced, remains single stranded and is stabilized by either RNA (RITOLS, cyan) or mtSSBP (SDM, orange). When the replication machinery has synthesized two thirds of the new H-strand, O_L is exposed and L-strand synthesis is initiated. Since the parental H-strand is already single stranded, no TWINKLE is necessary. Both replication machineries continue till mtDNA is replicated. **B) D-loop formation:** Synthesis of the daughter H-strand can be terminated after 650 nt at the TAS region, resulting in the 7S DNA. The D-loop is formed as the 7S DNA remains at the mtDNA and the parental H-strand remains displaced. Depending on the organism and cell type the D-loop has a specific lifetime after which the 7S DNA dissociates from the mtDNA.

Studies favoring RITOLS and SDM show strong evidences that the displaced H-strand is in most cases covered with protein or RNA, but not undergoing replication of a classical lagging strand including the formation of Okazaki fragments. There is no consensus if mtDNA replication follows RITOLS or SDS, since there is strong evidence for RNA and

mtSSBP to cover the displaced lagging strand (Yasukawa et al., 2006; Fuste et al., 2014). It has been suggested that both RNA and mtSSBP are involved in this process. Studies show that at least 80% of the displaced DNA strand is covered with RNA and single stranded stretches are not longer than 100-200 nt. These gaps could be filled with mtSSBP (Pohjoismaki et al., 2010; Wanrooij and Falkenberg, 2010).

Some scientists claim that replication of mtDNA may not only have a single mechanism or even a single origin of replication, but different mechanisms initiated at different positions. An indication for that could be the presence of several mitochondrial DNA polymerases found in Trypanosomes which could be required for different replication mechanisms. Also in humans, a second polymerase was found to be active in mitochondria: PrimPol. Multiple polymerase would provide another degree of freedom to regulate mitochondrial replication and thereby there might not exist only one single mode of mtDNA replication (Klingbeil et al., 2002; Holt et al., 2012; Garcia-Gomez et al., 2013). However, all data suggest the majority if replication occurs with an displaced strand that is covered with RNAs and mtSSBP, as well (Yasukawa et al., 2006; Wanrooij and Falkenberg, 2010; Holt et al., 2012, Fuste et al., 2014)

1.4.4 Termination of replication

Like termination of transcription, the termination of replication is not well understood. When POLγ finished a complete round of replication and reached O_H respectively O_L, it starts to idle. It initiates cycles of polymerization and degradation at the nick. When POLγ loses its 3'-5'-exonuclease activity and thereby its possibility to idle at the nick, POLγ starts to continue synthesis of DNA into the dsDNA area, creating a 5'-flap which cannot be ligated (Macao et al., 2015). Ligation in mitochondria is mediated by DNA ligase III at O_H and O_L and its loss causes mtDNA deletion (Lakshmipathy et al., 1999). There is hardly any knowledge about the mechanism, the structure and the involved factors of mitochondrial termination. Like it is true for transcription, proteins of the MTERF-family seem to be involved in the termination of replication. Loss or overexpression of MTERF1 and MTERF3 leads to impaired termination (Hyvarinen et al., 2011). Although it is poorly understood how the termination of functional replication is realized, there is mounting evidence for premature termination of replication leading to the formation of a structure termed the D-loop.

1.4.5 The D-loop

In some cells up to 95% of all replication events are terminated prematurely in a region termed termination associated sequence (TAS), resulting in a 650nt product, termed the 7S DNA according to its properties in sedimentation experiments. The 7S DNA is able to be incorporated into the mtDNA, which leads to a triple stranded region from O_H to TAS (Fig 1.10 B). This triple stranded structure is then termed the displacement loop (D-loop), which covers not the complete NCR. Therefore NCR and D-loop region do not describe the same area (Robberson and Clayton, 1972; Doda et al., 1981; Nicholls et al., 2014). D-loops have a half-life of up to 1h in mouse cells and at a given time only a proportion of mtDNA molecules contain a D-loop structure, e.g. 14% in cultured human fibroblasts and 95% in Xenopus oocytes (Hallberg 1974, Bogenhagen and Clayton, 1978; Kornblum et al., 2013). Different proteins specifically binding to the TAS region and thereby possible candidates for mediating termination have been found. Nevertheless, the distinct protein(s) required for D-loop formation could not be identified so far (Madsen et al., 1993; Nicholls et al., 2014)

The mitochondrial D-loop was initially discovered in the early 1970s in EM images of mouse and chicken mtDNA (Arnberg et al., 1971; Kasamatsu et al., 1971; Robberson et al., 1972). However, until today, there is no consensus about D-loop function. Studies show that POLγ can use the 7S DNA as a template to initiate replication in vitro. Thereby, 7S DNA can function as a primer for DNA synthesis. Other studies speculate that the D-loop is essential for coordinated termination and its presence reduces collisions of replication forks from H- and L-strand synthesis (Nicholls et al., 2014). Formation of the D-loop leads to an opening of the NCR. This could increase the access of DNA binding proteins like components of the replication and transcription machinery to the control region resulting in more active mtDNA (Berk and Clayton 1974; Nicholls et al., 2014). A potential involvement of the D-loop in the association from mtDNA to the inner membrane and the segregation on mtDNA is also proposed (He et al., 2007; Holt et al., 2007). In a nutshell, hypotheses of D-loop function in replication initiation, replication termination, stimulation of transcription and replication in general as well as location or distribution of mtDNA are available. Nevertheless, none of these functions could be shown in vivo.

1.5 Links between transcription and replication and its regulation

Since altered transcription and replication of mtDNA are strongly involved in clinical expression of diseases, these processes have to be well regulated. However, the regulation of both processes is one of the largest gaps in the understanding of mitochondria (Taylor et al., 1997; Montoya et al., 2006). Furthermore, the regulation of mitochondrial replication and transcription is an integral part of the current study.

Transcription and replication have to respond in a dynamic fashion to changes of the environment. Regulation can occur on different levels. Since the initiation of replication requires a transcript from LSP (see 1.4.2.1), it is very likely that most regulatory mechanisms affecting initiation of transcription will also affect replication. Therefore many regulatory mechanisms should regulate the general activity of mtDNA. Mechanisms which affect predominately replication and not transcription occur at the level of the initiation of replication after primer-formation or at the level of premature termination of replication at the TAS region. Another possibility to regulate mtDNA activity is the premature termination at CSB II. Influencing this premature termination can either trigger transcription when termination at CSB II is blocked, or trigger replication if termination is favored (Gustafsson et al., 2016; Agaronyan et al., 2015). In the literature many hypotheses of how mtDNA function is regulated and which proteins are involved can be found. In this section the mostly discussed concepts for regulation are highlighted.

1.5.1 Regulation of mtDNA activity

MtDNA activity can be regulated through effector proteins at the level of transcription initiation. Three topoisomerases have been found in mitochondria: The mitochondrial topoisomerase 1 (TOP1MT), mitochondrial topoisomerase 3α (TOP3A) and mitochondrial topoisomerase 2β (TOP2b) (Zhang et al., 2001 Wang et al., 2002; Low et al., 2003). In contrast to nuclear topoisomerases like TOP1, TOP1MT is not essential for maintaining transcription. Instead, it has a direct negative effect on mtDNA transcription. MEFs lacking TOP1MT show an increased number of transcripts. The mechanism of how TOP1MT can perform a negative impact on transcription is not known, since topoisomerases stimulate transcription of the nucleus by removing positive supercoils. One possibility is that erasing supercoils could impair the function of TFAM in creating a U-turn during transcription initiation (Sobek et al., 2013). Since TOP1MT is strongly enriched in the TAS region downstream of the D-loop, its influence may occur due to stabilization of this regulatory element. This theory is supported by

the observation that D-loop structures vanish upon inhibition of TOP1MT. This connection between TOP1MT and the D-loop could also be interpreted as a connection between TOP1MT and replication. However, an influence of the topoisomerase on replication could not be observed so far (Zhang and Pommier, 2008). Since TOP1MT is upregulated in cellular stress response, it might be involved in stress adaption of mtDNA and OXPHOS (Goto et al., 2006).

TFAM itself is also a very interesting candidate to regulate transcription and replication. Studies in mice show that overexpression of TFAM leads to an increased mtDNA copy number; a reduction of TFAM causes loss of the majority of mtDNA, indicating that TFAM is important for mitochondrial replication and/or mtDNA maintenance (Ekstrand et al., 2004). In cell culture, overexpression of TFAM can induce transcription but not replication of mtDNA (Maniura-Weber et al., 2004). As described above, some models suggest a function of TFAM in repressing specific transcripts and promoting others (see. 1.3.2.2).

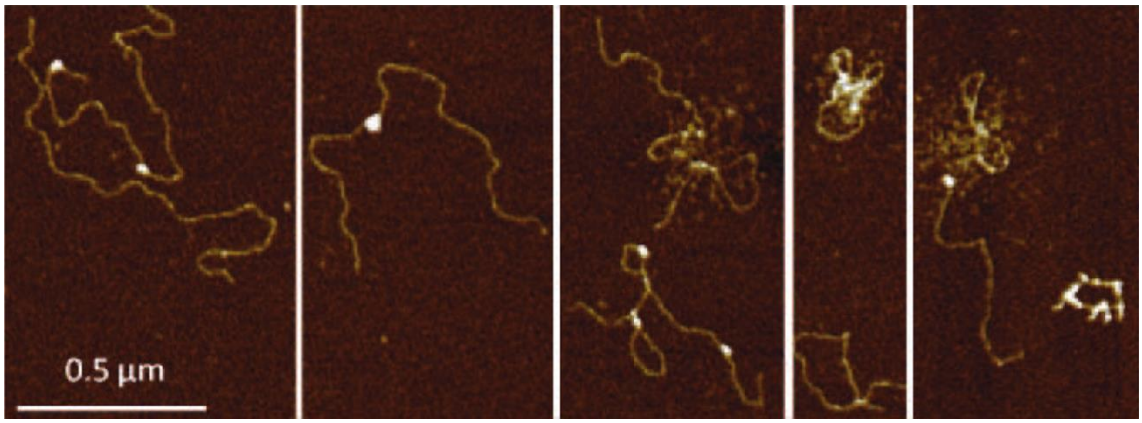

Figure 1.11 DNA compaction at a physiological TFAM level: A physiological TFAM level of one TFAM protein per 20 bp of DNA was added to naked DNA and then analyzed with atomic force microscopy. Different compaction levels can be observed (Modified after Farge et al., 2014).

TFAM's importance in regulating mtDNA activity becomes clear as studies show that the oncogene encoded protein c-Myc directly binds to the TFAM promotor and upregulation of c-Myc leads thereby to increased mitochondrial function and mtDNA content, which can be observed in many cancer patients. (Feng et al., 2005). Furthermore, studies based on atomic force microscopy show that under physiological levels of TFAM, DNA molecules show a high variation in their compaction level and that high TFAM levels inhibit melting of double stranded DNA (Fig. 1.11; Kaufman et al., 2007; Farge et al., 2014). It has been proposed that the compaction level could regulate if a nucleoid is

engaged in replication, transcription or both processes together (Gustafsson et al., 2016). In conclusion, there are a lot of reports indicating that the TFAM level stimulates the overall activity of mtDNA.

As mentioned above (section 1.4.3), the D-loop could also be involved in regulating the overall activity of nucleoids and its presence could stimulate transcription and replication due to the more open regulatory NCR. The proteins involved in D-loop formation and stabilization are therefore candidates for mtDNA regulation. Not only TOP1MT (see above), but also POLγB and TWINKLE are enriched at the TAS region. TWINKLE upregulation in this region can lead to increased replication using the 7S DNA as a primer (Jemt et al., 2015).

Transcription and replication could also be regulated by the ATP-level within the mitochondrial network. Since the priming nucleotide at LSP and HSP is an ATP, these promotors can sense the OXPHOS activity. Early studies show an ATP-dependent rate of transcription initiation at both promotors in vitro (Narasimhan et al., 1987; Amiott et al., 2006).

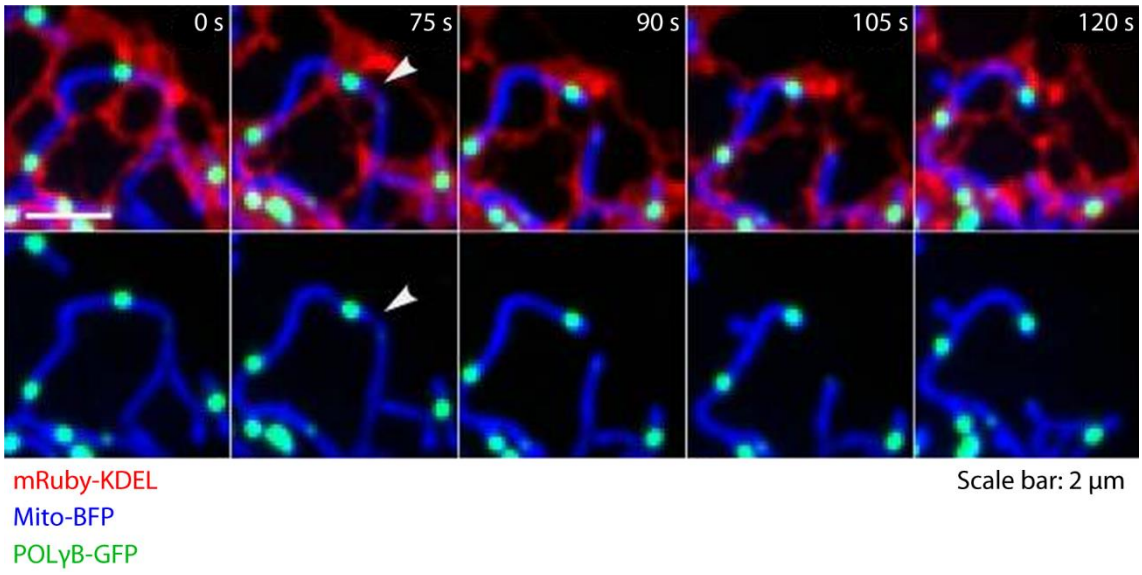

Figure 1.12 Mitochondrial replication is coupled with mitochondria-ER-contact sites and mitochondrial fission: U-2 OS cells expressing mRuby-KDEL (red) to label the endoplasmic reticulum and POLγB-GFP (green) to mark replicating mtDNAs. Additionally cells were incubated with Mito-BFP (blue) to label the mitochondria. Replicating mtDNAs colocalize with mitochondria-ER-contact sites and mark positions which will be involved in fission later (Modified after Lewis et al., 2014).

Also the position of mtDNA within the mitochondrial network could be important to regulate the behavior of mtDNA. The replication of mtDNA seems to be coupled on the

one hand with ER-mitochondria contact sites and on the other hand with fission of the mitochondrial network (Fig 1.14). This coupling of fission and mtDNA replication could be a mechanism of the cell to ensure equal distribution of mtDNA within the mitochondrial network. How far the ER-mitochondria contact sites and fission affect transcription has not been documented (Lewis et al., 2016).

1.5.2 Molecular switch between transcription and replication

Premature termination of transcription at CSB II is a very crucial process, since the decision whether mtDNA undergoes functional transcription or starts to initiate replication is made at this sequence (for CSB II termination see section 1.3.2.2). Mechanisms regulating CSB II termination would affect the ratio between transcription and replication and would thereby represent a powerful tool of the cell to adapt mtDNA function to its needs. Since the presence of TEFM prevents termination at CSB II, it is a promising candidate for a molecular switch between transcription and replication (Agaronyan et al., 2015).

A model of how TEFM can work as a molecular switch is based on its stabilizing effects on the elongation complex of POLRMT. In the presence of TEFM, transcription from HSP can proceed and create a near-genome length product. This is also true for LSP-products. TFAM prevents the formation of a G-quadruplex of the nascent RNA, avoiding premature termination. In the absence of TEFM, HSP will not produce near-genome length transcripts since the elongation complex shows low processivity of POLRMT. Without the presence of TEFM, LSP-transcripts are terminated at CSBII allowing primer formation for replication (section 1.4.2.1) (Agaronyan et al., 2015). Studies show that the loss of TEFM leads to a strong reduction of longer transcripts and an increased termination of transcription at CSB II in vitro. However, a negative influence of TEFM on replication as well as TEFM's importance in vivo are not mentioned (Agaronyan et al., 2015; Hillen et al., 2017(1)).

A second proposed molecular switch between replication and transcription is based on the concentration of POLRMT (Fig 1.13). Since POLRMT is required for transcription and formation of a replication primer, its knockout in mice leads to a huge reduction of transcripts and mtDNA copy number. However, a reduction of POLRMT causes a more versatile reaction of the cell. At low POLRMT levels the transcription initiation of LSP is better maintained since in vitro transcription assays show a much higher reduction of HSP-transcripts than of LSP-transcripts. Even in the complete absence of POLRMT in mice, Northern Blot analysis reveals the presence of LSP-transcript (Kühl et al., 2016).

In mice low POLRMT-levels cause an upregulation of TEFM and TWINKLE. The increased level of TEFM could compensate for the low POLRMT level to ensure functional transcription from LSP since heterozygous POLRMT knockouts to not show a reduced amount of transcripts. Neither the level of TFAM nor the level of TFB2M is affected upon POLRMT reduction. Hence, the different effect of POLRMT downregulation on both promotors is not caused by the level of transcription initiation. (Kühl et al., 2016).

The upregulation of TWINKLE could be a response to maintain the level of mtDNA replication. TWINKLE binds at the TAS and can reinitiate replication from D-loops 7S DNA (Jemt et al., 2015). Hence, less primer formation because of reduced LSP-transcription is compensated by more functional replication. The lack of D-Loops upon reduction of POLRMT in mice supports this theory (Kühl et al., 2016).

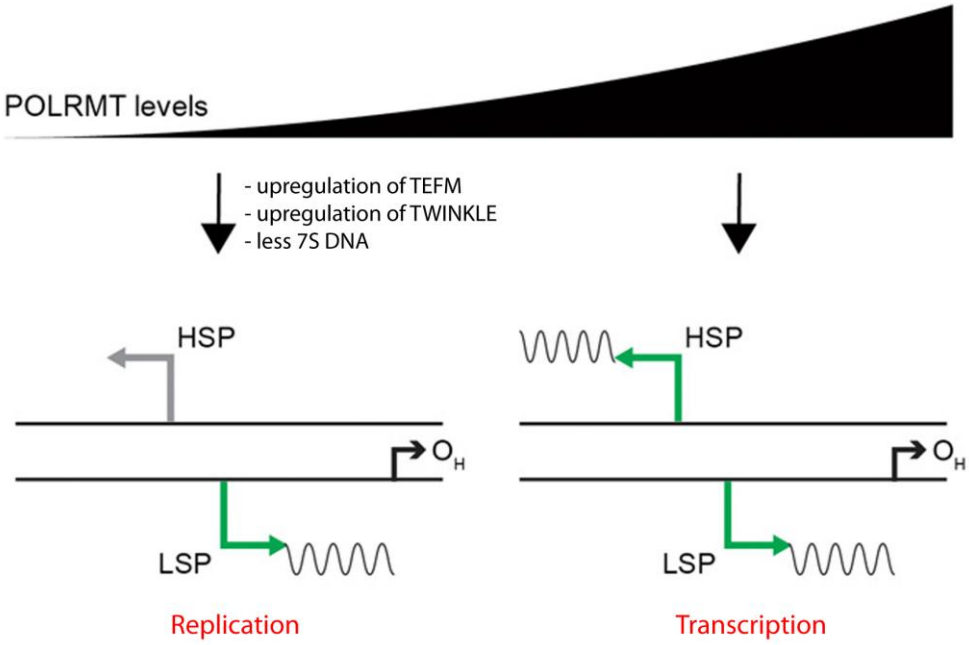

Figure 1.13 POLRMT level regulates transcription and replication in mitochondria: At low level of POLRMT HSP is totally inactive whereas transcription of LSP still occurs and ensures primer formation. Due to the upregulation of TEFM, functional transcription of LSP is maintained. Due to the upregulation of TWINKLE, replication is likely to be initiated using the 7SDNA as a primer as 7S DNA level are reduced. Hence, at lower POLRMT level mtDNA is triggered towards replication and at higher POLRMT level functional transcription is initiated at HSP and LSP (modified after Kühl et al., 2016).

In conclusion, at normal or high POLRMT level, transcription is initiated at HSP and LSP and functional gene expression from both strands occur. At low POLRMT level, transcription initiation is limited to LSP and no expression of heavy strand genes occur.

Upregulation of TEFM ensures functional LSP transcription whereas upregulation of TWINKLE ensures replication (Kühl et al., 2016).

1.6 Detection of transcription and replication via light microscopy

The investigation of transcription and replication in cells with light microscopy requires the labeling of these processes with florescent markers. In the literature different methods are described. In this section, some of these methods are highlighted.

One method to label mtDNA activity is the mitochondrial transcription and replication imaging protocol (mTRIP). mTRIP is a combination of DNA fluorescence in situ hybridization (FISH) and RNA FISH. In the first study describing this technique, 14 different fluorescent labeled DNA-probes were created with a length from about 700 to 1500 nt, complementary to the H- or L-strand of mtDNA (Chatre et al., 2013 (1)). mTRIP requires fixed cells, beyond that no further harsh treatment is necessary. It enables the investigation of the current amounts of mtDNA replication and transcription, but no analysis of the replication and transcription over longer periods. Sample analysis revealed that a subset of the probes specifically detects polycistronic RNA, whereas another subset recognizes the melted origin of replication. Therefore a pool of probes to detect transcription and another pool to detect replication was created. The study could detect three classes of mtDNAs: Replication and transcription positive, replication negative and transcription positive and totally inactive mtDNAs (Chatre et al., 201 (1); Chatre et al., 2013(2)). Although mTRIP appears to be very specific, there are only a limited number of publications available since it appears to be a quite challenging method.

The expression of fusion-proteins of components involved in replication and transcription is another way to investigate these processes. Since the essential components of the replication and transcription machinery of mitochondria (see 1.3.1 and 1.4.1) are identified, a wide selection of candidates for fusion proteins exists. A very prominent nucleoid protein to label is TFAM, since it is part of every nucleoid and thereby very applicable to mark the whole nucleoid population. The expression of fusion proteins is very suitable for live cell imaging and thereby for the analysis of nucleoid dynamics since no fixation is required. As it is true for mTRIP, no analysis of both processes over long periods is possible because one only observe current, ongoing activity. A disadvantage of this method is that overexpression of the nucleoid proteins can cause increased replication, altered replication and increased transcription (Maniura-Weber et al., 2004, Pohjoismäki et al., 2006; Ikeda et al., 2015; Kühl et al.,

2016). With the use of fusion-proteins, replication of mtDNA could be linked to the mitochondrial fission-machinery and ER-mitochondria contact sites. Furthermore a reduced mobility of replicating nucleoids could be observed, showing the possibility of analyzing nucleoid dynamics (Lewis et al., 2016).

Another method to visualize mtDNA activity is based on the integration of synthetic nucleoside analogues during replication and transcription. The most common nucleoside analogues are shown in Fig. 1.14. These molecules contain a nucleobase analogue and a sugar. The most famous ribonucleoside to mark transcription is 5'-Bromouridine (BrU). BrU is taken up by the cell and then converted to the nucleoisidetriphosphate BrUTP. After incorporation into nascent RNA instead of uridine, it can be detected with immunohistological stainings (Eidinof et al., 1959; Vanderlaan et al., 1985).

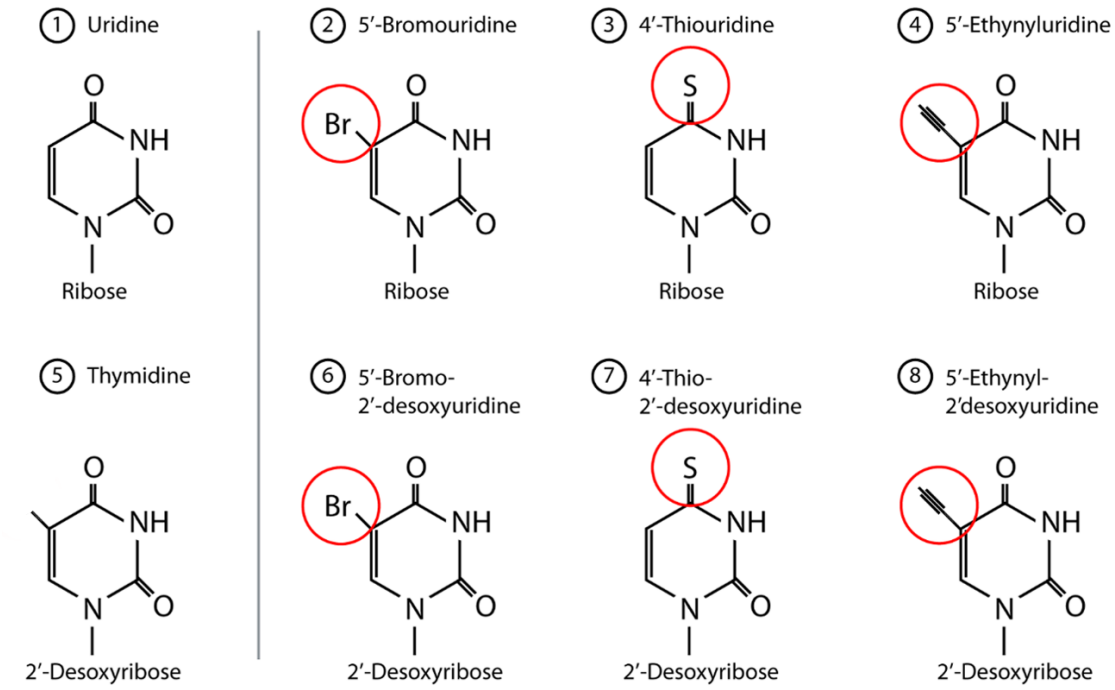

Figure 1.14 Synthetic nucleosides: 1) Uridine is part of the RNA and consists of the nucleobase Uracil and ß-D-Ribose. 2) 5'-Bromouridine is a Uridine with a Bromine at the 5'-C at its pyrimidine structure. 3) 4'-Thiouridine is a Uridine with a Sulfur at the 4'-C at its pyrimidine structure. 3) 5'-Ethynyluridine is a Uridine with an Ethynyl-group at the 5'-C at its pyrimidine structure. 5) Thymidine is part of the DNA contains of the nucleobase Thymine and ß-D-2'-Desoxyribose. 6) 5'-Bromo-2'-desoxyuridine is a Thymidine with a Bromine at the 5'-C at its pyrimidine structure. 7) 4'-Thio-2'-desoxyuridine is a Thymidine with a Sulfur at the 4'-C at its pyrimidine structure. 3) 5'-Ethynyl-2'-desoxyuridine is a Thymidine with an Ethynyl-group at the 5'-C at its pyrimidine structure.

Other less popular compounds to detect the transcription are 4'-thiouridine (4sU) and 5'-ethynyluridine (EU) (Hidenori et al., 2012; Fig 1.14). The most used detergent to detect replication is 5'-bromo-2'-desoxyuridine (BrdU). Similar to BrU, after uptake by the cell and decoration with phosphates, but is then incorporated into newly synthesized DNA instead of 5'-methyl-2'-desoxyuridine (thymidine). After incorporation, it can be detected via antibody staining. (Nowakowski et al., 1989; Gratzner 1982). Approximately a decade ago, 5'-ethyl-2'-desoxyuridine (EdU) was shown to be suitable to detect nascent DNA. EdU contains an alkene group and can be visualized by covalent addition of an azide-functionalized fluorophore in a copper catalyzed alkyne-azide cycloaddition (CuAAC) also termed "click-reaction" (Rostovtsev et al., 2002; Tornoe et al., 2002; Salic and Mitchison, 2008; Fig 1.14).

An advantage of synthetic nucleoside analogues is that you can apply longer incubation times and analyze how many mtDNA molecules were active during a chosen time period. The disadvantage is that some components have toxic side effects when concentrations are too high. Especially the toxicity of BrdU is well analyzed. High levels of BrdU lead to impaired replication of the nucleus (Taupin et al., 2007). Studies using synthetic nucleosides revealed that replication of mtDNA is randomly distributed throughout the mitochondrial network and is independent from the cell cycle. The half-time of newly synthesized RNA was shown to be about 45 min using BrU as a marker (Iborra et al., 2004).

1.7 Aims of the study

Mitochondrial DNA (mtDNA) is organized into distinct structures called nucleoids that are involved in transcription and replication. However, despite numerous studies on the two processes, the regulatory mechanisms that determine whether a nucleoid is engaged in transcription or replication or is alternatively inactive are poorly understood.

Investigation of these regulatory principles, though, requires an analysis of single nucleoids. This analysis is impeded by their small size of ~80 nm and their tendency to form clusters unresolvable by conventional confocal microscopy. Therefore, stimulated emission depletion (STED) nanoscopy will be used to analyze transcription and replication of single nucleoids.

Initially, the development of a robust and reliable approach for the visualization of both processes with STED nanoscopy must be established. This approach should function as a universal tool to analyze the proteins engaged in replication or transcription.

Consequently, it must also be independent from any protein involved in one of these processes.

With such a method, functional heterogeneity of nucleoids within single cells could then be visualized using multi-color STED nanoscopy. This would allow the fundamental question of whether all nucleoids within a single cell are equally active to be addressed.

Moreover, this method should also enable analysis of knockdown cell lines of the mitochondrial RNA polymerase POLRMT and the mitochondrial transcription elongation factor TEFM with STED nanoscopy to detect changes in the fraction of nucleoids engaged in transcription and replication. Such studies will offer important insights into the regulation of nucleoid activity.

2. Material and Methods

2.1 Materials

2.1.1 Antibodies

Antibodies were used for immunofluorescence (IF) and for Western Blot analysis (WB). Primary antibodies are listed in Tab. 2.1 and secondary antibodies are listed in Tab 2.2. The majority of the secondary antibodies were ordered unlabeled and decorated with fluorophores according to the protocol described in section 2.2.1.2. When an antibody was ordered unlabeled it is marked with an asterisk. The given manufacturer and catalogue number refers to the unlabeled antibody. Information about the fluorophores are listed in section 2.1.2.

Table 2.1 Primary antibodies

Target	Host	Method	Used Dilution	Manufacturer and catalogue number
αAlexa Fluor 488	rabbit	IF	1:200	Thermo Fisher Scientific (A-11094)
Aβ-Actin	mouse	WB	1:3000	Sigma-Aldrich (A5441)
αATP Synthase β	mouse	IF	1:400	Abcam (ab5432)
αBr(d)U	rat	WB	1:100	Abcam (ab6326) oder NovusBio (NB500-169)
αBrdU	mouse	IF	1:100	5-Bromo-2'-deoxy-uridine Labeling and Detection Kit II from Merck
αdsDNA	mouse	IF	1:2000	Abcam (ab27156)
αMic60	rabbit	IF	1:100	Proteintech (10179-1-AP)
αPOLR	rabbit	IF	1:100	Abcam (ab32988)
αPOLγ	rabbit	IF	1:100	Abcam (ab123875)
αTFAM	mouse	IF	1:100	Abnova (H00007019-B01)
αTFB2M	goat	IF	1:100	Abcam (ab118321)
αTEFM	rabbit	IF	1:100	Thermo Fisher Scientific (PA5-46121)
		WB	1:250	
αTWINKLE	rabbit	IF	1:100	Abcam (ab83329)

Table 2.2 Secondary antibodies

Target	Host	Attached marker	Method	Used Dilution	Manufacturer and catalogue number
mouse	goat	Abberior STAR RED*	IF	1:100	Dianova (515-005-062)
mouse	goat	Alexa Fluor 594	IF	1:100	Thermo Fisher Scientific (A11032)
mouse	sheep	Alexa Fluor 488*	IF	1:100	Dianova (515-005-003)
		Atto 490ls*	IF	1:100	
mouse	goat	Horseradish Peroxydase	WB	1:5000	Dianova (115-035-062)
rabbit	goat	Abberior STAR RED*	IF	1:100	Dianova (111-005-144)
rabbit	goat	Alexa Fluor 594	IF	1:100	Thermo Fisher Scientific (A11037)
rabbit	goat	Horseradish Peroxydase	WB	1:5000	Dianova (111-035-144)
goat	donkey	Atto647N*	IF	1:100	Dianova (705-005-147)
rat	goat	Alexa Fluor 594*	IF	1:100	Dianova (112-005-167)

2.1.2 Fluorophores

Fluorophores were ordered as an N-hydroxysuccinimide (NHS) ester to enable their covalent attachment to secondary antibodies. Values for absorption and emission are given for fluorophores with NHS-ester in aqueous solution. The used fluorophores were stored in the dark at -20°C before coupling to a secondary antibody. All used fluorophores are listed in Tab 2.3. The distinct values for the absorption and emission spectra can be found on the manufacturer's webpage.

Table 2.3 Fluorophores

Fluorophore	Absorption maximum	Emission maximum	Manufacturer and catalogue number
Abberior STAR RED	638 nm	655 nm	Abberior (1-0101-011-3)

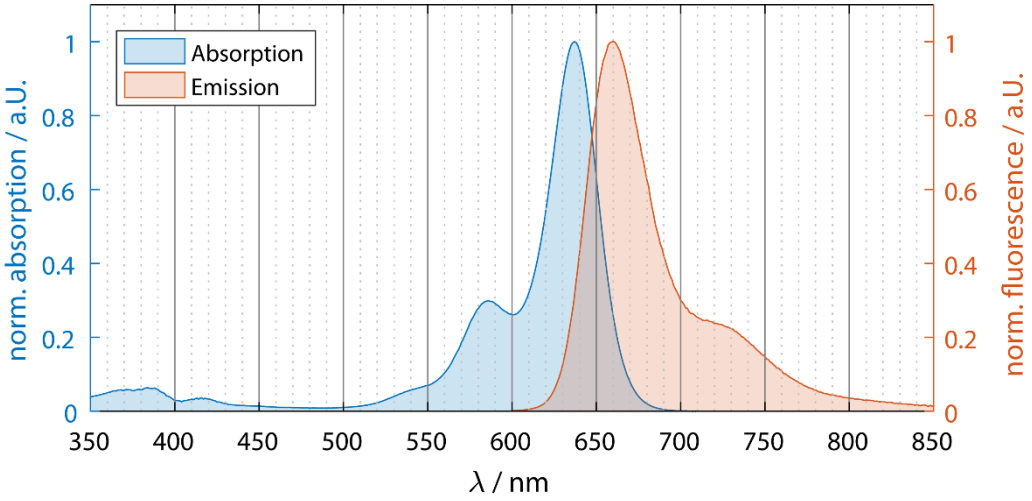

Figure 2.1 Absorption and Emission spectra of Abberior STAR RED

Alexa Fluor 488	494 nm	517 nm	Thermo Fisher Scientific (A20000)

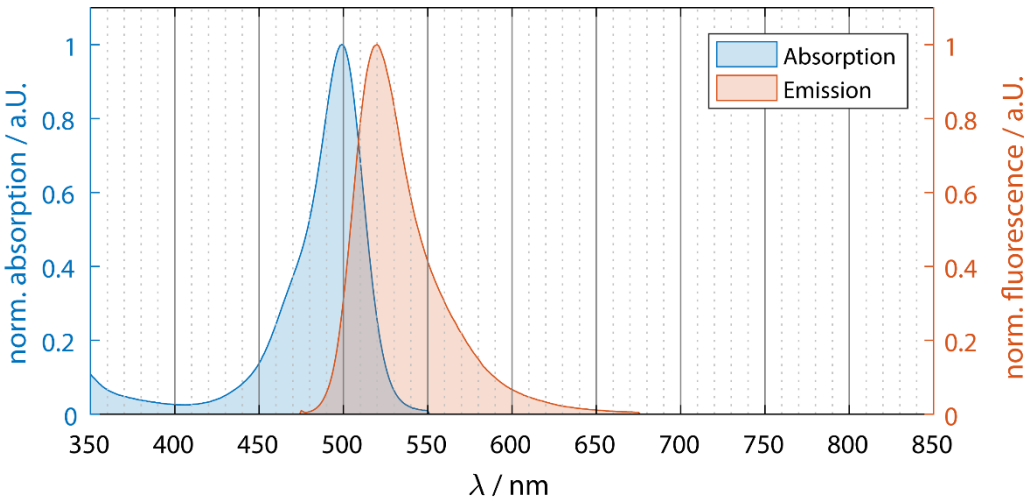

Figure 2.2 Absorption and emission spectra of Alexa Fluor 488

Alexa Fluor 594	590 nm	617 nm	Thermo Fisher Scientific (A20004)

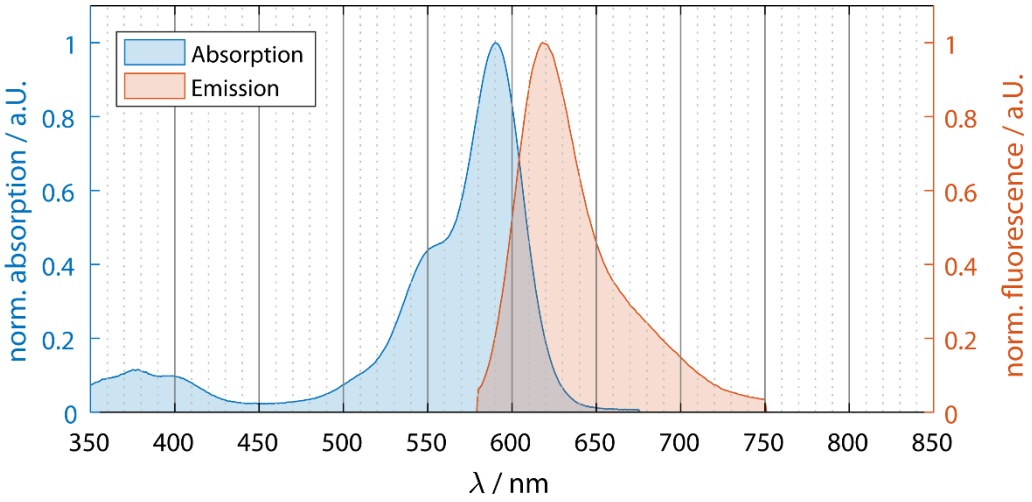

Figure 2.3 Absorption and emission spectra of Alexa Fluor 594

Atto 490ls	496 nm	661 nm	Atto-Tec (AD 490ls-35)

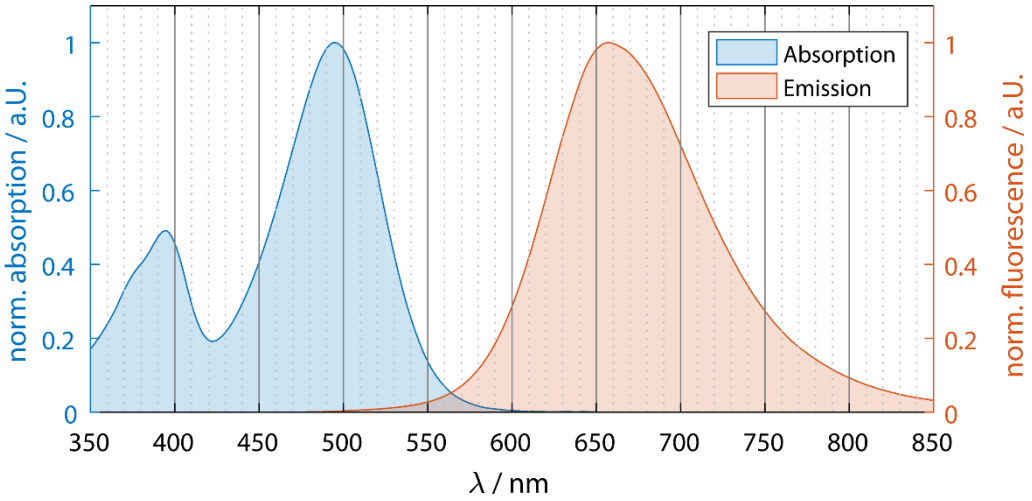

Figure 2.4 Absorption and emission spectra of Atto 490ls

Atto647N	646 nm	664 nm	Atto-Tec (AD 647N-35)

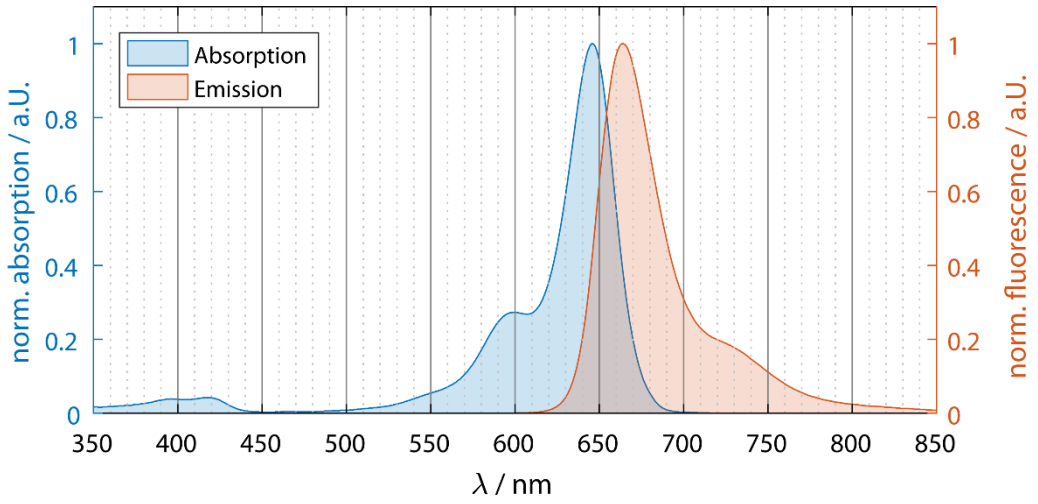

Figure 2.5 Absorption and emission spectra of Atto647N

2.1.3 Chemicals

Chemicals were sourced from the companies Sigma-Aldrich (Munich, Germany), Merck (Darmstadt, Germany), Carl Roth (Karlsruhe, Germany) or Applichem (Darmstadt, Germany).

2.1.4 Cell lines

The used human cell lines are listed in Tab 2.4.

Table 2.4 Cell lines

Cells line	**Tissue**	**Manufacturer and catalogue number**
Primal Dermal Fibroblast; Normal, Adult (HDFa)	skin	ATTC (PCS-201-012)
U-2 Osteosarcoma (U-2 OS)	bone	ECACC (92022711)

2.1.5 siRNA Pools

All siRNA pools used in this study are composed by siTOOLS BIOTECH GmbH (Planegg / Martinsried, Germany) and are listed in Tab 2.5.

Table 2.5 siRNA Pools

Target gene	Order details
Mitochondrial Transcription Elongation Factor (TEFM)	siPool targeting human TEFM, NCBI Gene ID 7019, 5 nmol siPool
Mitochondrial RNA Polymerase (POLRMT)	siPool targeting human POLRMT, NCBI Gene ID 7019, 5 nmol siPool
Control siPool	Unspecific siPool, 5 nmol siPool

siRNAs and RNA interference:

Small interfering RNAs (siRNAs) are small double stranded RNA-molecules with a size of 20-25 base pairs and were first observed during transgene- and virus-induced silencing in plants (Mello and Conte, 2004). SiRNAs interfere with the expression of specific target genes and can thereby be used for their temporary gene silencing.

Once siRNAs enter the cell they are recognized by proteins of the RNA-induced silencing complex (RISC) forming the pre-RISC. The RISC is important for melting of the double stranded RNA resulting in a matured RISC containing only one single stranded RNA molecule. The single stranded RNA guides the RISC complex to the target RNA forming the siRNA-mRNA-duplex. Afterwards the mRNA is cleaved by proteins of the Argonaute family which are part of RISC. This cleavage causes degradation of the mRNA and thereby a silencing of the targeted gene. Usually, a siRNA is designed to target RISC to a specific mRNA and causing gene silencing of the gene of interest (Carthew and Sontheimer, 2009).

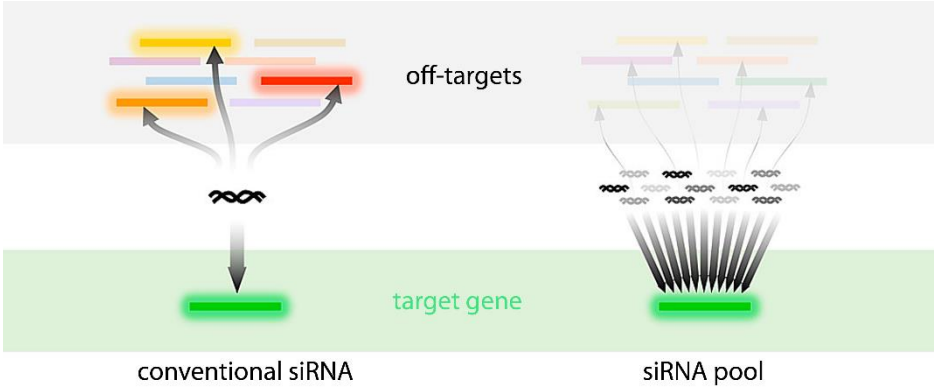

Figure 2.6 RNAi with siPools: SiPools consist of up to 30 different siRNAs targeting the same gene with minimal off-target effects (Modified - siTOOLS BIOTECH webpage).

siRNA Pools:

siPools from siTOOLS BIOTECH GmbH consist of 30 different siRNAs which target the same mRNA and ensure a high on-target effect. However, each siRNA within the pool is only present in a very low concentration to reduce potential off-target effects (Fig. 2.6; Hannus et al., 2014).

2.2 Methods

2.2.1 Imaging techniques

2.2.1.1 Indirect immunostainings

The protocol for EdU and BrdU samples are different and are listed in section 2.2.1.4 respective 2.2.1.5. The protocol for the normal indirect immunostaining is shown in Tab 2.6. Phosphate-buffered saline (PBS) was used during indirect immunostainings to perform washing steps. PBS was prepared as a 20-fold stock solution according to Tab. 2.7. The pH-value was adjusted to 7.4 with 1M Hydrochloric acid (HCl).

Table 2.6 Protocol for indirect immunostaining

Fixation	Cells were fixed with 4% formaldehyde (w/v) in PBS (see section 2.1.6) for 5 minutes at room temperature.
Washing	After fixation cells were washed three times with PBS.
Permeabilization	Cells were permeabilized with 0.5% Triton-X-100 (v/v) in PBS for 5 minutes at room temperature.
Washing	After permeabilization cells were washed three times for 2 minutes with.
Blocking	Cells were blocked with 5% BSA (w/v) in PBS for 5 minutes at room temperature.
Primary antibodies	Primary antibodies (see section 2.1.1) were diluted in 5% BSA (w/v) in PBS. Cells were incubated with the antibody solution in a wet chamber for 1 hour at room temperature.
Washing	After antibody binding cells were washed three times for 2 minutes with PBS.
Secondary antibodies	Secondary antibodies (see section 2.1.1) were spun down to remove aggregated antibodies and then diluted in 5% BSA (w/v) in PBS. Cells were incubated with the antibody solution in a wet

	chamber for 1 hour at room temperature. Secondary antibodies were labeled with fluorophores.
Washing	After antibody binding cells were washed three times for 5 minutes with PBS.
Embedding	Samples were embedded in Moviol with DABCO.

Table 2.7 Recipe for 20x PBS stock solution

Chemical	**20x PBS stock solution**	**Concentration in 1x PBS**
Na_2HPO_4	35.6 g	10 mM
KH_2PO_4	4.8 g	1.76 mM
KCl	3.95 g	2.68 mM
NaCl	160.1 g	137 mM
ddH_2O	Add to 1L	

2.2.1.2 Labeling of secondary antibodies with fluorescence dyes

The majority of the used secondary antibodies from section 2.1.1 are not commercially available. Therefore, antibodies had to be decorated with fluorescent dyes using the following protocol:

The dyes were coupled to the antibodies through their NHS-group. Prior to coupling the dye was dissolved in Dimethylformamide (DMF) to a final concentration of 10 mg/ml. The antibody-solution was free of Bovine Serum Albumine and contained a total amount of 1-2 mg of antibody with a concentration of about 1 mg/ml. 1M $NaHCO_3$ (10% of the total volume) was added prior the coupling to provide a pH value between 8.0 and 8.5. After preparation of both solutions the dye was added slowly to the stirred antibody-solution. The mixture was then stirred gently for 2 hours at room temperature. The reaction was stopped by adding 20 µl of 1.5 M NH_2OH (pH =8.0-8.5).

Purification of the labeled antibodies was done by size exclusion chromatography with a PD10 Sephadex G25 column. The column was equilibrated with 30 ml PBS (pH 6.0-6.5). The antibody-solution was transferred into the column and eluted with PBS (pH 8.0-8.5). Fractions of 0.5 ml of the antibody-solution were collected (Fig. 2.7). The uncolored fractions were discarded and the colored fractions were analyzed with the BioRad Protein-Assay from BioRad (Hercules, USA) according to the manufacturer's specifications to determine the concentration of the antibody.

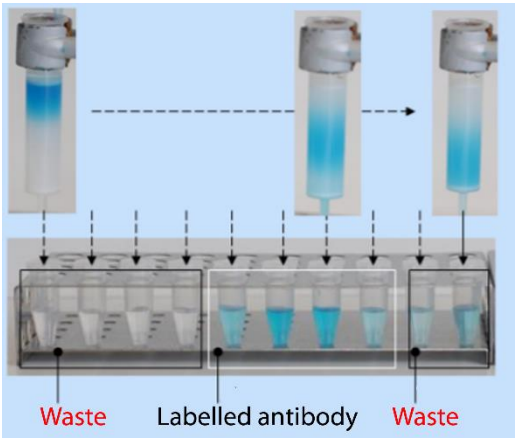

Figure 2.7 Collected fractions after elution of the antibody solution from the PD10 Sephadex G25 column: Only the most colored fractions were analyzed to determine the antibody concentration. (Modified - Abberior GmbH webpage).

2.2.1.3 Copper catalyzed alkyne-azide cycloaddition (CuAAC)

The copper catalyzed alkyne-azide cycloaddition (CuAAC) also termed "click-reaction" was essential to label incorporated EdU and thereby to label mtDNA replication. The principle of the click reaction is shown in Fig. 2.8. The protocol and the used components are based on the Click-iT EdU Alexa Fluor 488 Imaging Kit from Thermo Fisher Scientific (Massachusetts, USA). Only minor changes of the composition of the click cocktail were introduced (Tab 2.8). All components were dissolved in distilled water instead of Dimethylsulfoxid (DMSO).

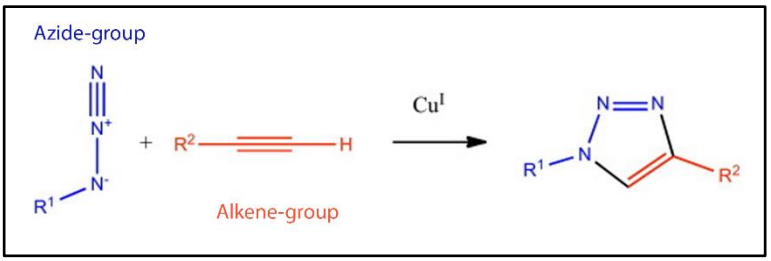

Figure 2.8 Principle of the copper catalyzed alkyne-azide cycloaddition (CuAAC) (Modified - Liang and Astruc, 2011)

Table 2.8 Click cocktail

1x Click iT reaction buffer (from kit)	322 µl
$CuSO_4$ (100mM freshly diluted from a self-made and sterile filtered 1M $CuSO_4$ solution in ddH_2O)	15 µL
Alexa 488 azide (from kit)	0.9 µl
Reaction buffer additive (from kit)	37 µl

The click cocktail was prepaid freshly for each experiment. Samples were incubated with the click cocktail under smooth swiveling for exactly 30 minutes. As solid material forms within the click cocktail during the incubation time the solution has to be removed quickly to avoid that the solid material covers the sample. After removal of the click cocktail the samples were intensively washed with PBS (see section 2.1.6) 10 to 15 times. Samples were always processed immediately.

2.2.1.4 EdU-labeling

EdU-labeling was performed to label newly synthesized DNA. Cells were fed with 20 µM 5'Ethynyl-2'-desoxyuridine (EdU) which is part of the Click-iT EdU Alexa Fluor 488 Imaging Kit from Thermo Fisher Scientific (Massachusetts, USA) (see section 2.2.1.1). Cells were threated in a six-well plate and were covered with 1.5 ml of DMEM (see section 2.2.4.1) prior EdU incubation. To start the EdU-incubation 1.5 ml of DMEM with 40 µM EdU were added to reach the final concentration of 20 µM. The EdU-DMEM-solution was freshly prepared prior to each experiment.

EdU labeling without signal enhancement by indirect immunofluorescence:

After EdU incubation cells were briefly washed with warm DMEM and then fixed, permeabilized and blocked according to the indirect immunostaining protocol (see section 2.2.1.1). Afterwards a click reaction was performed according to the protocol explained in section 2.2.1.3. If further structures had to be stained with antibodies, samples were blocked again with 5% BSA in PBS (see section 2.1.6) for 5 minutes and the indirect immunostaining protocol was carried on.

EdU labeling with signal enhancement by indirect immunofluorescence:

To enhance the signal, EdU labeled DNA was decorated with fluorophores via a click reaction and the signal was afterwards additionally amplified with Antibodies against

Alexa Fluor 488. Samples were processed like previously described in the protocol for "*EdU labeling without signal enhancement by indirect immunofluorescence"*. Afterwards, the attached Alexa 488 was decorated with an antibody against Alexa 488 and a suitable secondary antibody. Antibody staining was performed like previously described in section 2.2.1.

2.2.1.5 BrdU-labeling

BrdU-labeling was used to mark newly synthesized DNA. Labeling was performed based on the protocol of the 5-Bromo-2'-deoxy-uridine Labeling and Detection Kit II from Merck (Massachusetts, USA). Cells were incubated with 20 µM BrdU. Cells were threated in a six-well plate and were covered with 1.5 ml of DMEM prior BrdU incubation. To start the BrdU-incubation 1.5 ml of DMEM with 40 µM BrdU were added to reach a final concentration of 20 µM. The BrdU-DMEM-solution was freshly prepared prior to each experiment. Cells were incubated at 37°C and 5% CO_2.

BrdU labeling without additional staining of DNA:

After incubation with BrdU cells were briefly washed with warm DMEM and then fixed with an ice-cold 70% (v/v) EtOH (15mM Glycine, pH 2.0) for 20 minutes at -20°C. After intense washing with PBS (see section 2.1.6), samples were briefly washed with 0.5% Triton-X-100 in PBS (v/v) and then blocked with 5% BSA in PBS for 5 minutes. One color BrdU stainings were performed according the manufacturer's specifications with only one exception. After incubation with the αBrdU-working solution for 30 minutes at 37°C, cells were covered with αBrdU in 5% BSA for additional 30 minutes at room temperature to enhance the BrdU signal. When further structures were stained with antibodies, primary antibodies were added in both BrdU steps. Staining was continued according to the protocol for indirect immunostainings (see section 2.2.1).

BrdU labeling with additional staining of DNA:

When BrdU and DNA were stained together a modified BrdU-labeling protocol was used. After incubation with BrdU cells were briefly washed with warm DMEM and then fixed with an ice-cold 70% EtOH-solution pH 2.0 containing 15mM Glycine for only 10 minutes at -20°C. Afterwards cells were additionally fixed with 4% formaldehyde in 1xPBS (w/v) for 10 minutes at room temperature. Samples were then intensively washed with 1xPBS and permeabilized with 0.5% Triton-X-100 in 1xPBS (v/v) for 5 minutes at room temperature. The BrdU staining was performed according the manufacturer's specifications with the mentioned exception. After incubation with the αBrdU-working

solution for 30 minutes at 37°C, cells were additionally covered with αBrdU in 5% BSA in 1x PBS for 30 minutes at room temperature.

Since αBrdU and αdsDNA antibodies were both produced in the mice, a special staining protocol to enable the usage if two primary antibodies from the same host species was used. BrdU staining was first finished according to the protocol for indirect immunostainings (see section 2.2.1). Afterwards, samples were not embedded in Moviol, but processed like described in Tab. 2.9.

Table 2.9 Protocol for indirect immunostaining with primary antibodies from the same host species.

Samples were incubated with the first set of primary and secondary antibodies according to the protocol for indirect immunostaining (see section 2.2.1). In case of the BrdU-DNA double staining cells were already decorated with αBrdU antibody from mouse and a suitable secondary αmouse antibody.	
Washing	After antibody binding cells were washed three times with PBS for 5 minutes per washing step.
Blocking of the free binding sites of the first secondary antibody	Incubation with an unspecific "blocking-antibody" which is recognized by the first secondary antibody diluted in 5% BSA in PBS for 1h at room temperature. In case of the BrdU-DNA double staining an unspecific antibody produced in mice was used.
Blocking of the free binding sites of the first primary antibody and the previously used "blocking-antibody"	Incubation with an unlabeled Fab-fragment recognizing the first primary antibody and the "blocking-antibody". For the BrdU-DNA double staining a αmouse Fab-fragment was used.
Washing	After antibody binding cells were washed three times with PBS for 5 minutes per washing step.
Post-fixation	Samples were fixed with 4% formaldehyde (w/v) in PBS for 15 minutes at 37°C.
Washing	After post-fixation cells were washed three times with PBS.
Washing with detergent	Cells were washed with 0.5% Triton-X-100 in PBS for 5 minutes at room temperature.
Washing	Cells were washed three times with PBS for 2 minutes per washing step.

Blocking	Cells were blocked with 5% BSA in PBS for 5 minutes at room temperature.
Second round of primary and secondary antibodies.	Second set of antibodies were used according to the protocol of indirect immunostainings (see section 2.2.1) In case of the BrdU-DNA double staining cells were decorated with αdsDNA antibody and a suitable αmouse antibody.

2.2.1.6 BrU-labeling

BrU-labeling was used to mark newly synthesized RNA during transcription. Prior each experiment a 250 mM BrU solution was freshly prepared by dissolving BrU in distilled water. This BrU solution was added directly to the cultured cells to reach a final concentration of 20 µM BrU (HDFA) or 5 µM (U-2 OS). After BrU incubation for 25 minutes cells were briefly washed with warm DMEM and afterwards processed according to the protocol for indirect immunostainings (see section 2.2.1).

2.2.1.7 PicoGreen-labeling

PicoGreen can be used to label mtDNA. Cells were fixed either with 4% formaldehyde or with ice-cold MeOH. Afterwards cells were incubated in 0.1% Tween in PBS with 10 µg/ml RNAse A (Sigma-Aldrich; Munich, Germany) for 2 h at 37°C. After a short washing step with PBS, cells were incubated with 1:50 PicoGreen (Quant-iT PicoGreen dsDNA Reagent from Molecular Probes; Oregon, USA) in PBS for 30 min at room temperature. After a short washing step, the samples were embedded in Moviol with DABCO.

2.2.1.8 Confocal microscopy

For confocal microscopy the TSC Leica SP8 from Leica (Wetzlar, Germany) was used. The used excitation lasers had the wavelength of 488 nm, 561 nm and 633 nm. Photomultiplier tubes (PMTs) were used to detect the signal. The detection windows were freely adjustable. Images were taken with a HC PLAPO CS2 63x/1.40 oil objective. The scanning speed was 200 Hz and the pinhole had a size of one Airy Unit (AU). The used pixel size was 50-70 nm.

2.2.1.9 STED microscopy

STED microscopy

For high resolution STED microscopy a 2c 775 QUAD scanning nanoscope from Abberior Instruments (Goettingen, Germany) was used. The used laser and the dyes which were excited are listed in Tab 2.10. The built-in detection channels and the corresponding dyes which were detected are listed in Tab 2.11. The used objective was an UPlanSApo 100x/1.40 Oil [infinity]/0,17 / FN26.5 objective from Olympus (Tokio, Japan).

Table 2.10 Laser of the STED microscope

Wavelength	Excited Dyes	Laser and manufacturer
485 nm	Atto 490ls, PicoGreen	LDH-D-C-485 (PicoQuant, Berlin, Germany)
594 nm	Alexa Fluor 594	(Abberior Instruments, Goettingen, Germany)
640 nm	Abberior StarRed	LDH-D-C-640 (PicoQuant, Berlin, Germany)
775 nm	for STED	Katana-08 HP (Onefive GmbH, Regensdorf, Swiss Confederation)
595 nm	for STED (only of PicoGreen /different STED-Setup	Katana-06 HP (Onefive GmbH, Regensdorf, Swiss Confederation)

Table 2.11 Detection channels of the STED microscope

Detection channels	Detection window	Detected Dyes
GFP	525/50	PicoGreen
Cy3	615/20	Alexa594, Atto 490ls
Cy5	685/70	Abberior StarRed, Atto 490ls

For single and two-color imaging Abberior StarRed and/or Alexa Fluor 594 were used. A pixel size of 15 nm and a dwell time of 40 nm per pixel with a line accumulation of two was applied. For three color imaging Abberior StarRed, Alexa Fluor 594 and Atto 490ls were used. The pixel size was then increased to 20 nm whereas dwell time and line accumulation remained the same. The used pinhole size was 0.9 Airy Units (AUs).

2.2.2 Evaluation of the images

Postprocessing of the STED images were based on the usage of consecutive working MATLAB (Mathworks, Massachusetts, USA) analysis scripts.

2.2.2.1 Subtraction of the spectral crosstalk

The spectral crosstalk was determined for each sample with one color measurements using the same parameters as in the multicolor measurements.

The nucleus was automatically detected (see 2.2.2.2) and subtracted from each image in the one color control images. Afterwards single mtDNA, BrU and EdU spots were detected choosing a threshold manually (the principle is described in 2.2.2.4). The spectral distribution of each dye was computed as distribution of the signal in the spots on the different data channels. The average spectral distribution n for the three color STED images is shown in Tab 2.12. About 95% of the fluorescence signal remains in the respective channel whereas about 5% of the signal can be detected as bleed through in the remaining detection channels. These data were used for the linear unmixing of the multicolor STED images (see 2.2.2.3) before the spot detection.

Table 2.12 Distribution of the fluorescence in the three color STED images:

Labeled structure	Dye	Detection channel	Detected in DNA channel	Detected in BrU channel	Detected in EdU channel
DNA	Atto 490ls	Cy3 and Cy5	96.2%	2.9%	1%
BrU	Alexa Fluor 594	Cy3	2.1%	96.9%	1.1%
EdU	Abberor StarRed	Cy5	3.1%	2.2%	94.7%

2.2.2.2 Detection and subtraction of the nucleus

The nucleus was subtracted in each image as only the signal of the mitochondrial nucleoids was of interest. Nuclei were detected in confocal images (experiments in section 3.4) or directly in the STED images (experiments in section 3.5).

To subtract the nucleus, a binary mask of this structure had to be created. First, the image was smoothed with a 2D Gaussian with a width of 0.6 µm. Afterwards the image was binarized with a relative threshold of 0.2. Connected areas were identified and the holes within these segments were filled. All segments that were smaller than 14 pixel were discarded as they represented the nucleoids. Finally the still existing areas, representing the nucleus /nuclei, were enlarged by 0.2 µm in all directions to ensure a covering of the complete nucleus. If the detected area was not covering the edges of

the nucleus, the detected area was enlarged by 0.5 instead of 0.2 µm. All of the resulting nucleus masks were inspected visually and in some cases (<10% of all cases) the parameters (threshold, smoothing width) were adapted to better cover the nucleus.

2.2.2.3 Linear unmixing of the smoothed data before spot detection

All available channels in the multicolor STED images were smoothed with a 2D Gaussian of 0.1 µm width to remove the noise. A linear equation system was solved pixel wise to unmix the contributions of all channels given the spectral distribution matrix estimated from single dye measurements of the similar day (see 1.2.2.3). Negative values were set to zero.

2.2.2.4 Detection of mtDNA, BrU and EdU spots

After subtraction of the nucleus (see 1.2.2.2) and unmixing (see 1.2.2.3) the background in each channel was subtracted. The background was estimated by smoothing the linear, unmixed data with a 2D Gaussian of 0.6 µm width. A background corrected image was produced by subtracting 75% of the estimated background from the linear unmixed data and setting negative values to zero. All local maxima above a certain threshold are taken as spot centers. The threshold was manually chosen and afterwards a model function was fitted to each spot.

2.2.2.5 Fitting of the detected spots and estimation of spot width

The result of the manual thresholding was a list of spot positions with pixel accuracy. To get sub-pixel accuracy and to estimate the width of the spots, a 2D Gaussian, symmetrical peak function with a locally constant background was fitted to each spot on small cutouts of 0.4 x 0.4 µm from the original data of the respective channel. The fit was performed as a “least square”. Furthermore a “minimization no provision” for the influence of nearby other spots was done. However, nearby other spot potentially did bias the results, for example leading to overestimated widths.

2.2.2.6 Colocalization analysis of mtDNA, BrU and EdU spots

A colocalization analysis of the signals in the two or three color STED images was performed by assigning BrU or EdU spots to mtDNA spots. The positions of the BrU, EdU or mtDNA spots were taken from the fits (see 2.2.2.5). BrU and EdU spots were

separately colocalized to the mtDNA spots. Those who were assigned to the same mtDNA spots were regarded as triple BrU-EdU-DNA colocalization events.

To determine if a BrU or EdU spot colocalizes with a mtDNA signal, the Euclidian distances of all BrU and EdU spots to all mtDNA spots were computed to find pairs with smallest distance. If distance is smaller than threshold (0.1 µm for EdU, 0.2 µm for BrU; see Fig 3.10) the respective pair was counted as a colocalization. If multiple BrU or multiple EdU spots colocalized with the same mtDNA only the pair with the shortest distance was counted as a colocalization. Non-colocalized BrU or EdU spots were disregarded in any further processing. In contrast, non-colocalized mzDNA spots were regarded as single mtDNA spots. For further processing, like the determination of the distance to the nucleus, the positions of the assigned mtDNA spot were used.

2.2.2.7 Calculation of the distance between nucleoids and the nucleus

The distance of single nucleoid to the nucleus was defined as the shortest distance to the edge of the nucleus. The positions of all DNA spots was taken and the distance of them to the nucleus was computed as the smallest distance to any pixel of the nucleus along the edge of the nucleus.

2.2.2.8 Determination of the area covered by mitochondria

The determination of the area covered by the mitochondria within cells important to calculate a value representing the density of nucleoids (Fig 3.18) and worked similar to the detection of mtDNA, EdU and BrU spots (see 2.2.2.4). The mitochondrial network was labeled with antibodies against Mic60 and confocal images were analyzed. The nucleus was subtracted like described in 2.2.2.2. The remaining Mic60 signal was taken and smoothed with a 2D Gaussian of 0.3 µm width. Background was subtracted and the image was binarized by manually choosing a threshold.

2.2.3 Methods of protein biochemistry

2.2.3.1 Isolation of proteins from total cells

Cells were washed with warm PBS (see section 2.1.6) three times to remove the culture medium. Afterwards cells were covered with lysis buffer (Tab 2.13) for 30 min at 4°C. If cell debris had to be removed they were spun down for 10 minutes with 13000 x g at RT.

Table 2.13 Lysis buffer

Chemical	Concentration
Tris-Base pH 6.8	50 mM
$MgCl_2$	4 mM
Dithiothreitol (DTT)	0.1 mM
Sodiumdodecylsulfat (SDS)	1% (w/v)
Benzonase Endouclease 10 U/µl (Merck, Darmstadt, Germany)	0.1% (v/v) freshly added before use

2.2.3.2 Determination of the protein concentration

Protein concentration was determined with the Pierce BCA Protein Assay Kit from Thermo Fisher Scientific (Massachusetts, USA) according the manufacturer's specifications.

2.2.3.3 SDS Polyacrylamide Gel Electrophoresis

SDS Polyacrylamide Gel Electrophoresis was performed to separate proteins according their molecular size. The used buffer were prepared like it is described in Laemmli et al. 1970. After separation proteins were transferred to a nitrocellulose membrane by a Western Blot (see section 2.2.3.4)

Samples were heated in Laemmli sample buffer (Tab 2.13) for 5 to 10 minutes at 95°C and then loaded into Mini-PROTEAN TGX Precast Gels from Bio-Rad (Hercules, USA) with 12% acrylamide. As a standard the Page Ruler Prestained Protein Ladder from Thermo Fisher Scientific (Massachusetts, USA) was used. Gel electrophoresis was performed in the Mini-PROTEAN Tetra Cell System from Bio-Rad with Laemmli running buffer (Tab 2.15) to close the electric circuit. For separation a constant voltage of 80 V was applied.

Table 2.14 Laemmli sample buffer

Tris-Base pH 6.8	100 mM
DTT	200 mM
SDS	4% (w/v)
Brome phenol blue	0.02% (w/v)
Glycerin	20% Glycerine (w/v)

Table 2.15 Laemmli running buffer

Tris-Base pH 6.8	25 mM
SDS	0,1% (w/v)
Glycine	192 mM

2.2.3.4 Western Blot

After proteins were separated by SDS page they were transferred to a Hybond ECL nitrocellulose membranes from GE Heathcare (Little Chalfont, England). For transfer the polyacrylamide gel was directly placed on the nitrocellulose membrane. Membrane and gel were covered with three filter paper and one small sponge on each side and placed in a tank blot (Fig. 2.10). As the SDS-protein complexes has a negative charge the protein transfer is mediated by an electric field. The anode is attached on the side of the nitrocellulose membrane and the cathode is attached on the side of the polyacrylamide gel (Fig. 2.4). Negative charges like the SDS-protein complexes are then transferred from gel to the membrane. The tank was filled with transfer buffer (Tab 2.16) and a current of either 160 mA (overnight) or 250 mA (for 3 h on 4°C) was applied per membrane.

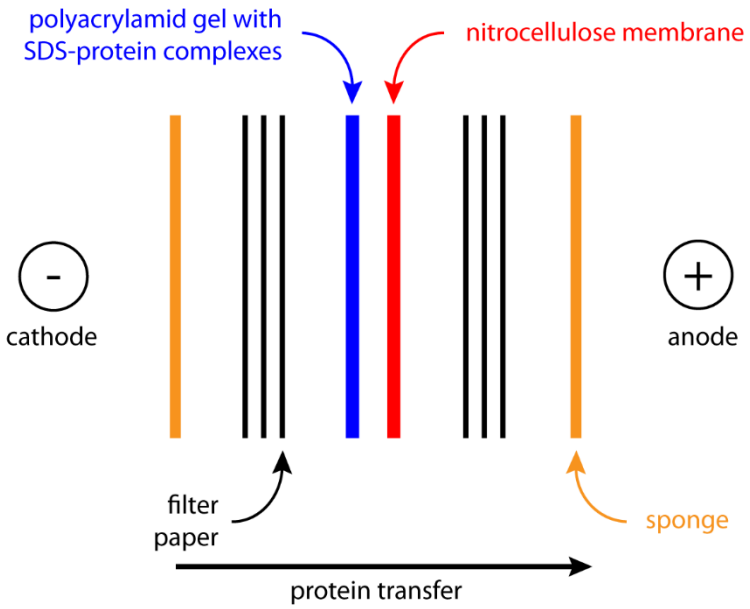

Figure 2.9 Structure of the Western Blot: Gel and membrane are covered by three filter paper and a thin sponge on each side. Negatively charged SDS-protein complexes move towards the anode and are thereby transferred to the membrane.

Table 2.16 Transfer buffer

Tris-Base pH 8.5	20 mM
Glycin	150 mM
MeOH	20% (v/v)

2.2.3.4 Ponceau staining of the nitrocellulose membrane

Ponceau-S binds to the positively charged amino-groups of the membrane bound proteins. This binding is reversible and can be easily removed with TBS. Ponceau staining was used to confirm the transfer of proteins to the nitrocellulose membrane. Membranes were covered with the Ponceau-S-solution (Tab. 2.17) for 10 minutes at room temperature.

Table 2.17 Ponceau-S-solution

Ponceau S	0.3% (w/v)
Trichloroacetic acid	3% (v/v)

2.2.3.5 Staining of the nitrocellulose membrane

After the protein transfer (see section 2.2.3.4) was confirmed with Ponceau S (see section 2.2.3.4) the nitrocellulose membrane was stained with antibodies to detect specific proteins. The used protocol is described in Tab 2.18. Tris-buffered saline (TBS) was used to perform the washing steps. TBS prepared as a 20-fold stock solution according to Tab. 2.19. The pH-value was adjusted to 7.4 with 12M HCl.

Table 2.18 Staining of a nitrocellulose membrane

Blocking	Membrane was blocked with 5% milk powder (w/v) in TBS for 2 hours at room temperature.
Primary antibodies	Membranes were incubated with primary antibodies in 5% milk powder (w/v) in TBS over night at 4 °C or for 1h at room temperature
Washing	After antibody incubation the membranes were washed three times with TBS + 0.05% Tween20 at room temperature.
Secondary antibodies	Membranes were incubated with secondary antibodies in 5% milk powder (w/v) TBS over night at 4°C.
Washing	After antibody incubation the membranes were washed three times with TBS + 0.05% Tween20 at room temperature.

Table 2.19 Recipe for 20x TBS stock solution

Chemical	20x TBS stock solution	Concentration in 1x TBS
Tris-Base pH 6.8	24g	50 mM
NaCl	88g	150 mM
ddH_2O	Add to 1L	

2.2.3.6 Recording of the nitrocellulose membrane

After the proteins on the membrane were decorated with antibodies (see section 2.2.3.6) membranes were processed with the Western Lightning Plus-ECL substrate from PerkinElmer (Massachusetts, USA) according to the manufacturer's specifications. The ECL-solution works as a substrate for the horseradish peroxidase (HRP) which is coupled to the secondary antibody. HRP catalyzes the chemiluminescence reaction and the resulting signal is detected with the Amersham Imager 600 from GE Healthcare (Little Chalfont, England).

2.2.4 Cell culture

2.2.4.1 Cultivation of HDFa and U-2 OS cells

Cells were grown in an incubator with 5% CO_2 at 37 °C. The used culture medium was Dulbecco's Modified Eagle's Medium (DMEM) with 4.5 g/l glucose, GlutaMAX and phenol red from Thermo Fisher Scientific (Massachusetts, USA). Fetal Bovine Serum (FBS), sodium pyruvate, penicillin and streptomycin were added like described in Tab 2.20. For splitting and seeding of the cells DMEM was replaced with warm PBS (see section 2.1.6) for washing and the cells were detached by incubation with a trypsin solution for 5 minutes at 37°C. Trypsin was afterwards inactivated with at least 5 volumes of DMEM.

Table 2.20 Culture medium

Ingredient	Concentration
DMEM, GlutaMAX, High Glucose	Basis solution
FBS	10% (v/v)
Penicillin	100 U/ml
Streptomycin	100 µg/ml
Sodium pyruvate	1 mM

2.2.4.2 Transfection of cells

Transfection of siRNAs was done with the transfection reagent Lipofectamine RNAiMAX from Thermo Fisher Scientific (Massachusetts, USA).

For each transfection 246 µl Opti-MEM from Thermo Fisher Scientific (Massachusetts, USA) without FBS were mixed with 4 µl of the transfection reagent. In parallel 210 µL DMEM without FBS were mixed with 40 µl of a 0.3 µM siRNA Pool solution.

RNAiMAX dilution and siPool solution were then mixed by intense vortexing and afterwards incubated for 5-10 min at room temperature. Afterwards, the transfection mix was added to seeded cells together with 1.5 ml of DMEM (see. 2.2.4.1).

2.2.4.3 Toxicity tests

The toxicity of the nucleoside analogues EdU, BrdU and BrU was tested with the NucleoCounter NC 3000 from ChemoMetec (Lillerod, Denmark). The “Cell Cycle” and the “Vitality” assay were performed according the manufacturer’s specifications.

3. Results

Replication and transcription of mitochondrial DNA (mtDNA) are essential cellular processes whose malfunctions can be linked to several diseases. However, their regulation is poorly understood and it is one of the biggest gaps in our understanding of mitochondria. Biochemical studies have helped to identify key players in the replication and transcription machinery, as well as proteins that are crucial for the regulation of both of these processes. Conventional light microscopy has provided deep insights into the dynamics of mitochondrial replication and transcription and the influence of the submitochondrial localization of mtDNA-molecules. Albeit, all studies so far lacked the resolution to analyze single mtDNA molecules since they cannot be resolved due to their density in mitochondria and their small diameter below the diffraction limit of 200 nm.

In contrast to previous works, in this study superresolution microscopy, namely Stimulated Emission Depletion (STED) nanoscopy, is used to analyze single mtDNA-molecules, which are indistinguishable in clusters of molecules when conventional diffraction limited microscopy methods are applied (Kukat and Wurm et al., 2011).

To analyze the regulation and connection of mitochondrial replication and transcription, the development of a protocol to visualize both processes was crucial. The first part of this study deals with the establishment of a fluorescence-microscopy based approach allowing to detect replication and transcription using STED nanoscopy. Thereby, the visualization of mtDNA activity is required to be independent from the proteins of the replication and transcription machinery as the developed protocol should be also used to analyze mtDNA activity in knockdown cell lines of these proteins afterwards.

In the second part of this study, the developed staining and imaging approach is applied to uncover the activity of mtDNA molecules in wild type cells as well as the regulatory mechanisms behind mitochondrial replication and transcription in wild type cells and knockdown cell lines.

The experiments were performed in fixed adult human dermal fibroblasts (HDFa) and human bone osteosarcoma cells (U-2 OS). These cell lines were chosen as they show preferable properties for light microscopy. Both cell types appear wildly spread and are therefore very plane. As a result, the majority of nucleoids are localized in the same focal plane and can be observed easily with STED nanoscopy.

3.1 Nanoscopy is essential to visualize single nucleoids

To visualize mitochondria and mitochondrial DNA (mtDNA), HDFa cells were incubated with antisera against double stranded (ds)DNA as well as the mitochondrial protein Mic60 and subsequently imaged with a confocal microscope. The cells show numerous dots of extranuclear DNA (magenta) exclusively located within the mitochondria (green, Fig 3.1 A). In confocal images, the mtDNA is found in clusters (Fig 3.1 B-G). STED nanoscopy of this single confocal DNA signals uncovers that these confocal signals can originate from a varying amount of single nucleoids (Fig 3.1 B'-G'). Hence, diffraction limited microscopy can only investigate nucleoid clusters containing an unknown amount of nucleoids, whereas the increased resolution of STED nanoscopy facilitates the investigation of single mitochondrial nucleoids in such clusters.

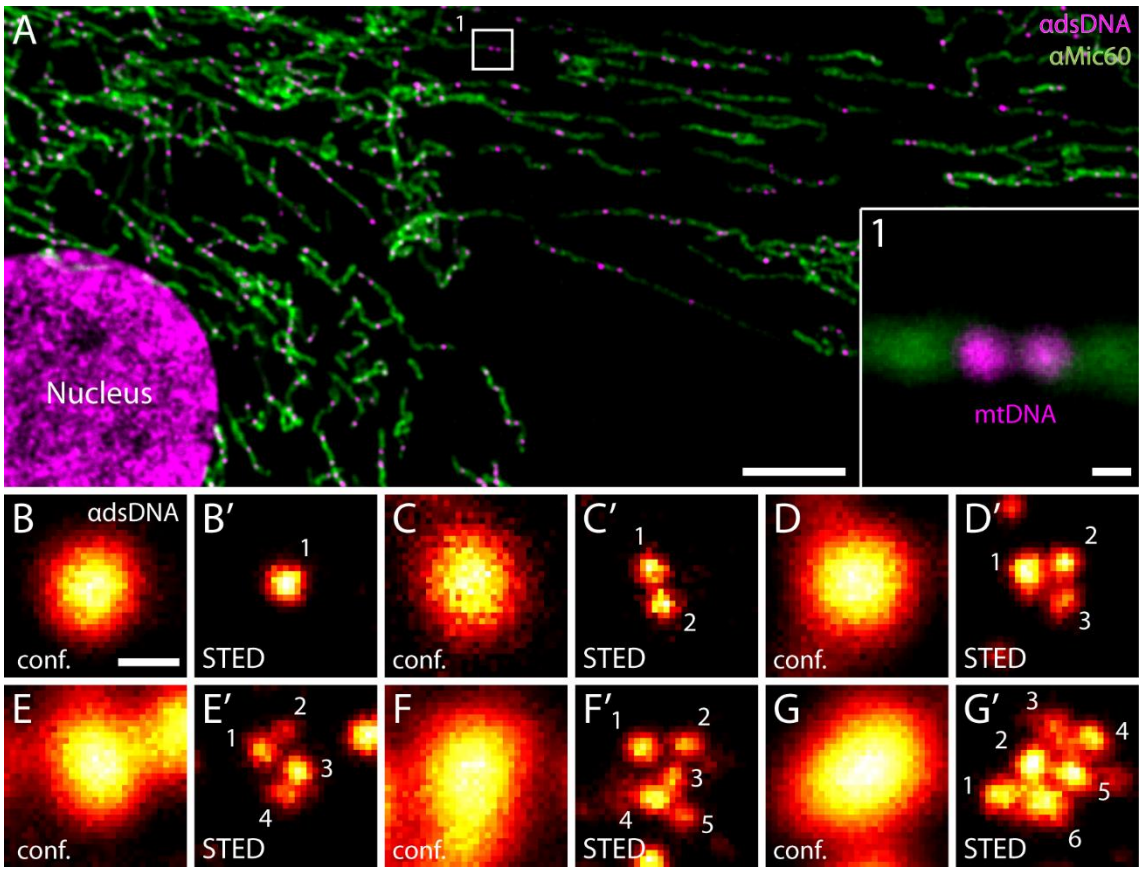

Figure 3.1 Nanoscopy is essential to visualize single nucleoids: A) HDFa cell incubated with antisera against dsDNA (magenta) and the inner mitochondrial membrane protein Mic60 (green). Mitochondrial DNA (mtDNA) appears as extranuclear DNA signal within the mitochondrial network. **B-G')** Comparison between mtDNA signals recorded with conventional confocal microscopy and STED nanoscopy. Identical sections were recorded with the same excitation laser power and the same pixel size. Whereas confocal images show a single DNA signal, STED images reveal different amounts of nucleoids. Raw data with 5% subtraction of the background. Scale bar in A: 5µm and in 1 and B-G': 200 nm

The visualization of cellular structures in the nanoscale by super-resolution microscopy requires dyes with specific properties, especially high brightness and contrast. Furthermore, the labeling has to be very specific because small artefacts that are undetectable in confocal microscopy can affect the nanostructure. Moreover, visualization of nucleoids should not influence mtDNA activities as this study focusses on their regulation. Therefore, it was crucial to select a labeling method which is not affecting the replication and transcription.

3.1.1 Antibodies against DNA provide the best properties to label nucleoids

The labeling of nucleoids can be done by labeling of the nucleoid proteins or the nucleic acids. Detecting nucleoids using reporter gene fusion proteins was dismissed as the additional expression of nucleoid proteins can alter mitochondrial replication and transcription (Maniura-Weber et al., 2004, Pohjoismäki et al., 2006; Ikeda et al., 2015; Kühl et al., 2016). For example, the mitochondrial transcription activator TFAM is a very abundant core structural protein of mitochondrial nucleoids and is a commonly used protein to label nucleoids by its fusion to reporter proteins. However, since it is strongly involved in transcription, additional expression of TFAM is sufficient to stimulate RNA synthesis (Maniura-Weber et al, 2004). Endogenous tagging to circumvent the problem of overexpression was suspended as primary cells are used in some experiments.

In this work, three different methods were tested to label the mitochondrial nucleoids (Fig. 3.2). Cells were incubated either with antibodies against dsDNA (A), antibodies against the nucleoid core protein TFAM (B) or with the DNA intercalator dye PicoGreen (C) and imaged in the confocal- (A-C) or STED-mode (D-F). All three methods give rise to bright signals with very good contrast. Furthermore, the three labeling methods can be used in STED nanoscopy to resolve single nucleoids within a cluster.

The signal of antibodies against dsDNAs reveal nucleoids with a very uniform size and shape like their appearance is described in literature when STED is applied (Fig 3.2 D). This is in agreement with previous findings (Kukat and Wurm et al., 2011). In contrast, antisera against TFAM result in uneven labeling with inconsistent size and irregular shape (Fig 3.2). This could be a result of inhomogeneous TFAM-binding to mtDNA (Gustafson et al., 2016). Furthermore, TFAM is one of the candidates involved in the regulation of mtDNA activity as its presence primes mitochondrial transcription. Therefore the labeling of nucleoids should be independent of TFAM to allow a future research of the analysis of nucleoid activity upon varying protein level of this mitochondrial transcription factor. Hence, TFAM is not a suitable nucleoid marker for

this study as it does not provide a uniform labeling of nucleoids throughout all experiments.

PicoGreen requires no detection with antibodies as it is fluorescent on its own and shows an increase of fluorescence intensity upon intercalation into the DNA, resolving single nucleoids and displaying good contrast and brightness (Fig 3.2 F). However, PicoGreen has drawbacks making it unsuitable for this study. First, the stain is not specific for dsDNA, but also recognizes structured RNA. Therefore, a crucial step to provide good contrast is the complete digestion of RNA within the cell, but that eliminates the possibility to mark transcription by labeling RNA directly in following steps. Second, labeling of the DNA by PicoGreen has a rather short life time. After preparation of the sample, the dye starts to dissociate from the DNA. About 4 hours after sample preparation, single nucleoids can hardly be identified by the decreased contrast (Supplement Fig. 9.1). The irregular shape of nucleoids labeled with PicoGreen might be a result of the dissociation of the stain (Fig 3.2 F).

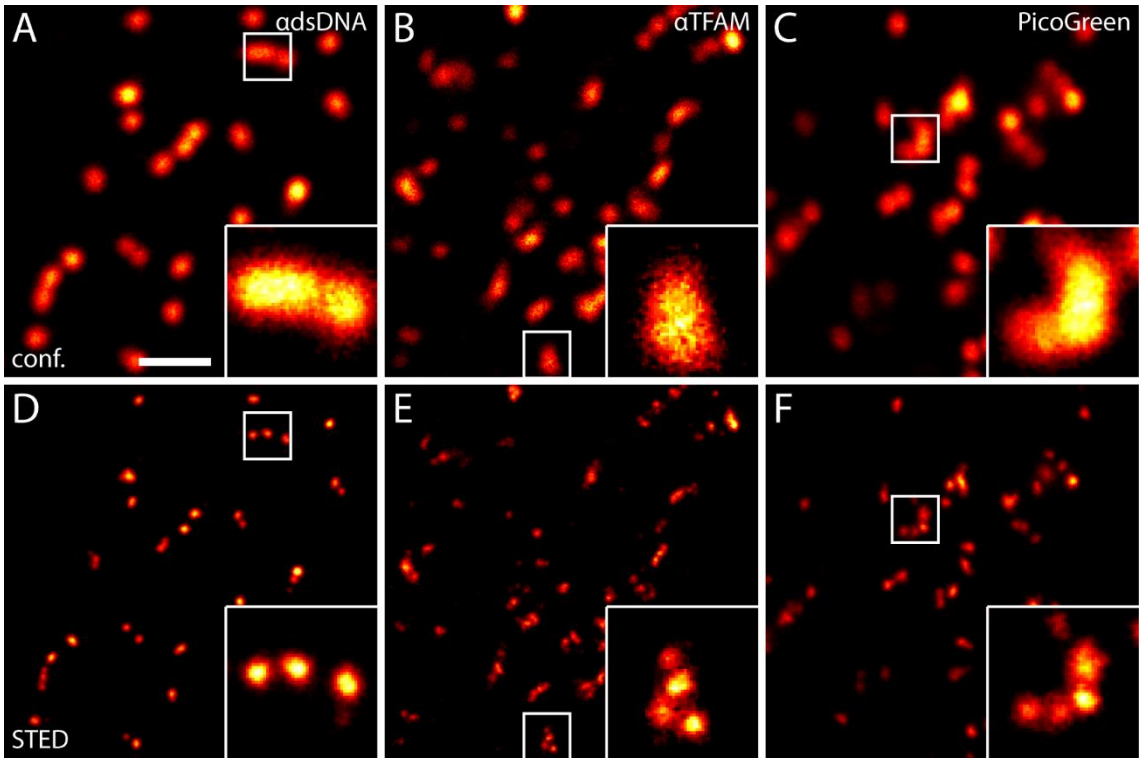

Figure 3.2 Different methods to visualize mtDNA: A-C) HDFa cells were incubated with antibodies against dsDNA (A), the nucleoid core protein TFAM (B) and the DNA intercalator PicoGreen. All three methods were suitable to detect mtDNA and images were recorded with conventional confocal microscopy. **D-F)** same sections like in A-C are recorded with STED nanoscopy using identical excitation power and pixel size. The enhanced resolution reveals that some single confocal signals originate from cluster of several mtDNA molecules. Nucleoids decorated with αdsDNA (D) show a uniform size and shape in contrast to αTFAM (E) and PicoGreen (F) stainings in which nucleoids appear in a higher variety. Scale bar: 500 nm

Summarizing, antisera against dsDNA provide the best properties to image nucleoids in this study as they do not influence mtDNA activity at any stage and label nucleoids with high contrast. In the following, structures engaged in the process of replication and transcription respectively will be analyzed based on this visualization of single nucleoids.

3.2 Labeling of mtDNA activity with nucleoside analogues

The imaging of mtDNA activity is used to analyze the influence of key players of mitochondrial replication and transcription later in this study. These factors are the mitochondrial transcription elongation factor TEFM and the mitochondrial RNA polymerase POLRMT, as they are linked to the regulation of mtDNA activity in the literature (Minczuk et al., 2011; Agaronyan et al., 2015; Kühl et al., 2016; Gustafsson et al., 2016). As the imaging approach should work as a universal tool to investigate the influence of all factors involved in mitochondrial replication and transcription, the method to detect mtDNA activity should be totally independent from any of these mitochondrial factors. Therefore, the labeling of components of the mitochondrial replication or transcription machinery is not the preferred method.

Nevertheless, it is important to test if one of the factors involved in mitochondrial replication and transcription enables one to detect the nucleoid activity since proteins of the replication machinery are often used to mark mtDNA activity (Example: Lewis et al., 2016). Proteins that specifically label mitochondrial transcription can act as a valid control throughout the experiments. Hence, immunostainings of main factors of both processes were carried out.

3.2.1 Antibody labeling of the replication and transcription machinery do not specifically mark mtDNA activity

Important proteins involved in replication are the mitochondrial single strand binding protein (mtSSBP), the mitochondrial DNA polymerase γ (POLγ) and the helicase TWINKLE (see 1.4.1). Antibodies against all three components were tested in HDFa and U-2 OS cells to identify a suitable marker for replication in two-color stainings together with a mitochondrial marker or an mtDNA marker to identify their localization.

The αmtSSBP signal (magenta) is restricted to mitochondria marked by antibodies against the β-subunit of the ATP synthase (green, Fig 3.3 A-A''). Brighter spots of αmtSSBP signal show a partial colocalization with nucleoids (green, Fig 3.3 B-B''). Colocalization is highlighted with circles and separate localization is framed by squares.

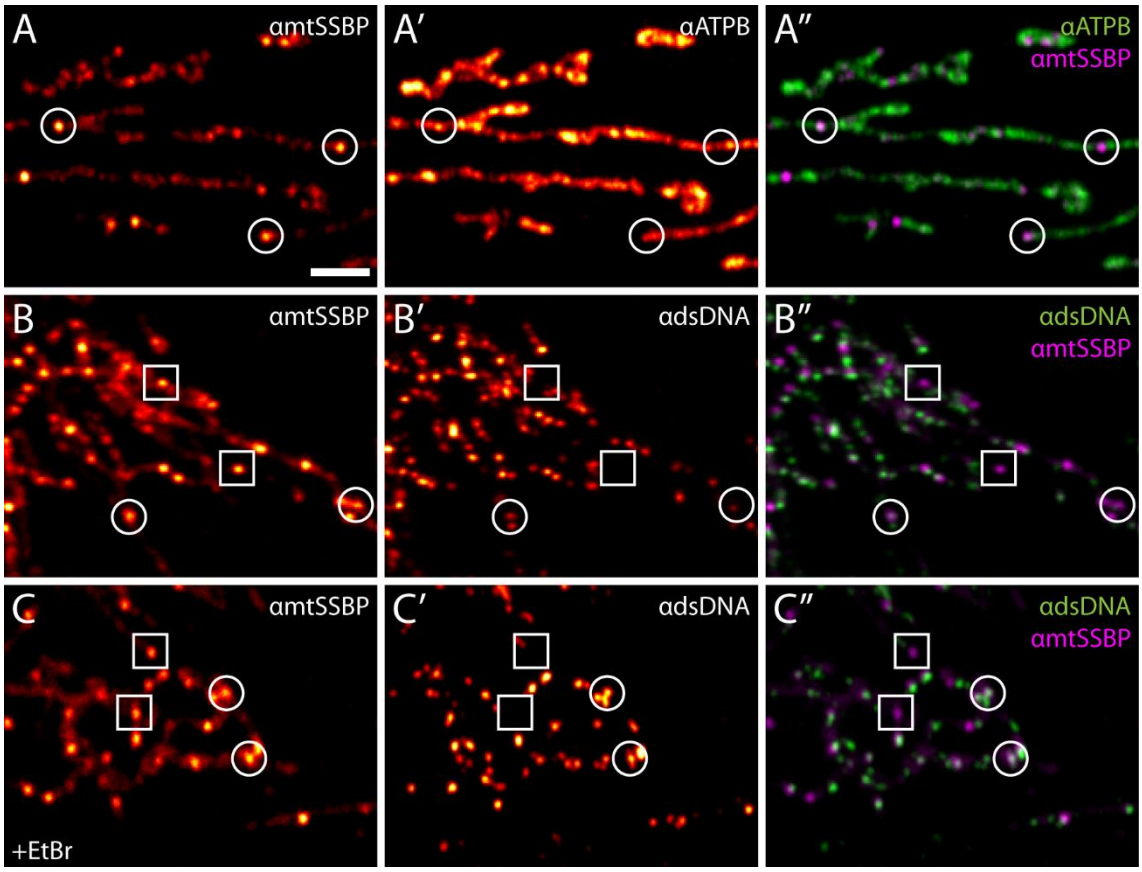

Figure 3.3 mtSSBP is not a suitable marker for replication of nucleoids: U2-OS cells were incubated with antisera against the mitochondrial single strand binding protein mtSSBP together with antibodies against the ß-subunit of cristae-protein ATP-synthase (ATPB) as a mitochondrial marker or against DNA to visualize the mtDNA. **A-A'')** mtSSBP is located within the mitochondrial network and is enriched in distinct dots**. B-B'')** Spots of enriched mtSSBP signal colocalize only partially with mtDNA. Colocalization is marked with circles, discrete localization is highlighted with squares. **C-C'')** 2 µg/µl ethidium bromide is added to the cells for three hours prior the fixation to block mitochondrial replication. To some extent accumulations of mtSSBP still colocalize with mtDNA. Colocalization is again marked with circles, separate localization is highlighted with squares. Scale bar: 2 µm

To test whether the mtSSBP signal is not restricted to nucleoids but mtSSBP positive nucleoids are indeed undergoing replication, cells were treated with ethidium bromide (EtBr). EtBr intercalates predominantly into mtDNA and thereby inhibits melting of the DNA, leading to impaired mitochondrial replication and transcription (Hayakawa et al., 1998; Holt and Reyes, 2012). Although mitochondrial replication is blocked, mtSSBP is still found in defined spots with a partial colocalization with mtDNA (Fig 3.3 C-C''). Hence, mtSSBP binds to nucleoids even if they are not involved in ongoing replication. Later experiments show that the EtBr control works also reliably if specific replication markers are used (see 3.2.3). The mtSSBP data are a typical example for the lack of specificity of components involved in mitochondrial replication to label nucleoid activity.

Also antibody stainings against TWINKLE labeled a subset of nucleoids upon EtBr treatment. Antisera against POLγ were not able to label nucleoids (Supplement Fig. 9.2). Identical experiments were performed in HDFa cells. Antibodies against mtSSBP labels a subset of nucleoids, even when EtBr was added. Antisera against TWINKLE and POLγ did not produce a specific signal (Supplement Fig. 9.2).

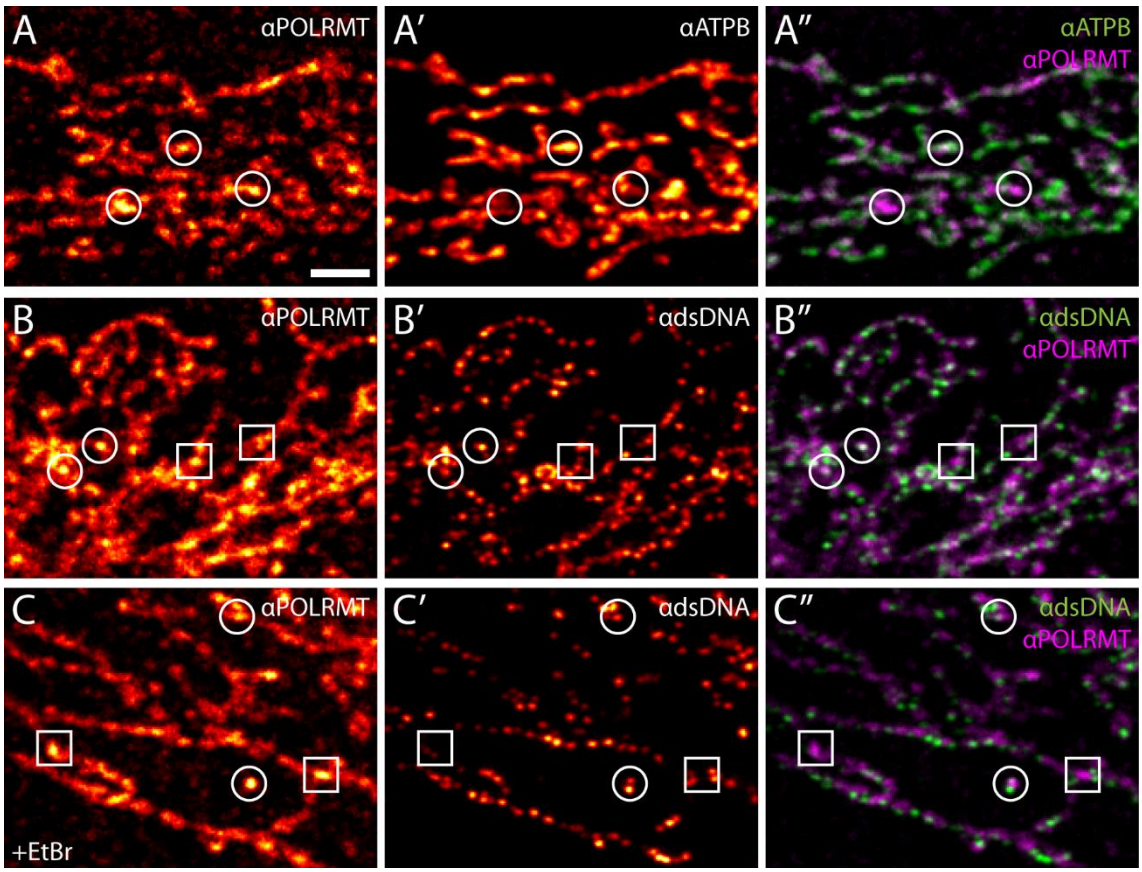

Figure 3.4 POLRMT is not a specific marker for transcription: U-2 OS cells were incubated with antisera against the mitochondrial RNA polymerase POLRMT together with antibodies against the ß-subunit of cristae-protein ATP-synthase (ATPB) as a mitochondrial marker or against dsDNA to label the mtDNA. **A-A'')** POLRMT is enriched in mitochondria. Within the mitochondrial network, spots with enhanced signal are present. **B-B'')** Areas with an increased level of POLRMT do not always colocalize with mtDNA, however, structures of enriched POLRMT are often attached to an mtDNA molecule. Colocalization is highlighted with circles, separate localization and attachment to mtDNA with squares. **C-C'')** 2 µg/µl ethidium bromide was added to the cells for three hours prior the fixation to block mitochondrial transcription. POLRMT spots still show colocalization or agglomeration to the mtDNA. Colocalization is again highlighted with circles, discrete localization and attachment to mtDNA with squares. Scale bar: 2µm

Although proteins of the replication machinery do not prove to be suitable markers for mitochondrial replication, it was tested, whether stainings of components involved in mitochondrial transcription work as reliable marker for nucleoid activity. Identified factors involved in mitochondrial transcription are TFAM, the mitochondrial transcription factor B2 (TFB2M), POLRMT and TEFM (see 1.5.1). TFAM is not suitable to

label transcription since it is very abundant and labels the complete nucleoid content of a cell (see Fig 3.2)

Stainings against the polymerase POLRMT together with stainings against the β-subunit of the ATP synthase as a mitochondrial marker and against dsDNA as a marker for nucleoids reveal that POLRMT (magenta) strongly colocalize with the mitochondrial network (green, Fig 3.4 A-A'') but only partially with nucleoids (green, Fig 3.4 B-B''). Colocalization is highlighted with circles and separate localization with squares. This partial colocalization of POLRMT is also not disturbed by a treatment of the cells with EtBr that blocks mitochondrial transcription. In conclusion, POLRMT is found associated with nucleoids even when transcription is blocked. Therefore antibody stainings against POLRMT cannot be used to detect transcription specifically. Later experiments will show that the EtBr control works reliable if specific transcription marker are used (see 3.2.3). The results shown for POLRMT are exemplary for the TEFM staining, as it shows a partially colocalization with mtDNA which is unaffected by the EtBr treatment (Supplement Fig. 9.3). The used antibodies against TFB2M showed no specific signal (Supplement Fig. 9.3). No antibody against proteins involved in mitochondrial transcription show any specific signal in HDFa cells (Supplement Fig. 9.3).

In conclusion, no protein of the replication and transcription machinery is a reliable marker for mtDNA activity. A labeling method which is independent from those components is therefore needed. An approach which is rarely used to label mtDNA activity but nonetheless displays promising results in the literature is the treatment of cells with nucleoside analogues.

3.2.2 Synthetic nucleoside analogues label mtDNA activity

Synthetic nucleoside analogues added to the cells, are incorporated into nascent DNA and RNA during replication and transcription, respectively. The concentration and incubation time has varying effects in different mammalian cells, and therefore has to be adjusted for each cell line to exclude effects limiting the signal and imaging quality. Determination of these optimal conditions, as well as exemplary effects caused by deviations from these conditions, are shown in (Supplement Fig. 9.4). The optimized protocols can be found in 2.2.1.4 – 2.2.1.6).

Two nucleoside analogues to detect mitochondrial replication and one analogue to label transcription were examined. Replication was labeled with the two thymidine analogues 5'-Ethynyl-2'-desoxyuridine (EdU) and 5'-Bromo-2'desoxyuridine (BrdU).

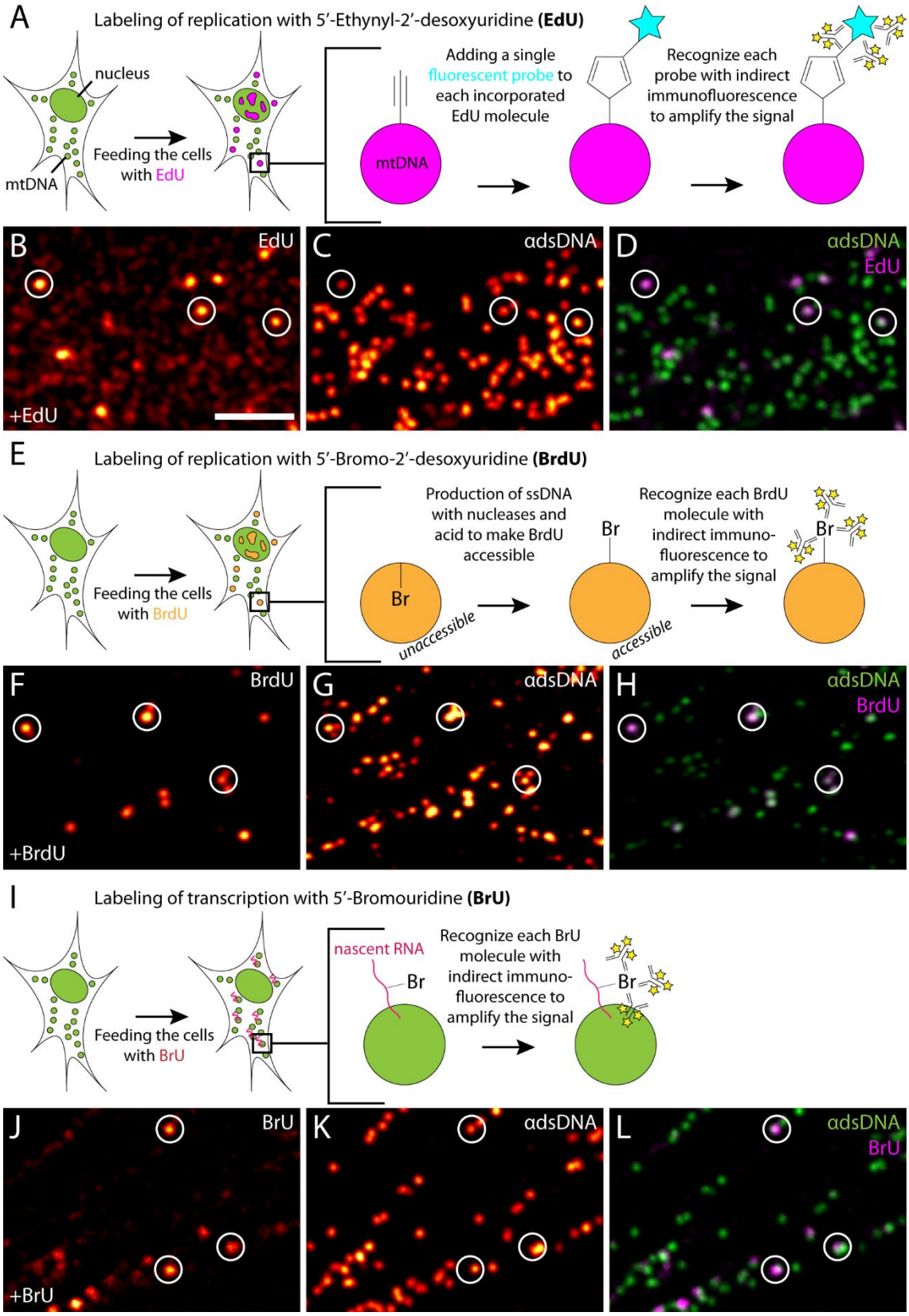

Figure 3.5 Nucleoside analogues mark mtDNA activity: A) To label replication with EdU, the nucleoside analogue is added to the medium prior to fixation for incorporation into the nascent DNA. EdU molecules contain an alkene group that reacts with an azide group in a copper catalyzed alkyne-azide cycloaddition (CuAAC). This reaction is used to add a single fluorescent probe to each EdU molecule. The EdU signal can be enhanced with an antibody staining against the fluorescent probe. **B-D)** HDFa cells were incubated

with 20 mM EdU for 2 h. CuAAC was performed with Alexa Fluor 488-azide that afterwards was recognized with αAlexa Fluor 488 antibodies. Foci of EdU signal (magenta) specifically colocalize with mtDNA (green). **E)** BrdU was added into the medium and incorporated into the newly synthesized DNA during replication. Acid and nucleases were applied to produce fragments of single stranded DNA and make BrdU accessible to antibodies. Afterwards BrdU was labeled with indirect immunofluorescence. **F-H)** HDFa cells were fed with 20 µM BrdU for 2 h. BrdU signal shows strong colocalization with mtDNA. **I)** BrU was used to label transcription as it is incorporated into nascent RNA. After incorporation it was recognized via antibodies. **J-I)** HDFa cells were incubated with 20 µM BrU for 30 min prior to fixation. BrU signal is always associated with mtDNA. Scale bar: 2 µm

In contrast to thymidine, EdU is functionalized with an alkene group which can be used to label each EdU-molecule with an azide-functionalized probe in a copper catalyzed alkyne-azide cycloaddition (CuAAC), colloquially termed “click reaction”. When a fluorophore is used as a probe, it can be used directly to visualize replicating DNA. However, the signal intensity can be further amplified by performing an indirect immunostaining against the probe. During this study, EdU was labeled with Alexa Fluor 488-azide and the signal afterwards enhanced with an antibody staining against Alexa Fluor 488. Fig 3.4 A shows the workflow of an EdU-labeling. Fig 3.5 B-D shows a HDFa cell fed with EdU. Foci of EdU (magenta) signal exclusively colocalize with mtDNA labeled with αdsDNA (green).

BrdU possesses a Bromine atom at the 5’-Carbon of the nucleobase which can be recognized by specific antibodies. When BrdU is incorporated into DNA, a very harsh protocol is required to make the Bromine atom accessible for antibodies. This protocol includes acid ethanol fixation to produce single stranded DNA followed by an incubation with nucleases to create small fragments of DNA. Afterwards, the BrdU can be decorated with antibodies. The basic workflow of BrdU labeling is shown in Fig 3.5 E. A section of an HDFa cell incubated with BrdU and treated with the mentioned protocol is displayed in Fig 3.5 F-G. The BrdU signal (magenta) is strongly restricted to mtDNA molecules and labels a subset of the nucleoids (green).

Finally, a nucleoside analogue to detect transcription was tested. 5’-Bromouridine (BrU) differs from BrdU by an additional oxygen at the 2’-Carbon of the ribose. As a result, it is incorporated into nascent RNA instead of DNA replacing uridine. BrU can be detected with the same antibodies like BrdU since they recognize the Bromide atom shared by both nucleosides. Since BrU incorporated into RNA is accessible without previous melting or digesting of the nucleic acid, it can be visualized through a conventional antibody staining without any harsh treatment of the cell. Fig 3.5 I shows the schematic workflow of BrU usage to label transcription. Fig 3.5 J-L reveal that every BrU spot is associated with a nucleoid.

The nucleoside analogues are incorporated into DNA and RNA during the complete incubation time. To ensure that predominantly ongoing transcription and replication is measured, the incubation time with each nucleoside has to be as short as possible. Images in the following sections show cells which were incubated with BrdU and EdU for 2 h and BrU for 30 min showing bright signal with high contrast. The shortest incubation times suitable for nucleoside analogues to detect replication were 70 min in HDFa cells and 55 min in U-2 OS cells. The shortest incubation times for BrU suitable to detect transcription were 25 min in HDFa cells and 20 min in U-2 OS cells. No specific signal could be detected using shorter incubation times (Supplement Fig. 9.4).

To test if this labeling protocols are reliable, all three labeling approaches were performed without the previous feeding of the respective nucleoside. Furthermore, it was tested if the three synthetic nucleoside were incorporated into DNA or RNA, respectively upon EtBr treatment. As mentioned above, EtBr intercalates predominantly into mtDNA and causes a block of mitochondrial replication and transcription as well (Hayakawa et al., 1998; Holt and Reyes, 2012). Fig 3.6 shows the results of both experiments. The EdU protocol is highly specific as no distinct signal was detected when EdU was absent (Fig 3.6 A-A'). Furthermore, EdU incorporation into DNA is totally blocked upon EtBr treatment (Fig 3.6 B-B'). Hence, EdU only forms foci colocalizing with nucleoids after incorporation into DNA during replication.

Identical results could be obtained for BrdU (Fig 3.6 C-D'). The appearance of BrdU signal localizing to mitochondrial nucleoids require the presence of the nucleoside itself and ongoing replication as EtBr treatment efficiently blocks the incorporation of BrdU into mtDNA.

Finally, Fig 3.6 E-F' shows the controls for the labeling of transcription by BrU. The protocol used for the visualization of incorporated BrU is also highly specific since no signal could be detected when BrU is missing (Fig 3.6 E-E'). BrU incorporation into RNA should be blocked by EtBr due to impaired mitochondrial transcription. Fig 3.6 F-F' reveals that the BrU signal totally vanishes when transcription is inhibited.

In conclusion, the nucleoside analogues EdU, BrdU and BrU are specific markers to label mtDNAs activity as they survive the EtBr control. Furthermore, the visualization of mitochondrial replication and transcription via incorporated nucleosides is independent from components of both machineries. Hence, the usage of nucleoside analogues provides the possibility to analyze the regulation of mtDNA activity upon different genetic situations with varying protein levels, without influencing the imaging system itself. However, it has to be determined whether the incorporation of synthetic nucleosides alter the behavior of the cells or has toxicity effects.

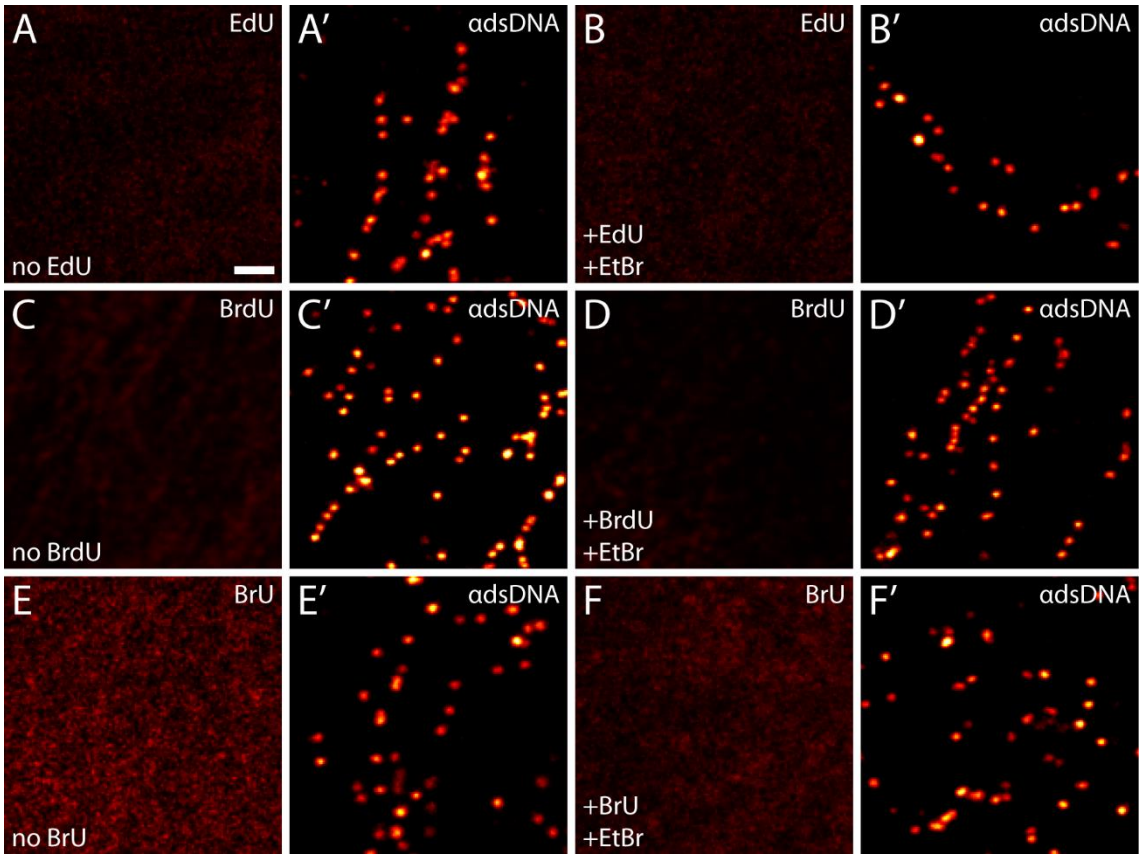

Figure 3.6 Nucleoside analogues are a specific method to label mitochondrial replication and transcription: HDFa cells were used to test the specificity of EdU, BrdU and BrU. **A-A')** Without previous EdU incubation, no EdU signal can be detected. **B-B')** Cells were incubated with 20 µM EdU for 2 h and 2 µg/µl EtBr for 3 h. Upon treatment with EtBr, no incorporation of EdU into the DNA can be observed. **C-C')** The BrdU staining protocol produces no specific signal without previous feeding of the cells with BrdU. **D-D')** Cells were treated with 20 µM BrdU for 2 h and 2 µg/µl EtBr for 3 h. Blocking of mtDNA activity with EtBr blocks BrdU incorporation as no BrdU signal is detected. **E-E')** Cells show no BrU signal when BrU is not added prior to the fixation. **F-F')** Cells were incubated with 20 µM BrU for 30 min and 2 µg/µl EtBr for 3 h. No specific BrU signal can be identified. Scale bar: 1 µm

3.2.3 Short treatment with nucleoside analogues has no toxic side effects

The toxicity of EdU and BrdU has been described in some reports (Taupin et al., 2007; Ligasova et al., 2015). The observed toxicity depends on the concentration used, the incubation time and the resulting incorporation rate of the nucleoside analogues into the newly synthesized DNA. However, there is strong evidence that toxicity of at least EdU strongly depends on the used cell type (Ligasova et al., 2015). Potential negative side effects of BrU are not discussed in the literature.

To evaluate whether the used nucleoside analogues affect the cells, three parameters were analyzed. The cell cycle was evaluated by automated computer based analysis of a DAPI staining. Cells in the G1, G2 or S-phase can be quantified to identify arrest in the cell cycle upon nucleoside analogue treatment. The viability was tested by a computer

based analysis of the cell's membrane integrity. Therefore, Acridine Orange was used to label the total cell population as it is cell permeable. Cells were simultaneously incubated with DAPI that will only penetrate cells with impaired plasma membrane and label the nucleus. Finally, the number of nucleoid cluster within the mitochondria were analyzed with confocal microscopy. 20 µM EdU, BrdU and BrU were added to HDFa cells for two and 48 hours. As a control 20 µM Aphidicholin was added to the cells. Aphidicholin leads to an arrest of the cells in the S-Phase or G2-phase since it inhibits the DNA polymerase activity. Three independent experiments with over 10^5 cells for each condition were performed to analyze the cell cycle and viability. For the determination of the nucleoid number, 10 cells per approach were analyzed with confocal microscopy. Tab 3.1 shows the average values (Raw data shown Supplement Tab. 9.1).

Table 3.1 Toxicity of nucleotide analogues: HDFa cells were treated with 20 µM Aphidicholin, EdU, BrdU and BrU for 2 and 48 hours. The cell cycle as well as the viability of the cells was analyzed. DAPI-stainings of the nucleus were used to distinguish between G1- S- and G2-phase of the cell cycle. Membrane integrity was analyzed to determine the viability of cells. Furthermore, the amount of nucleoid cluster within a cell was determined with confocal microscopy. As a control, cells without previous treatment were analyzed. In each experiment, more than 10^5 cells were studied and three independent experiments were performed. For the estimation of the nucleoids within a cell, 10 cells were analyzed for each situation. Average values are shown. Incubation of cells with one of the tested components for 2 hours cause no alterations of the cell cycle, viability or the number of nucleoids. After 48 h, cells treated with Aphidicholin show an enrichment of cells in the S- and G2-phase. Furthermore, the viability is decreased. EdU causes no decreased viability but an enrichment of cells in the G2-Phase. The cell cycle upon BrdU treatment appears normal. However, the viability is slightly decreased. BrU treatment for 48 h has no effect on the cell cycle or the viability. The amount of nucleoid cluster is slightly decreased when cells are treated with Aphidicholin. Incubation with one of the nucleoside analogues has no influence on the number of nucleoid cluster.

	untreated	Aphidicholin	EdU	BrdU	BrU
Cells in G1-Phase (2 h)	**86.3%**	88.1%	85.7%	85.9%	87.1%
Cells in S-Phase (2 h)	**4.4%**	4.3%	5.1%	4.9%	4.3%
Cells in G2-Phase (2 h)	**8.1%**	6.9%	8.5%	8.4%	7.7%
Viability (2 h)	**88.9%**	88.1%	89.5%	91.3%	88.5%
Nucleoid Cluster (2 h)	**327**	311	319	332	313
Cells in G1-Phase (48 h)	**90.6%**	83.3%	82.5%	90.1%	89.5%
Cells in S-Phase (48 h)	**2.5%**	7.5%	2.8%	2.0%	2.9%
Cells in G2-Phase (48 h)	**6.0%**	8.1%	13.7%	6.7%	6.6%
Viability (48 h)	**94.3%**	81.1%	91.3%	87.3%	91.9%
Nucleoid Cluster (48 h)	**292**	269	279	287	301

After a short incubation time of two hours, neither EdU, nor BrdU, nor BrU show negative effects on the cell cycle, viability or the number of nucleoid cluster in the cells. A longer incubation time of about 48 hours revealed differences between the tested components.

Upon Aphidicholin treatment cells show a decrease of viability. Furthermore, the cells got stuck in the S- and G2-phase of the cell cycle. The amount of nucleoid cluster is only slightly reduced. Hence, toxicity can be detected with the used approached. EdU and BrdU have different influences on the cells. EdU leads to an enrichment of cells in the G2-phase of the cell cycle. However, the viability of the cells is not decreased and the amount of nucleoid cluster is not altered. In contrast, BrdU has no effect on the cell cycle as cells are distributed in G1-, S- and G2-phase like the untreated control. However, when fed with BrdU, cells show a slight decreased viability. The number of nucleoids is not changed upon BrdU treatment. Feeding of the cells with BrU for 48 h has no influence on the tested parameter.

In conclusion, short incubation times of the nucleoside analogues do not affect the cells. At least not when analyzed with the used approaches. As the majority of the experiments in this study were performed with incubation times below 70 minutes to detect replication and below 30 minutes to label transcription, the usage of the nucleosides can be considered as harmless for the cells. When longer incubation times are used, it should be noted that this might affect the cell cycle or the viability of cells. However, the amount of nucleoids is not affected at all by the tested nucleoside analogues.

Since all nucleoside analogues display perfect specificity and no toxicity using short incubation times, it has to be determined which nucleosides or which combination of nucleosides is more suitable to investigate nucleoid behavior and activity in the following.

3.2.4 Combination of EdU and BrU treatment enables labeling of the overall nucleoid activity

HDFa cells were simultaneously incubated with EdU and BrdU to check whether both nucleoids label the same mitochondrial nucleoids. Unfortunately, the used protocols to label EdU and BrdU are not combinable, as the usage of acid is one of the core steps of BrdU labeling (see Fig 3.5 E). Using samples fixed with ethanol at a neutral pH instead of acid ethanol, incorporated BrdU is not detected using the applied antibodies. Fig 3.7 A-A’ displays a section of a HDFa cell that was incubated with EdU and BrdU

simultaneously. Cells are fixed with ice cold ethanol with a neutral pH-value of 7.4. EdU signal forms distinct foci as it is incorporated into mitochondrial nucleoids. However, BrdU labeling leads to no distinct signal. Fig 3.7 B-B' shows cells which are treated exactly like cells in A-A' with the only exception that the cells are fixed with ethanol-HCl having a pH value of 2.0. As soon as acid is applied to a sample, click reactions do not label incorporated EdU. The EdU signal totally vanishes whereas incorporated BrdU can now be decorated via an indirect immunostaining.

The results shown in Fig 3.7 A-B' demonstrate that although both EdU and BrdU can be incorporated into replicating DNA simultaneously. However, they cannot be visualized simultaneously because of their incompatible staining protocols. An analysis of the amount of EdU and BrdU labeled nucleoids upon an equal incubation time and concentration revealed that both nucleoside analogues label the same amount of structures (Fig 3.7). This is a strong hint that both replication markers label the same population of nucleoids representing another proof for their specificity.

Since, mitochondrial replication and transcription could be visualized by the incorporation of nucleoside analogues, their compatibly was analyzed next. Using them simultaneously would allow to answer whether all nucleoids within a cell are equally active or if different subpopulations with specific functions exist. It would enable one to identify inactive nucleoids that are not engaged in at least one of both processes. Therefore, simultaneous detection of replication and transcription is essential to describe the activity pattern of a single nucleoid.

As mentioned above, BrdU incorporated in DNA and BrU incorporated in RNA were visualized using the same antibodies. Hence, both nucleosides cannot be labeled specifically when they are used together. In contrast, EdU and BrU can be separated since both nucleosides are detected with different methods. Fig 3.7 D-D'' shows nucleoids of a HDFa cell which was fed with EdU and BrU simultaneously. Nucleoids and incorporated BrU were decorated with antibodies against dsDNA and BrU and incorporated EdU was marked with Alexa Fluor 488-azide within a click-reaction and the signal afterwards enhanced by an antibody staining against Alexa Fluor 488. Nucleoids without any signal of EdU and BrU are apparent (1) as well as nucleoids only positive for EdU (2) or BrU (3), respectively can be detected. Furthermore, mitochondrial nucleoids positive for both nucleoside analogues exist (4). Hence, EdU and BrU can be used simultaneously to identify the behavior and activity of mitochondrial nucleoids.

Nucleoids engaged in replication and transcription, as well as nucleoids engaged in both processes were identified. However, as Fig 3.7 shows, confocal data alone cannot

determine whether single nucleoids or cluster of nucleoids are observed. To connect a specific activity to a single nucleoid, multicolor nanoscopy was necessary.

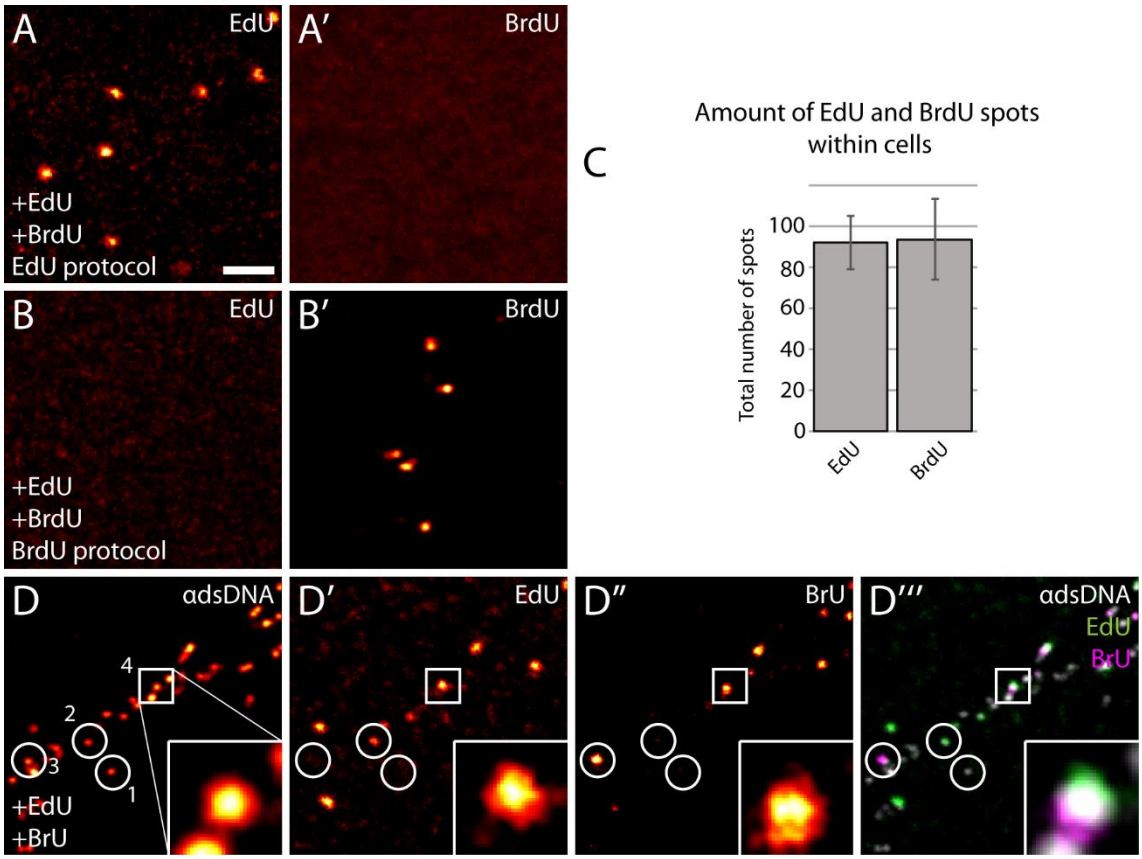

Figure 3.7 Simultaneous incorporation of EdU and BrdU to label mitochondrial replication and transcription together: HDFa cells were treated with combinations of EdU, BrdU and BrU. **A-B')** When cells were simultaneously fed wit 20 µM EdU and BrdU for 2 h both, nucleosides could not be visualized together. If the protocol was triggered towards EdU signal (A-A'), no BrdU signal can was detected. Usage of a BrdU protocol (B-B') led to a clear BrdU signal but no EdU signal. **C)** 15 HDFa cells incubated with 20 µM EdU and BrdU for 2 h were analyzed. Both nucleosides label the same amount of nucleoids within the cells. **D-D''')** Cells were incubated with 20 µM EdU for 2 h and 20 µM BrU for 30 min. EdU (replication, green) and BrU (transcription, magenta) can be used to label nucleoid activity together. One nucleoid without nucleoside signal (1), an EdU positive nucleoid (2) as well as one nucleoid positive for BrU (3) and both marker (4) are highlighted. Image in the magnified area is interpolated to enhance the amount of pixel by a factor of 2. Scale bar: 1 µm

3.3 Nanoscopy of single, active nucleoids.

A feature of this study is the analysis of single nucleoids with STED nanoscopy. As demonstrated in the beginning of this study, nucleoids tend to form clusters and single nucleoids can only be visualized using nanoscopy. To assign a specific action to a single nucleoid, two-color nanoscopy of a nucleoside analogue with a nucleoid marker is necessary. Since EdU and BrU can be used simultaneously to label mtDNA, both nucleosides were favored over BrdU. Furthermore nanoscopy revealed that nucleoids

appear with an irregular shape after incubation with nucleases during the BrdU staining protocol. Single nucleoids and background signal could not be separated clearly anymore (Supplement Fig. 9.5). Therefore, the following section covers the visualization of EdU- and BrU-positive nucleoids with STED nanoscopy, similar experiments with BrdU-positive nucleoids can be found in Supplement Fig. 9.5.

It was shown that EdU is a specific marker for replication since its incorporation is impaired when replication is blocked. Its localization is restricted to DNA and colocalized with a subset of mitochondrial nucleoids in confocal images. To test if EdU works with STED nanoscopy and whether single EdU-positive nucleoids can be identified, two-color STED of EdU labeling and an antibody staining against DNA was performed in HDFa cells. EdU incubation time was set to 70 minutes which represents the shortest incubation time to detect a specific signal. Fig 3.8 A-A'' shows a confocal signal which appears as a single EdU positive nucleoid. Two color STED of the same section in Fig 3.8 B-B'' reveals that the confocal signal originates from two single nucleoids (green) from which both show EdU incorporation (magenta). Fig 3.8 C-C'' displays another confocal nucleoid signal which is positive for EdU and that is comparable to the confocal images shown in A-A''. STED nanoscopy in Fig 3.8 D-D'' of the same section reveals that the confocal signals again originate from two single nucleoids (green). However, this time only one of both nucleoids shows EdU incorporation (magenta). Hence, STED nanoscopy of EdU is essential for the identification of single replicating nucleoids. Not only the correct amount of nucleoids can be estimated, but also single replicating nucleoids within a cluster can be identified.

A similar experiment was performed with HDFa cells after BrU incorporation to identify single nucleoids involved in transcription. The BrU incubation time was set to 25 min representing the shortest incubation time producing a specific signal. Cells were decorated with antibodies against dsDNA as well as antibodies against BrU. Afterwards, cells were investigated with two color STED nanoscopy. Fig 3.8 E-E'' and G-G'' show in each of the images a single nucleoid signal (green) positive for BrU (cyan) detected with confocal microscopy. STED nanoscopy of the same sections in Fig 3.8 F-F'' and H-H'' reveal that a single confocal event can originate from two single nucleoids (green) with only one engaging in transcription and thereby associated with BrU (cyan, F-F'') or from a single nucleoid with two separate transcription signals (H-H''). It becomes apparent that BrU signal is always slightly shifted to the nucleoid signal, whereas EdU signal shows a nearly perfect colocalization with mitochondrial nucleoids. This result meets the expectations as EdU is incorporated into the DNA and is therefore part of the nucleoid, whereas BrU labels the RNA that can be found in close proximity of the nucleoid but is

not part of it. In conclusion, STED nanoscopy is necessary to identify single nucleoids engaged in transcription. As demonstrated for the EdU-staining, confocal microscopy cannot resolve the information hidden in the diffraction limited signal.

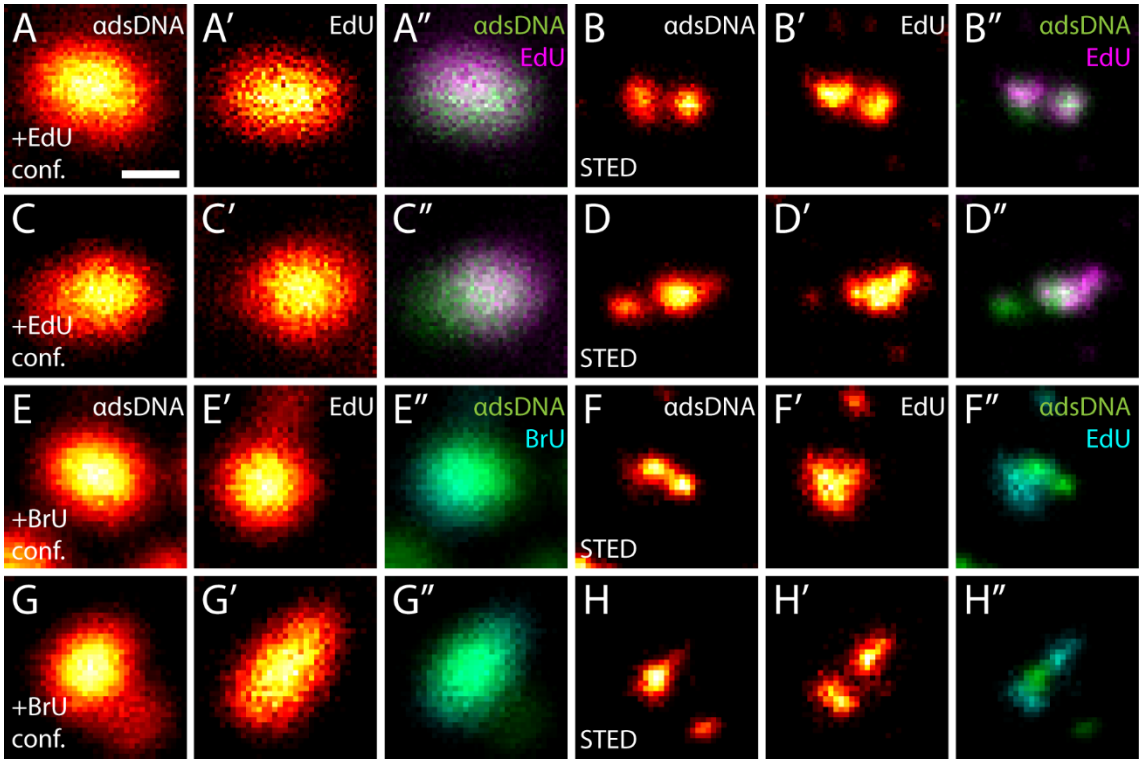

Figure 3.8 Nanoscopy of active nucleoids: HDFa cells were incubated with 20 µM EdU for 70 min or 20 µM BrU for 25 min. Afterwards EdU was labeled with Alexa Fluor 488 within a CuAAC and the signal enhanced by indirect immunofluorescence. BrU and DNA were detected with antisera. **A-B'')** Images in A-A'' show a single EdU positive nucleoid signal. STED nanoscopy of the same structure in B-B'' reveals that the confocal images in A-A'' originate from two EdU positive nucleoids. **C-D'')** Like in A-A'', C-C'' exhibit a single EdU positive nucleoid signal. STED nanoscopy of the same section in D-D'' resolves two single nucleoids only one being EdU positive. **E-F'')** Confocal images in E-E'' display a single BrU positive nucleoid signal. Applying STED nanoscopy in F-F'' leads to the identification of two nucleoids but only one is positive for BrU. **G-H'')** Confocal microscopy in G-G'' displays another single BrU positive nucleoid signal. In contrast, nanoscopy of the same section in H-H'' displays a single nucleoid with two separate BrU spots. Raw data with 5% subtraction of the background. Scale bar: 200 nm

After the establishment of two color STED to visualize single nucleoids engaged in replication and transcription, three color STED to visualize single nucleoids which are positive for both labels was applied.

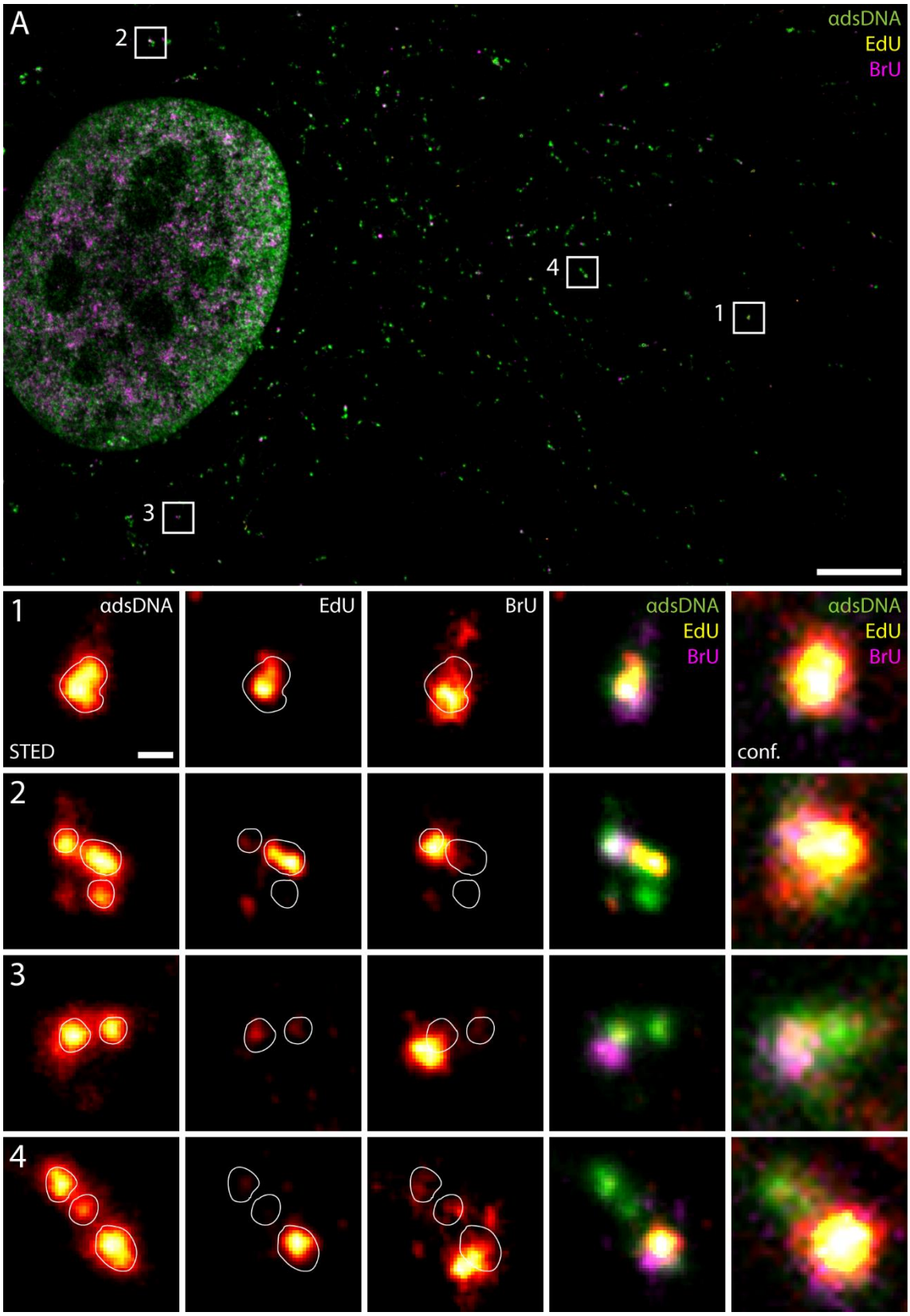

Figure 3.9 Three color nanoscopy to visualize the overall activity of single nucleoids: HDFa cells were incubated with 20 µM EdU for 70 min or 20 µM BrU for 25 min. EdU was afterwards labeled with Alexa Fluor 488 within a CuAAC and the signal enhanced by indirect immunofluorescence. BrU and DNA were detected with antisera. **A)** Three color STED nanoscopy of DNA (green), EdU (replication, fire) and BrU

(transcription, magenta). 1-4) Sections from A divided into the single STED channels. The merged image is shown as a STED image and a conventional confocal image. All STED images are shown as raw data with 8% subtraction of the background. The confocal images were interpolated to enhance the pixel number by a factor of 2.5. Scale bar in A: 5 µM and in 1-4: 200 nm.

To test if three color nanoscopy is suitable to visualize single nucleoids involved in replication and transcription within the same measurement, HDFa cells were incubated with EdU and BrU simultaneously. The incorporated EdU and BrU were labeled together with the nucleoids and STED nanoscopy was applied afterwards. The dyes used, detection channels and parameters for three color STED can be found in the materials and methods section. A combination of nucleoside analogues and three color STED enables one to identify single nucleoids positive for EdU, BrU or even both nucleosides as well as inactive nucleoids (Fig 3.9). Fig. 3.9 shows a very large section of an HDFa cell recorded with three color STED nanoscopy.

Four nucleoids and cluster of nucleoids are highlighted. Single DNA, EdU and BrU channels are shown, as well as a merged image. For comparison the merged image is additionally displayed as a confocal image. Fig 3.9 (1) shows a single nucleoid positive for EdU and BrU. Like shown above the BrU signal is slightly shifted to the nucleoid signal, whereas Fig 3.9 (2) displays a cluster of nucleoids. Within this cluster, one nucleoid is positive for EdU and another nucleoid shows a BrU signal. A third nucleoid is negative for both. The confocal image of the same cluster reveal none of these information. Fig 3.9 (3) shows two nucleoids in close proximity from which only one exhibits a BrU signal. Finally, Fig. 3.9 (4) shows a cluster of two inactive nucleoids and a third nucleoid which is positive for EdU and BrU.

In conclusion, identification of single nucleoids positive for EdU and BrU with multicolor nanoscopy is reliable accomplished. As the incubation time with both nucleoside analogues is set to a minimum, EdU and BrU positive nucleoids should represent structures with ongoing replication and transcription. Multicolor STED nanoscopy, requires all fluorophores feature an emission maximum within a similar spectral range. This is a drawback, especially using three color STED nanoscopy (Tab 2.3 in the Material and Methods section). Therefore crosstalk between the fluorescent dyes can be a significant issue. To solve this problem, a data processing pipeline was used to subtract the specific crosstalk for each pixel. Furthermore, semi-automated analysis was necessary to quantify the amount of single nucleoids engaged in replication and transcription within the images, because cells contain up to several hundreds of nucleoids. During the analysis of the STED images, the average diameter of nucleoids was estimated to ensure that the achieved resolution is sufficient to identify single

nucleoids. Furthermore, EdU and DNA signal are a nearly perfect colocalization whereas BrU and DNA where also slightly shifted. This difference in the signal pattern was also analyzed during the evaluation.

3.3.1 Automated analysis of single nucleoids

The STED images were postprocessed with different scripts for data evaluation. This data processing pipeline was essential to analyze mitochondrial replication and transcription as it enables one to analyze a large number of cells and single nucleoids later in this study. The postprocessing of the images included crucial steps like removing the crosstalk of the different fluorophores in the EdU, BrU and DNA channel. Afterwards single EdU and BrU as well as DNA signals were semi-automatically recognized to detect nucleoids engaged in transcription or replication. During the evaluation of the images, additionally two parameters were analyzed. First, the average size of single nucleoids in the different experiments was determined (Tab 3.2). This value was important to ensure that that in every experiment indeed the activity of single nucleoids was investigated. Previous studies revealed an average diameter of single nucleoids measured with nanoscopy of 99 nm (Kukat and Wurm et al., 2011; decorated with antibodies; STED) or 110 nm (Brown et al., 2011; without antibodies; dSTORM). Whereas in these studies nanoscopy was optimized towards the best resolution to determine nucleoid size, the current study focused on the regulation of mitochondrial DNA.

Table 3.2 Determined sizes of nucleoids with different dyes and fluorophores in this work and previous studies:

	Fluorophore	Nucleoid diameter	Microscope technique
This study (section 3.5 transcription staining)	Abberior StarRed	94 nm	2C-STED
This study (section 3.5 replication staining)	Alexa Fluor 594	111 nm	2C-STED
This study (section 3.4)	Atto 490ls	120 nm	3C-STED
Kukat and Wurm et al., 2011	Abberior StarRed	99 nm	1C-STED
Brown et al., 2011	PicoGreen	110 nm	dSTORM

As a result, multicolor STED nanoscopy and the usage of different fluorophores were necessary, which decreased the possible resolution. Although the average diameter of single nucleoids appears slightly enlarged in the three color STED measurements, in all

experiments nucleoids display a size, comparable to the size of single nucleoids described in previous studies (Tab 3.2).

Another important value was the distance between detected EdU and BrU spots to the mtDNA. EdU and BrU spots were detected according to the intensity of their fluorescence. Afterwards, the distance between each EdU or BrU spot and the closest nucleoid was determined (Fig 3.10).

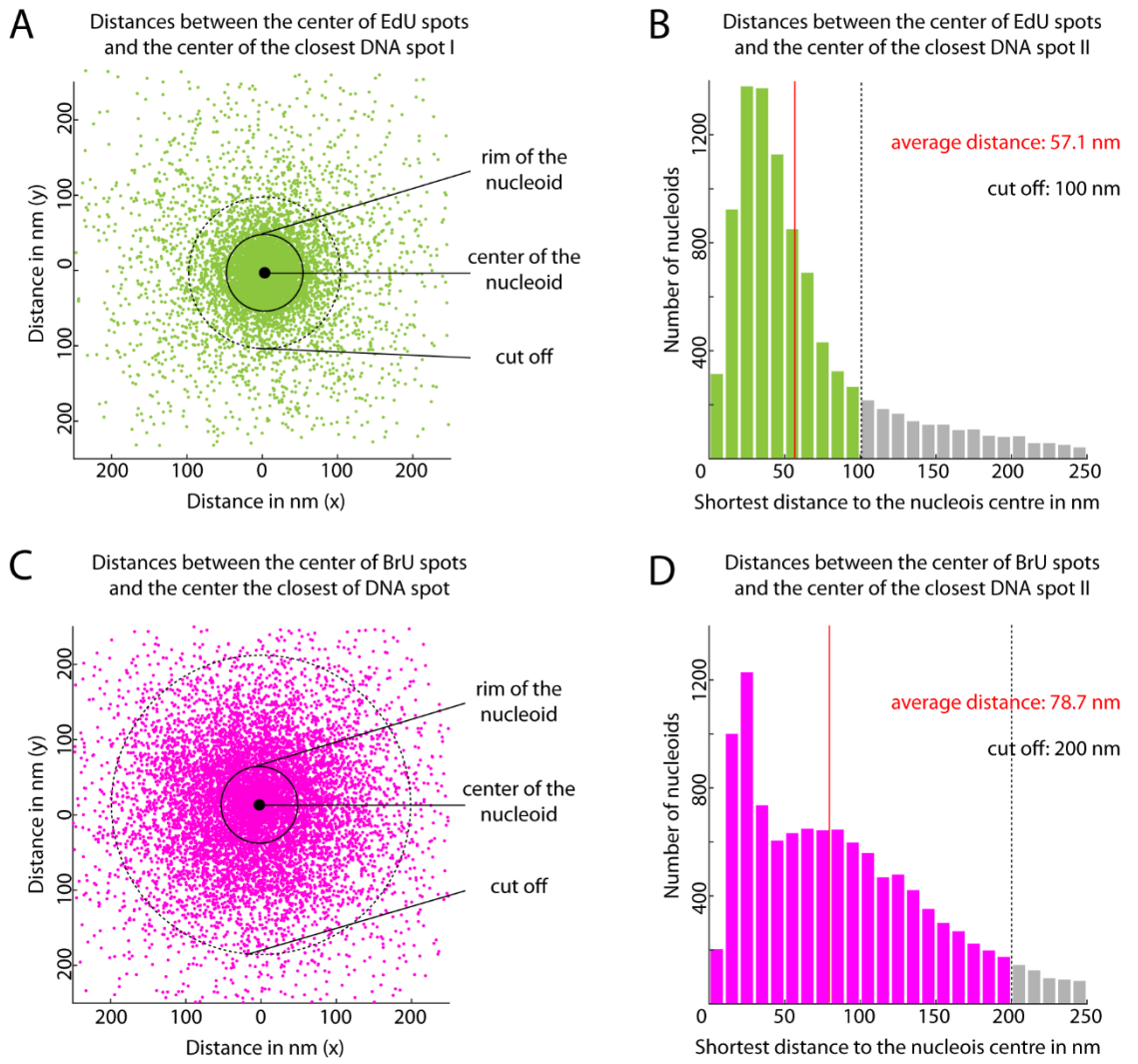

Figure 3.10 Difference in the EdU- and BrU-signal pattern in relation to the mtDNA: Distances between the centers of EdU or BrU spots and the closest mtDNA signal. **A and B)** The majority of EdU spots are located in close proximity to nucleoids and reveal overlapping signal with the mtDNA. In average, the center of every detected EdU (including green and gray bars) signal is 57.1 nm away from the center of the next mtDNA molecule. To separate between background and specific EdU signal was dismissed when the distance to the nearest mtDNA was above 100 nm. The rim of the nucleoids was delineated in (A) as a 100 nm structure. **C-D)** BrU spots do not always colocalize with mtDNA but are adjacent. In average the distance between the center of an identified BrU signal and the closest mtDNA is 78.7 nm. To separate between background and specific BrU signal was dismissed when the distance to the nearest mtDNA was above 200 nm. The rim of the nucleoids was delineated in (A) as a 100 nm structure.

The distance from the center of an EdU or BrU spot, independent if it was counted as a specific signal or as background, to the center of the nearest DNA revealed that on average EdU spots (57.1 nm distance) are closer to the nucleoids than BrU spots (78.7 nm). This confirms the observation that EdU signal appear within mtDNA whereas the majority of the BrU signal is slightly shifted to the DNA. This is a very strong hint that both nucleosides label different structures as they reveal a different signal pattern that fits to the respective expected localization (Fig 3.10). EdU is expected to locate closer to the nucleoid center as it is incorporated into the DNA itself. In contrast, BrU is incorporated into the RNA that is expected to be more often at the rim of the nucleoid or detached from the mtDNA after its synthesis.

In the EdU detection channel, as well as in the BrU detection channel, background cluster of signal were detected during the image analysis. A very efficient way to distinguish between background signal and specific signal that is in close proximity to nucleoids was the introduction of a cut off value (Fig 3.10). If the distance between a detected EdU spot and the closest DNA spot was above 100 nm, it was dismissed whereas the cut off value for specific BrU signal was 200 nm. These values were constant throughout all experiments and determined manually after an analysis of all measured samples.

The established approaches to label single nucleoids engaged in transcription and replication were used to analyze the behavior of nucleoids in wild type cells and the regulation of mitochondrial transcription and replication by POLRMT and TEFM. The automated image analysis assured a higher throughput of images.

3.4 Analysis of the functional heterogeneity of single nucleoids

Single cells contain multiple copies of the mitochondrial DNA and therefore a high number of nucleoids. STED analysis revealed that single human fibroblasts contain over 1100 nucleoids in average (Kukat and Wurm et al., 2011). So far, no functional difference between these nucleoids in a single cell could be identified, only increased replication rates of mutant mtDNAs were reported (Wallace, 1989; Wallace, 1992). In this study a fluorescence based approach to detect single nucleoids engaged in transcription and replication with STED nanoscopy was developed enabling the study of nucleoid activity in detail. In this section, human fibroblasts (HDFa) were analyzed to tackle the question if nucleoids within a single cell are equally active or if different subpopulations of nucleoids that differ in their function can be identified.

For this analysis HDFa cells were incubated with BrU to label transcription and EdU to label replication. The BrU incubation time was set to 25 min. Longer incubation times

led to a dissociation of the synthesized RNAs from the respective nucleoids resulting in a labeling of the total mitochondrial matrix (Supplement Fig. 9.4). In contrast, once EdU is incorporated into mtDNA it remains part of the nucleoid until the whole structure is degraded. Hence, longer incubation times of EdU enable one to analyze the amount of mitochondrial replication over longer periods. Therefore short incubation times with EdU can be used to mark current replication whereas longer incubation times can be used to identify nucleoid replication during a long period.

3.4.1 Nucleoids reveal subpopulations of active and inactive nucleoids

Fig 3.11 shows data of HDFa cells that were treated with BrU for 25 minutes and EdU for 70 minutes. As mentioned before, these were the shortest incubation times with the respective nucleoside analogues that enabled one to detect specific signals. Thereby ensuring that the nucleoside analogues label predominately ongoing activity of nucleoids. After labeling nucleoids simultaneously with both nucleoside analogues, three color STED was used to visualize single active nucleoids. Afterwards, the fractions of nucleoids engaged in transcription or replication, as well as structures engaged in both processes were estimated. Fig 3.11 A-D shows exemplary STED data of single nucleoids within HDFa cells treated with BrU and EdU simultaneously. The merged image as well as the single color channels of DNA (green), BrU (magenta) and EdU (green) are shown. Fig 3.11 A displays a nucleoid neither engaged in transcription, nor in replication. Fig 3.11 B shows a single nucleoid with incorporated BrU and Fig 3.11 C a single nucleoid with incorporated EdU. Finally, Fig 3.11 D reveals that nucleoids were engaged in transcription and replication simultaneously.

More than 50 cells with over 18,000 nucleoids in total were analyzed and the results are shown in Fig 3.11 E-H. The column chart in Fig 3.11 E reveals that 81% of the analyzed nucleoids showed no signs of transcription or replication whereas only 19% were involved in at least one of these processes. 11% of the nucleoids were only engaged in transcription and 5% were only engaged in replication. Nucleoids involved in both, transcription and replication reached a proportion of about 3%. In Fig 3.11 F nucleoids engaged in transcription and replication were divided into structures only engaged in one process or in both processes combined. 22% of all nucleoids engaged in transcription were also engaged in replication and 60% of all nucleoids engaged in replication were simultaneously engaged in transcription.

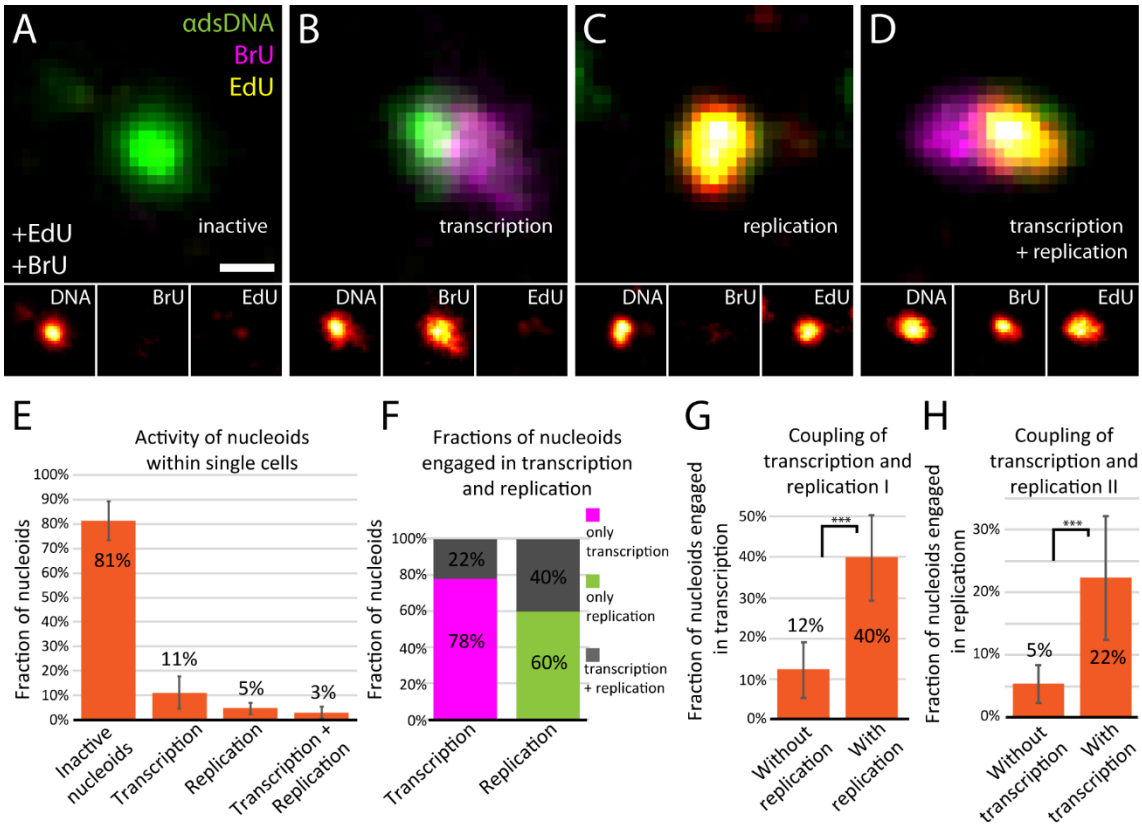

Figure 3.11 Activity of mitochondrial nucleoids: HDFa cells were incubated with 20 µM EdU for 70 min and 20 µM BrU for 25 min. Cells were afterwards processed to label the DNA, incorporated BrU and EdU. More than 50 cells with a total amount of over 18,000 nucleoids were measured with STED nanoscopy. **A-D)** Representative nucleoids (green) without incorporated EdU and BrU (A), with incorporated BrU (magenta; B), with incorporated EdU (green; C), and with an incorporation of both nucleoside analogues (D). **E)** Column chart showing the different activities of nucleoids within a single cell. The majority of nucleoids (81%) were inactive whereas only 19% were involved in transcription and/or replication. 11% of the nucleoids were only engaged in transcription and 5% were engaged in replication only. About 3% of the nucleoids within cells were engaged in both processes. **F)** Nucleoids engaged in transcription respective replication were divided in fractions of nucleoids only engaged in one or engaged in both processes. 22% of all nucleoids engaged in transcription were also engaged in replication. In contrast, 60% of all replicating nucleoids showed also transcriptional activity. **G)** Fraction of nucleoids engaged in transcription when they were simultaneously engaged in replication or when they were not replicating. Among nucleoids not engaged in replication, 12% were engaged in transcription. In contrast, among replicating nucleoids, 60% were engaged in transcription. **H)** Fraction of nucleoids engaged in replication when they were simultaneously engaged in transcription or when they did not show ongoing transcription. 5% of all nucleoids not engaged in transcription were engaged in replication. Among nucleoids that showed transcription, 22% were engaged in replication. Error bars display the standard deviation. Three asterisk represent a p value below 0.0001. Scale bar: 100 nm

In Fig 3.11 G nucleoids were classified into two groups: structures engaged in replication and structures without signs of replication. Replicating nucleoids (60%) were significantly more often engaged in transcription than non-replicating nucleoids (12%). A similar analysis is shown in Fig 3.11 H. In this column chart nucleoids were classified into a population that were engaged in transcription and nucleoids that did not reveal signs of transcription. The fractions of nucleoids engaged in replication were shown for

both subpopulations. Among nucleoids with ongoing transcription the fraction with EdU incorporation (22%) is significantly higher than the fraction without signs of transcription (5%).

In conclusion, the analysis of cells treated with nucleoside analogues for a very short period shows that nucleoids during replication have a higher probability to be also active in transcription and vice versa. This is a strong hint for the existence of at least two subpopulations of nucleoids within single cells, active ones and inactive ones. To further investigate this observations, cells were treated with EdU for increasing incubation times. This dataset should help to determine if all nucleoids within a cell are equally engaged in replication, or if again different subpopulations appear.

3.4.2 Different EdU incubation times reveal two populations of nucleoids

The analysis of EdU incorporation over increasing incubation times enables one to determine the replication rate of nucleoids. Moreover, it is possible to determine if all nucleoids are equally engaged in replication or if different levels of replication activity of nucleoids are present within a single cell.

First it was analyzed, if the functional heterogeneity that was observed for a short time scale (section 3.4.1) can also be observed when nucleoids activity is analyzed for a longer time scale.

HDFa cells were incubated with EdU for different incubation times between 1.5 h and 72 h. Nucleoids within the cells were afterwards labeled with antibodies against dsDNA. Incorporated EdU was additionally visualized. Samples were then measured with two color STED nanoscopy and the fraction of EdU positive nucleoids was determined for each incubation time (Fig 3.12).

Fig 3.12 A-D reveals that upon increasing incubation time with EdU more nucleoids (green) show EdU incubation (magenta). The column chat in Fig 3.12 E displays the increase of EdU-positive nucleoids within single cells.

To determine whether nucleoids within a cell are equally engaged in replication or if two subpopulations can be identified two different models were fitted to the data (Fig 3.12 F, detailed models: Supplement Fig. 9.6). The first model (black) is based on the assumption that every single nucleoid shows an equal level of activity and is therefore equally engaged in replication. The second model (red) is based on the previous observation that at least, two subpopulations of nucleoids can be identified within a single cell, namely active and inactive ones (Fig 3.11).

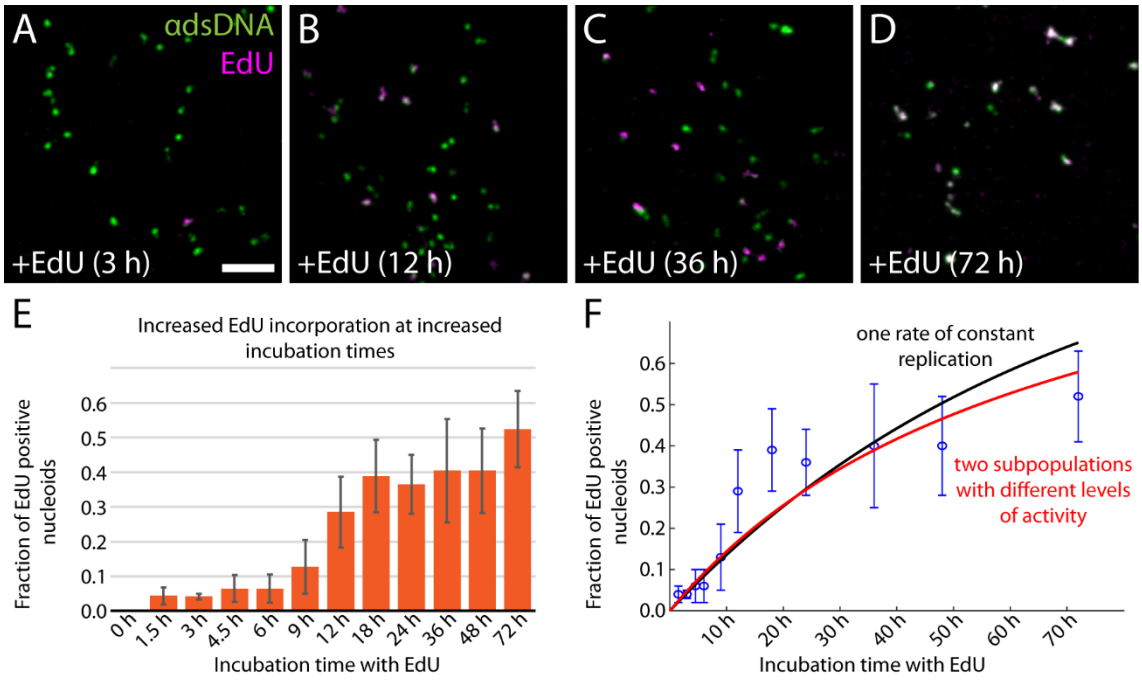

Figure 3.12 EdU incorporation at increasing incubation times: HDFa cells were treated with EdU for different periods of time from 90 min to 72 h. Afterwards the incorporated EdU was visualized and nucleoids were labeled with antibodies against dsDNA. **A-D)** Representative sections of HDFa cells upon different incubation times with EdU. The images reveal that an increasing amount of nucleoids (green) additionally labeled with EdU (magenta). **E)** Column chart displaying the increased fraction of EdU-positive nucleoids at longer incubation periods. **F)** Two different models were fitted to the data shown in (E). One model was based on the estimation that all nucleoids are equally engaged in replication (black) and a second model was based on the assumption that two subpopulations with a different level of activity are present in single cells (red). Error bars show the standard deviation.

Both models do not perfectly fit to the amount of replicating nucleoids upon different incubation times with EdU. The raw data display a very fast increase of the fraction of EdU positive nucleoids within the first 6 to 18 h. Afterwards, the proportion of nucleoids engaged in replication, during the chosen incubation time with EdU, reveals only a slight additional increase. Both tested models do not reflect the different involved kinetics. However, the model based on two different subpopulation with different levels of activity seems to reflect the raw data more precisely than the mono-exponential model based on a single population within the cell. Further parameters like degradation of nucleoids have to be analyzed to develop a model that fits to the shown data.

In conclusion, although the tested model based on two subpopulations do not perfectly fit to the data, it can be ruled out that nucleoids within a cell display a uniform activity.

3.4.3 Activity of nucleoids does not depend on their distance to the nucleus

The previous experiments revealed the existence of at least two subpopulations of nucleoids: active and inactive ones. It was tested if nucleoids activity depends on their distance to the nucleus as some properties of mitochondria are correlated with distance to the nucleus. One example for that dependence is the abundance of MICOS proteins of the inner mitochondrial membrane (Jans and Wurm et al., 2013). Furthermore, less nucleoids can be identified in the periphery of the cell (Kukat and Wurm et al., 2011).

To analyze the distribution of the engagement of nucleoids into transcription and replication the same dataset like in 3.4.1 was used. HDFa cells were incubated with BrU and EdU for only a short period to label ongoing activity

Fig 3.13 shows how current transcription and replication are distributed within the cell. Fig 3.13 A displays an HDFa cell after short incubation times with BrU and EdU. The shortest distance of each nucleoids center to the outer rim of the nucleus was estimated. Fig. 3.13 B displays the normalized amount of nucleoids with increasing distance to the nucleus. As mentioned above, it becomes apparent that the amount of nucleoids decreases in the periphery. For Fig 3.1 C-E the amount of nucleoids for each distance to the nucleus was always determined in relation to the number of total nucleoids. Fig. 3.13 C reveals that the fraction of active and inactive nucleoids remains constantly at about 20% from perinuclear areas into the periphery. Fig 3.13 D shows the distribution of replication and transcription within single cells. Both processes appear to be uninfluenced by the distance of the nucleoid to the nucleus. Fluctuations of the values at greater distances from the nucleus are the result of a smaller sample size as less nucleoids can be identified in the periphery of cells. Fig 3.13 E displays the distribution of nucleoids only engaged in transcription or replication, or involved in both processes simultaneously. Again, the position of the nucleoid within the cell shows no effect on nucleoids current activity.

The presented data in Fig 3.11 and 3.12 present evidence that nucleoids within a single cell form two different subpopulations, namely an active and an inactive population. Whether a nucleoid belongs to the active or inactive subpopulation does not depend on its distance to the nucleus (Fig 3.13). Parameters which are involved in the activation of nucleoids have to be identified in the future.

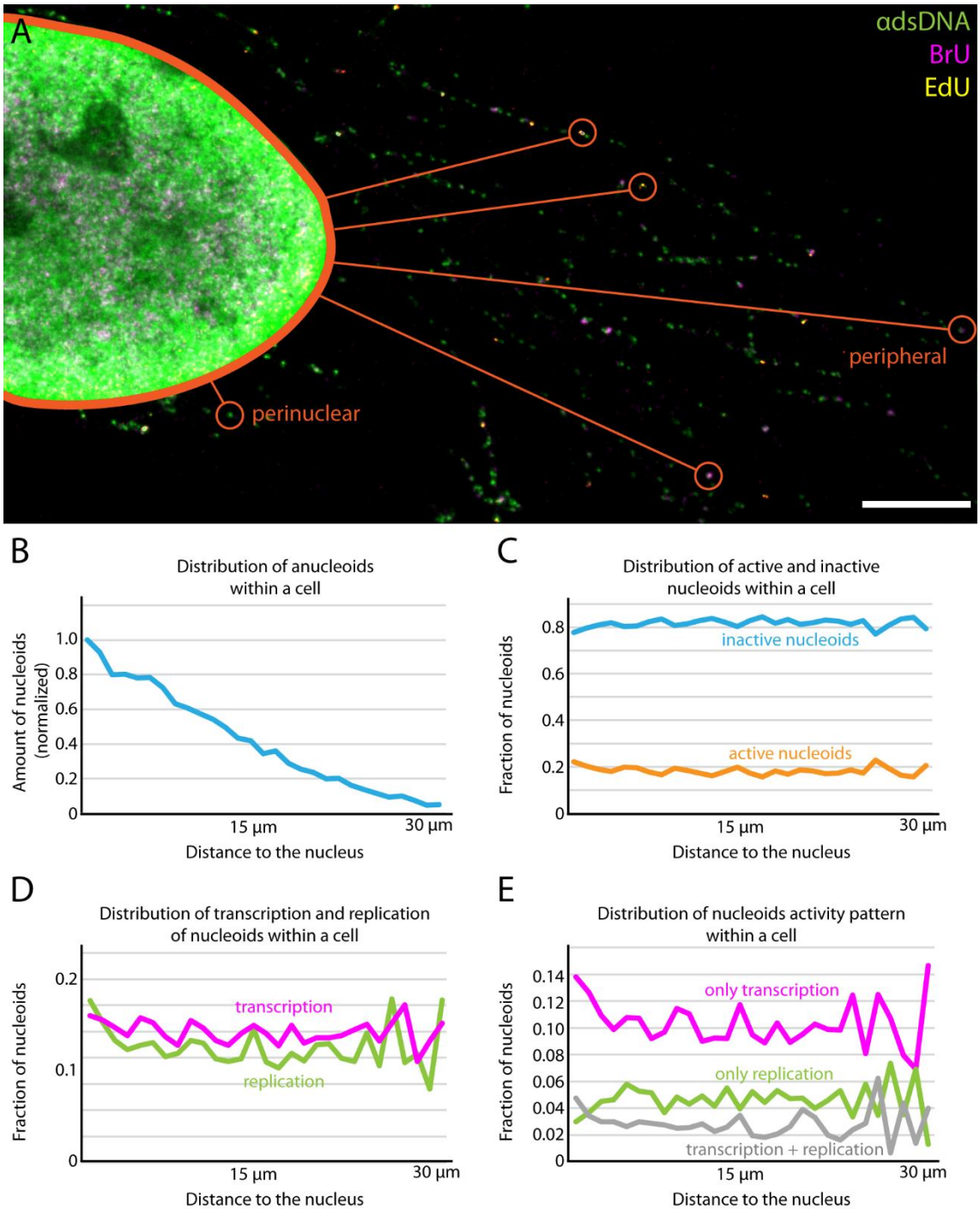

Figure 3.13 Intracellular distribution of mitochondrial transcription and replication: HDFa cells were incubated with 20 µM EdU for 70 min and 20 µM BrU for 25 min. Cells were afterwards processed to label the DNA, incorporated BrU and EdU. More than 50 cells with a total amount of over 18,000 nucleoids were measured with STED nanoscopy. **A)** Exemplary image to demonstrate the measurement of the distance between nucleus and nucleoid. The shortest distance between the center of each nucleoid signal and the outer rim of the nucleus was quantified. **B)** Within the cell, more nucleoids are located perinuclear than peripheral. When single cells are analyzed, the amount of nucleoids continuously decreases with an increasing distance to the nucleus. **C)** The distribution of active nucleoids engaged in replication and/or transcription was analyzed. The fractions of active and inactive nucleoids remains constant over the increasing distance to the nucleus. **D)** Distribution of nucleoids engaged in transcription and nucleoids engaged in replication was analyzed. No relationship between the distance of a nucleoid to the nucleus and an involvement in one of these processes could be observed. **E)** It was separated between nucleoids

engaged only in transcription or only in replication and nucleoids engaged in both processes simultaneously. Again, the distance to the nucleus does not affect the behavior of nucleoids. Scale bar: 5 µm

Whereas in this section, it was focused on the general activity of the general activity of nucleoids, the next section addresses the switch between transcription and replication of single nucleoids.

3.5 Analysis of single nucleoids in knockdowns of POLRMT and TEFM

Only a few aspects of the regulation of mitochondrial replication and transcription have been identified so far. As both of these processes are coupled in mitochondria, especially the factors that trigger nucleoids towards replication or transcription represent a field of intense research. Recently, the transcription elongation factor TEFM was identified as the molecular switch between transcription and replication of nucleoids (Minczuk et al., 2011; Agaronyan et al., 2015; Posse et al., 2015). Transcription of the light strand can be terminated just 100 bp after the promotor at a sequence termed CSBII. This termination results in the formation of a primer for mitochondrial replication instead of functional transcription. Processivity of mitochondrial transcription throughout CSBII or termination depends on the presence of TEFM (Agaronyan et al., 2015). During transcription the nascent RNA forms a G-quadruplex structure at CSBII (Hillen et al., 2017(2)). In the absence of TEFM, the G-quadruplex structure clashes with the mitochondrial RNA polymerase POLRMT leading to the dissociation of the transcription machinery and a primer that works as a substrate for the mitochondrial DNA polymerase POLγ. If TEFM is present, it forms a RNA exit channel leading to a suppression of an early formation of a G-quadruplex structure of the nascent RNA (Hillen et al., 2017(2)). Hence, the presence of TEFM promotes complete transcription.

Studies of a heterozygous knock out of POLRMT in mice revealed that POLRMT level influence the level of TEFM (Kühl et al., 2015). Reduced POLRMT level has no influence on the level of total transcripts in mice although transcripts from LSP occur with a higher frequency than transcripts from HSP. As LSP-transcription is important for the formation of a replication primer, it was proposed that replication is favored at low POLRMT level (Kühl et al., 2016). The influence of TEFM and POLRMT on nucleoid behavior and activity were analyzed with different biochemical methods like Western and Northern Blots so far (Kühl et al., 2015, Agaronyan et al., 2015; Posse et al., 2015).

In the present study an approach to visualize the activity of single nucleoids with STED nanoscopy was developed. Hence, it can be determined whether single nucleoids are

engaged in replication or transcription. To extend the understanding of how POLRMT and TEFM influence the switch between mitochondrial replication and transcription, single nucleoids upon reduction of these factors were analyzed. To ensure a controlled decrease of POLRMT and TEFM level within the cell, gene expression was reduced by RNA interference.

3.5.1 siPool mediated knockdown of POLRMT and TEFM

Downregulation of proteins via RNA interference provides some advantages compared to complete knockouts. First, the decrease of the protein level can be regulated and varies by adjusting the incubation time with the small interfering (si)RNA or short hairpin (sh)RNA. In contrast, knockouts provide only a single, not variable protein level for investigation. Moreover, experiments based on RNA interference are less time consuming in preparation and offer the possibility to analyze different knock downs and different genetic situations faster.

A drawback of RNA interference is the potential affection of off-targets. The usage of so called siPools reduces the unwanted influence of siRNAs on off-targets and thereby improves the quality of the results (Hannus et al., 2014). siPools consist of about 30 different siRNAs that are all designed against the desired target gene but all affect different off-targets. As every siRNA is only in very low concentration, their influence on each of the different off-targets is reduced to a minimum (see 2.5.1, Hannus et al., 2014). Therefore, to analyze the behavior of single nucleoids upon decreased level of POLRMT or TEFM as well as both factors, protein levels were reduced in U-2 OS cells via the usage of siPools. U-2 OS cells were used here instead of HDFa cells because the primary fibroblasts cannot be transfected with chemical reagents.

U-2 OS cells were incubated with a siRNAs against POLRMT or TEFM as well as an unspecific siPool as a control (Fig 3.14). Afterwards the cells were incubated with antiserum against POLRMT or TEFM to investigate the presence of the proteins. It was shown above that POLRMT localizes to mitochondria (Fig 3.4). Upon treatment with the control siPool, the POLRMT localization pattern appears to be unchanged since strong signals are detected within the mitochondria (Fig 3.14 A). 36 h after transfection with the siPool against POLRMT, the protein level is strongly reduced; no mitochondrial network can be detected but only diffuse fluorescence in the cytoplasm (Fig 3.14 B). After 72 h of gene silencing POLRMT, the signal in the mitochondrial network is still not detectable, but the POLRMT signal in the cytoplasm is further reduced (Fig 3.14 C). Fig 3.14 G shows the results of a Western Blot to determine the protein level of POLRMT and TEFM upon treatment of the cells with siPool against the RNA polymerase. The cells

were transfected with the siRNAs and proteins were extracted after five different incubation times between 24 h and 72 h. In the Western Blot POLRMT and TEFM as well as β-Actin as a loading control were detected. Upon longer incubation times the POLRMT level displays a continuously decrease. It appears that the level of TEFM is slightly increased upon reduction of POLRMT.

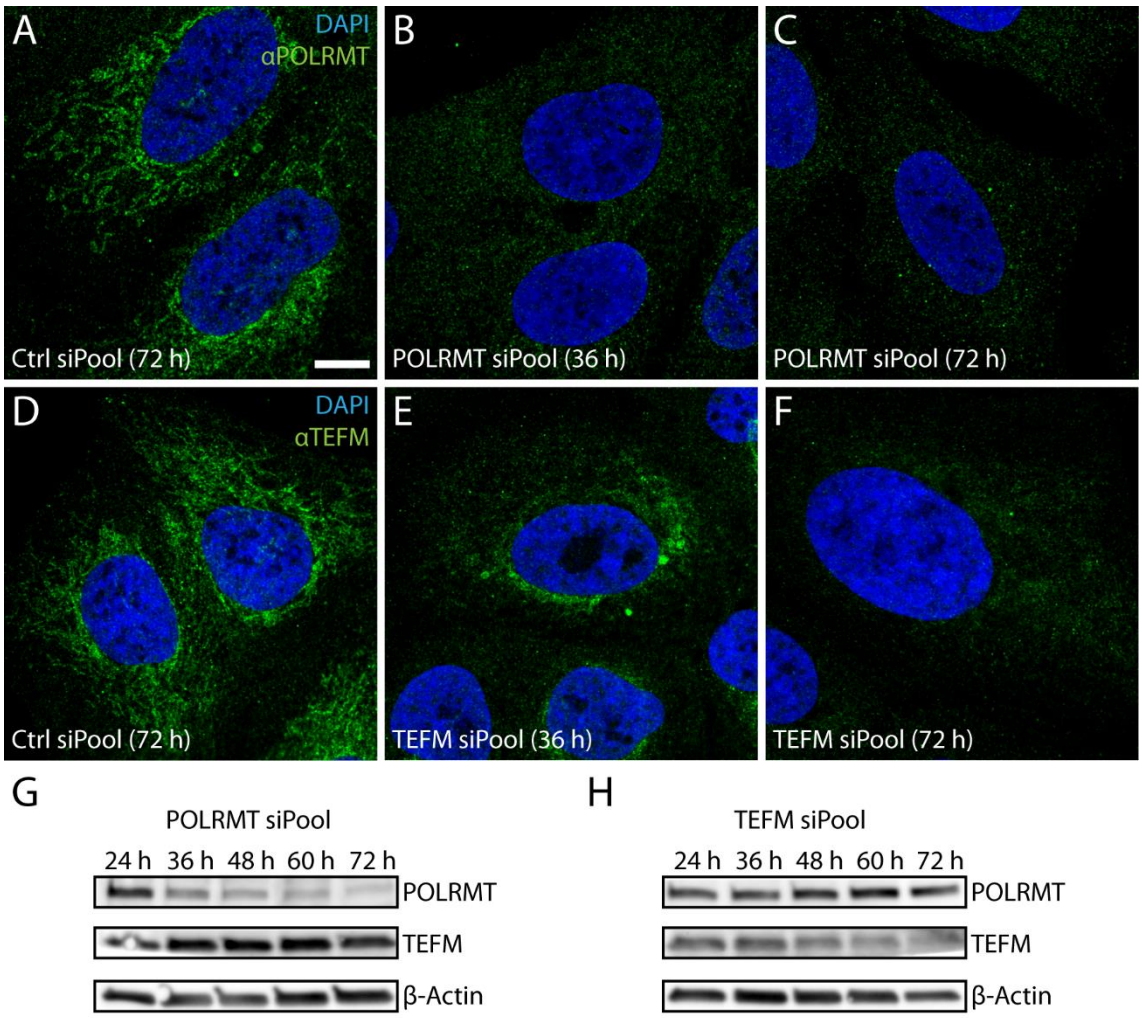

Figure 3.14 SiPool mediated knockdown of POLRMT and TEFM: U-2 OS cells were transfected with 6 µM of the control siPool (Ctrl) and 3 µM siPool against POLRMT or TEFM. **A-C)** Upon treatment with the control siPool for 72 h, POLRMT is visible within the mitochondrial network as was shown in Fig 3.4 (A). When cells were incubated with the siPool against POLRMT, the protein level is efficiently reduced as no mitochondrial network is detected, neither after 36 h of incubation (B), nor after 72 h after transfection. **D-E)** TEFM (green) localizes within the mitochondrial network upon incubation with the control siPool for 72 h (see Fig 3.4, D). 36 h after transfection (E) with the siPool against TEFM, the signal is reduced. However, strong perinuclear TEFM signal can be detected. After 72 h of siPool incubation, a weak signal of TEFM is apparent within the cell. **G)** Western Blot to display the reduction of POLRMT upon siPool treatment. Increasing incubation time leads to an increasing loss of POLRMT. A simultaneous increase of TEFM level can be observed. **H)** A Western Blot showing the decreasing level of TEFM upon increasing incubation time of the siPool against TEFM. A simultaneous increase of POLRMT level can be observed. Scale bar: 10 µm

The effects of a siPool designed against TEFM on U-2 OS cells is shown in Fig 3.14 D-F. Transfection with an unspecific control siPool reveals that the TEFM antibody gives rise to a specific signal within the mitochondria (Fig 3.14 E). 36 h after transfection the amount of TEFM is reduced (Fig 3.14 E). However, distinct signal around the nucleus and weak protein level in the mitochondria are still detectable. After 72 h of siPool incubation, TEFM is further reduced but still detectable (Fig 3.14 F). The immunofluorescence data reveal that the knock down of TEFM occurs slower than the knockdown of POLRMT and it reveals detectable protein level in the mitochondria after 72 h. Similar results are observed during Western Blot analysis of the TEFM knockdown. Fig 3.14 H shows the TEFM levels of U-2 OS cells after five different incubation times between 24 h and 72 h with siRNAs against TEFM. The TEFM decrease appears to be slower than the decrease of POLRMT shown before in Fig 3.14 G. Interestingly, upon reduction of TEFM, the level of POLRMT shows an increasement. In conclusion, siPools can be used to decrease the protein level of POLRMT or TEFM. Several cells were imaged and siPool treatment had a uniform effect on the cells as shown in Fig 3.14. Upon incubation with the siPool, no unaffected cell with a wild type signal pattern could be identified.

Before the nucleoid behavior was analyzed, it was checked whether the down regulation of the mitochondrial polymerase or the elongation factor influence the morphology of the mitochondrial network. Fig 3.15 shows U-2 OS cells 72 h after transfection with an unspecific siPool as a control (A), siRNA against POLRMT (B) or TEFM (C), respectively. Cells were decorated with antibodies against Mic60 to label the mitochondria (green) and against DNA to mark the nucleoids (magenta). The mitochondrial network shows no obvious changes of its morphology upon reduction of POLRMT or TEFM. Furthermore, nucleoids within the mitochondria are still present. Viability of the cells upon POLRMT and TEFM reduction was not determined, but no increased amount of dead cells could be observed.

The tested siPools are very efficient in downregulating of POLRMT or TEFM. However, downregulation of one factor causes a parallel increase of the other protein level (Fig 3.14 G and H). To circumvent this effect, it was tested if a simultaneous transfection with both siPools can cause a double knockdown of both factors. That would additionally allow to analyze the effects of a TEFM reduction in a POLRMT knockdown background and vice versa.

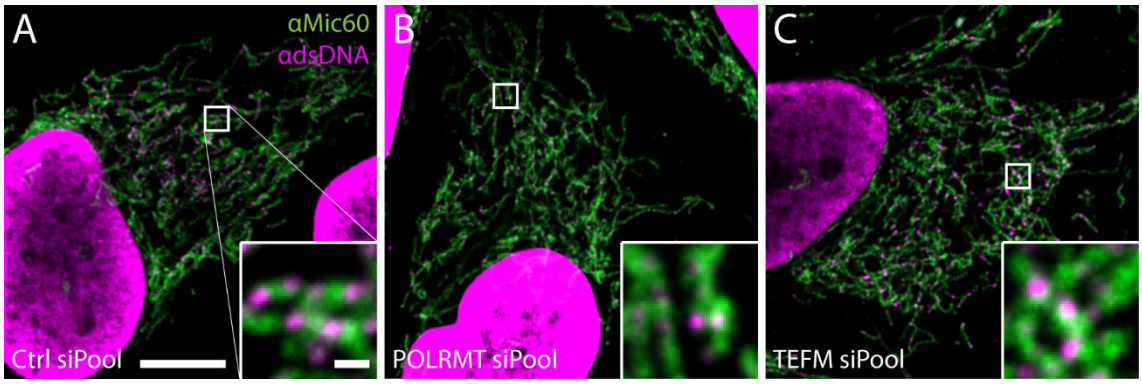

Figure 3.15 The morphology of the mitochondrial network appears unaffected upon POLRMT and TEFM knockdown: U-2 OS cells were incubated with 6 µM control siPool (Ctrl) or 3 µM POLRMT or TEFM siPool. Afterwards the cells were decorated with antisera against Mic60 as a mitochondrial marker (green) and against dsDNA to label nucleoids (magenta). The mitochondrial network appears unchanged upon POLRMT (B) and TEFM (C) knockdown when compared to the control (A). Scale bar: Large image: 10 µM Zoom: 1 µm

3.5.2 Simultaneous knockdown of POLRMT and TEFM

U-2 OS cells were transfected with both siPools to create a double knockdown of TEFM and POLRMT (Fig 3.16). Fig 3.16 A and D show the signal of a POLRMT (A) and TEFM (B) antibody staining. Both protein signals are localized in the mitochondria. After incubation with siPools against both of these factors, the protein level is strongly reduced after 36 h (B and E) and almost gone after 72 h (C and F). Like previously shown for the single knockdowns (Fig 3.14), the decrease of POLRMT occurs faster than the reduction of TEFM. Whereas POLRMT is strongly reduced after 36 h, TEFM shows still strong perinuclear signal. After 72 h of siPool treatment, the signal of TEFM is strongly reduced but still detectable. Measurements of several cells revealed a very uniform protein level and localization for both factors in all cells. No cell with a wild type level of protein could be identified, neither after 36 h nor after 72 h of siPool incubation. Hence, siPools are suitable and reliable to create a double knockdown of POLRMT and TEFM.

The morphology of the mitochondria appears unchanged (Fig 3.16 G-I). Double knockdowns of POLRMT and TEFM, as well as cells transfected with a control siPool, were labeled with antibodies against Mic60 (green) and dsDNA (magenta). Neither 36 h (H) nor 72 h (I) after transfection any obvious alteration of the mitochondrial morphology could be detected compared to the control cells (G).

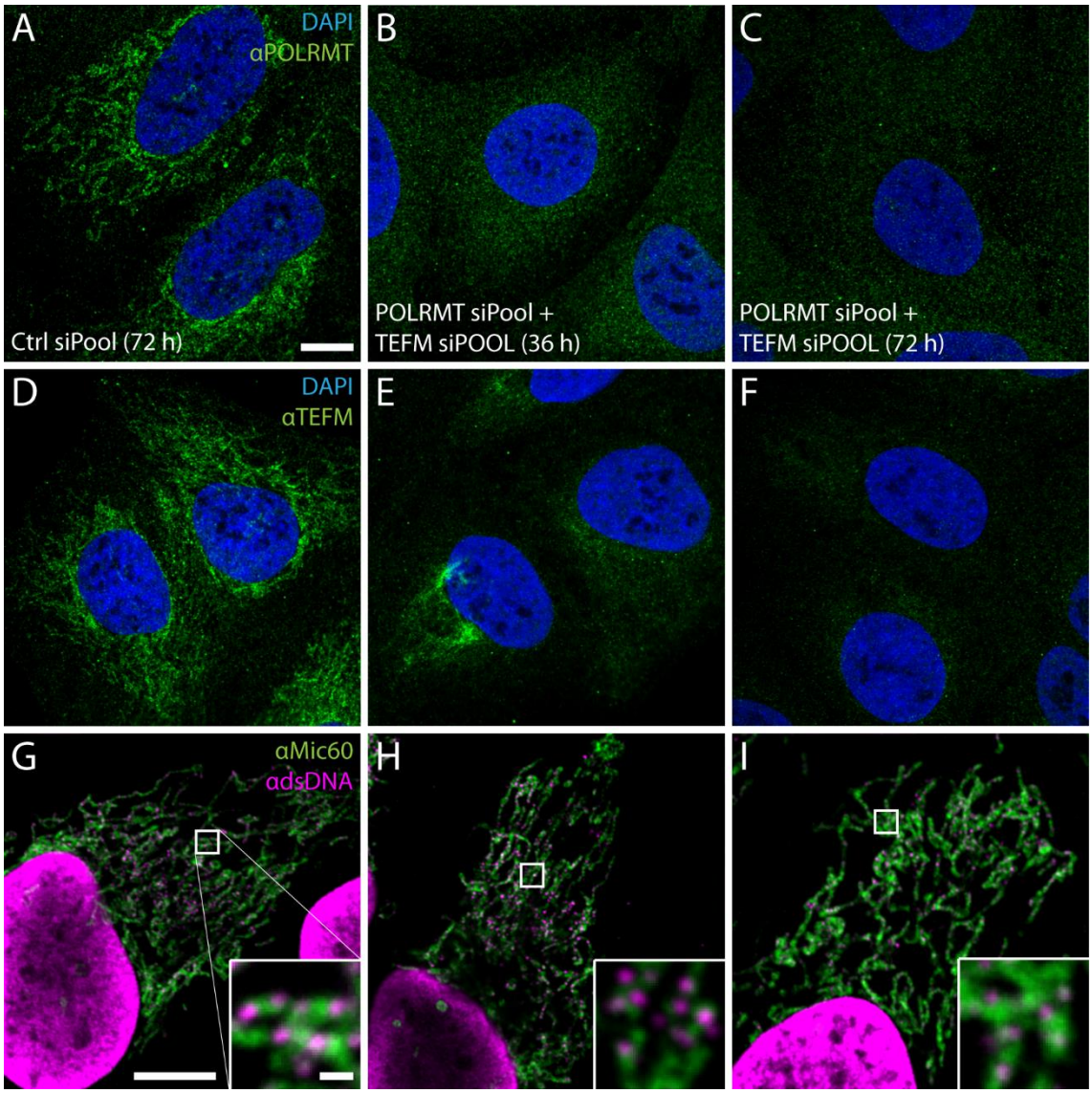

Figure 3.16 SiPool mediated double knockdown of POLRMT and TEFM: U-2 OS cells were transfected with 6 µm of a control siPool or with 3 µM of both, a siPool against POLRMT and TEFM to generate a double knockdown. Cells were incubated with the siPools for 36 h or 72 h. **A-C)** As shown before, POLRMT is located within the mitochondrial network upon treatment with the control (Ctrl) siPool (A). 36 h (B) and 72 h (C) after transfection with both siPools only weak POLRMT signal can be detected within the cell. The signal within the mitochondrial network vanished completely. **D-F)** In the control, TEFM is located within the mitochondria (A). After 36 h of incubation with siPool against TEFM and POLRMT, the signal of TEFM within the mitochondria is reduced but still apparent. In perinuclear regions, strong TEFM signal can be detected as shown before for the single knockdown of TEFM (B, Fig. 3.A). TEFM signal is further reduced after 72 h of siPool treatment (C). **G-I)** Labeling of the mitochondria with antisera against Mic60 (green) and labeling of the nucleoids with antibodies against dsDNA (magenta) reveals that the POLRMT and TEFM double knockdown shows no altered morphology of the mitochondrial network within the cell. Scale bar: 10 µm, scale bar in magnified images: 500 nm

In conclusion, three different genetic situations can be generated with the used siPools. First, knockdown of the RNA polymerase POLRMT with an increased level of TEFM, second, a knockdown of the elongation factor TEFM that displays a slightly increased

level of POLRMT and finally third, both protein levels can be reduced simultaneously. The activity of single nucleoids in all cell lines were analyzed using nucleotide analogues and STED nanoscopy to reveal the influence of POLRMT and TEFM on the regulation of nucleoid activity.

3.5.2 Low POLRMT level trigger nucleoids towards transcription

In the following, nucleoids in knockdowns of POLRMT, TEFM and in a double knockdown of both factors are analyzed concerning their activity in the process of transcription and replication. Therefore, U-2 OS cells 36 h and 72 h after transfection with the respective siPools as well as cells treated with an unspecific siPool as a control and untransfected cells were compared (Fig 3.17). After siPool treatment, the knockdowns were separately incubated with BrU for 20 minutes to label transcription and EdU for 55 min to label replication of nucleoids.

In principle, simultaneous imaging of transcription and replication in U-2 OS cells would be possible. However, in contrast to HDFa cells, simultaneous treatment of U-2 OS cells with BrU and EdU decreases the quality of the BrU-signal compared to cells treated with only one nucleoside.

After nucleoside incubation, cells were decorated with antibodies against dsDNA to detect nucleoids and treated with the respective staining protocol to visualize transcription or replication. Cells were then measured with STED nanoscopy. Fig 3.17 A and B show typical images of visualized transcription (A) and replication (B) in wild type U-2 OS cells. Nucleoids are shown in green and the respective BrU or EdU stain in magenta.

About 250 U-2 OS cells including more than 350,000 nucleoids were measured with two color STED nanoscopy and analyzed automatically to investigate the influence of the different knockdowns. Significance of the observed effects were calculated with an analysis of variance (ANOVA) test. The fractions of nucleoids engaged in transcription or replication are shown in Fig 3.17 C-F. An incubation of the cells with the different siPools for 36 h has no influence on the percentage of nucleoids engaged in transcription (Fig 3.17 C). After siPool treatments as well as in the control, 5-7% of the nucleoids show signs of transcription. Transcription seems to be unaffected in the knockdowns after 36 h.

In contrast, a siPool treatment of 36 h reveals effects of the used siRNAs on the fraction of replicating nucleoids (Fig 3.17 D). A knockdown of POLRMT (4%), TEFM (5%) or a double knockdown against both proteins (5%) exhibit a significant decrease of

replication compared to cells treated with the control siPool (8%). However, the control reveals a slight increase of replication compared to the wild type (7%). As a result, the fraction of replicating nucleoids in the TEFM knockdown and POLRMT + TEFM double knockdown is not significantly decreased compared to the wild type. The reduction of replicating nucleoids in the POLRMT knockdown remains significant compared to the wild type.

72 h after transfection with the siRNAs, the proportion of single nucleoids engaged in transcription is increased in the POLRMT knockdown (11%) in relation to the other knockdowns (TEFM: 5%, POLRMT +TEFM: 6%) and the wild type (8%; Fig 3.17 E) as well as the control (8%). In contrast, the amount of nucleoids engaged in transcription in the TEFM knockdown cells is significantly decreased, whereas the double knockdown reveals only a slight reduction. Finally, the fraction of nucleoids engaged in replication after 72 h of siPool treatment were analyzed (Fig 3.17 F). It becomes apparent that the proportion of nucleoids engaged in replication upon reduced POLRMT level (2%) is strongly reduced compared to the remaining samples. The fraction of replicating nucleoids in the POLRMT + TEFM double knockdown (4%) shows also a significant decrease related to wild type cells (7%), and the control (9%). Although the TEFM knockdown induces also a reduction of nucleoids engaged in replication, this difference is not significant.

To illustrate the different involvement of nucleoids in transcription or replication, a ratio between the fraction of replicating nucleoids and the ones engaged in transcription was calculated. This ratio was afterwards normalized to the quotient of the wild type cells (Fig 3.17 G-H). In the column charts the red line represents a ratio of 1. Values below 1 describe nucleoids which are more triggered towards replication in relation to the wild type cells and a value above 1 is the result of an increased amount of nucleoids engaged in transcription.

The nucleoid activity within cells after 36 h of siRNA treatment is shown in Fig 3.17 G. Nucleoids in the POLRMT knockdown appear to be triggered towards transcription. This tendency is strengthened when the knockdown cell lines after 72 h of siPool treatment are analyzed (Fig 3.17 H). Nucleoids within the POLRMT knockdown reveal increased involvement into transcription. TEFM knockdown cells reveal a slight shift towards mitochondrial replication. The remaining samples reveal similar ratios of transcription and replication.

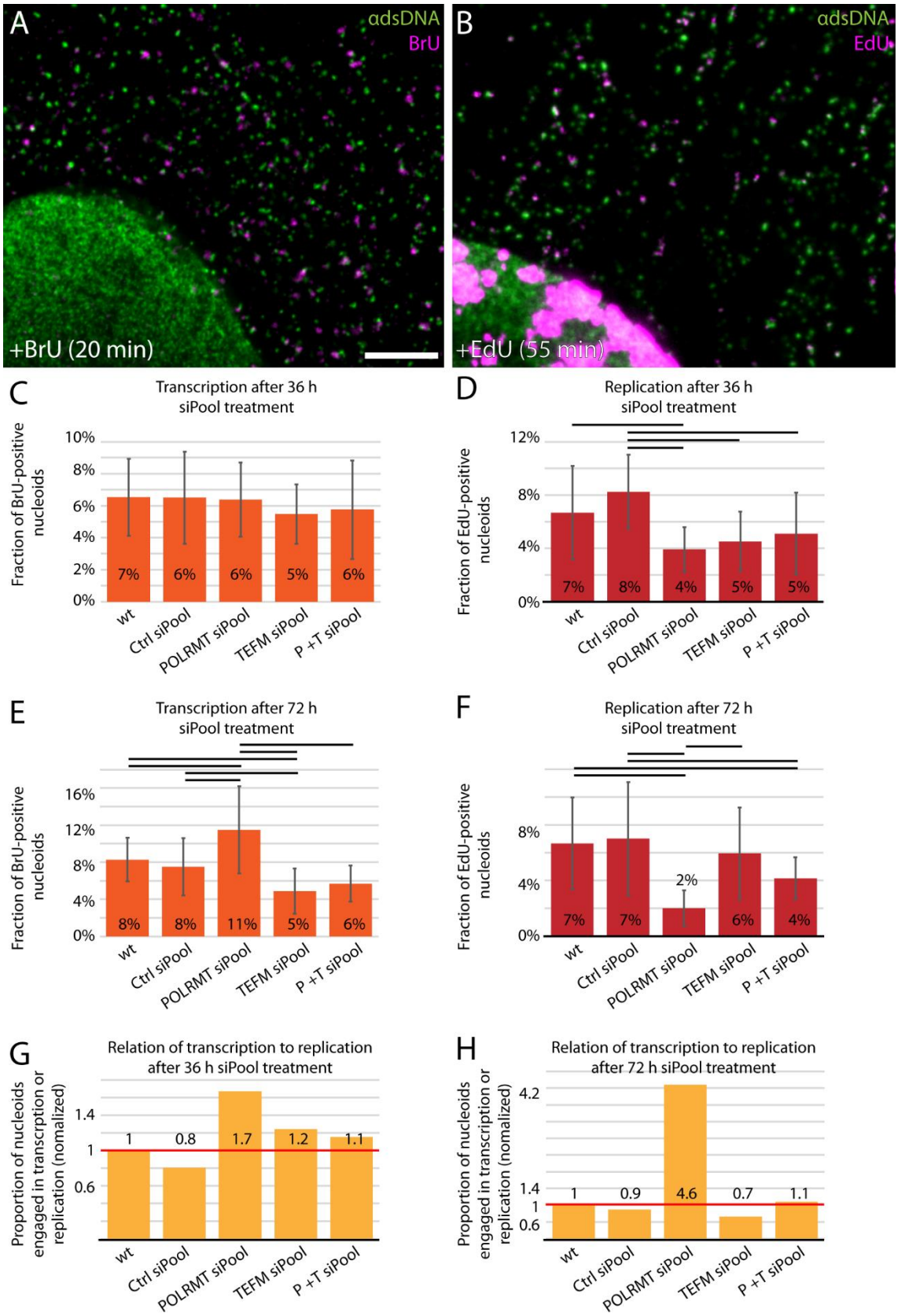

Figure 3.17 Low POLRMT level trigger nucleoids towards transcription: U-2 OS cells were incubated with siPools for 36 h or 72 h, respectively. An unspecific control siPool as well as siPools against POLRMT, TEFM and against POLRMT and TEFM together (P+T) were used. Cells were treated with EdU to label replication for 55 min or with BrU for 20 min to mark transcription. About 250 cells with over 350,000 nucleoids were

analyzed. **A and B)** Section of an wild type U-2 OS cell labeled with antisera against dsDNA (green) and additional visualization of transcription (magenta, A) or replication (magenta, B). **C)** Fraction of nucleoids engaged in transcription after 36 h of siPool treatment. No significant differences are detected. **D)** Proportion of nucleoids engaged in replication 36 h after transfection with the siPools. Horizontal bars indicate a significant difference. Cells after siPool treatment against POLRMT reveal a significant lower fraction of replication nucleoids compared to the control siPool and the wild type. **E)** Fraction of nucleoids engaged in transcription after 72 h of siPool treatment. Horizontal bars indicate a significant difference. After 72 h of incubation with a siPool against POLRMT, transcription is significantly increased compared to all other samples. In contrast, the siPool against TEFM caused a significant decrease of transcription compared to the control siPool and the wild type. **F)** Proportion of nucleoids engaged in replication 72 h after transfection with the siPools. Horizontal bars indicate a significant difference. 72 h after transfection with siPool against POLRMT, replication is reduced compared to every other sample. The double knockdown of POLRMT and TEFM reveals a significant decrease of replicating nucleoids compared to the wild type and control cells. **G and H)** The fraction of nucleoids engaged in transcription is divided by the proportion of replicating nucleoids to calculate a value representing nucleoid activity. This value was normalized to the wild type. If a value is below 1, nucleoids are more triggered towards replication compared to the wild type. If a value is above 1, nucleoids tend to be engaged in transcription. After 36 h treatment with the siPools (G), the POLRMT knockdown reveals nucleoids that tend to be engaged in transcription. The other sample shows no clear difference compared to the wild type. After an incubation of 72 h with the siRNAs, the activity of nucleoids in the POLRMT knockdown is shifted towards transcription whereas the TEFM knockdown is slightly shifted towards replication. The other samples show no clear difference compared to the wild type. Scale bar: 2 µm, error bars indicate the standard deviation, indicated significance was calculated with an OneWay ANOVA using α=0.05.

In conclusion, a reduction of POLRMT triggers nucleoids towards transcription. This effect vanishes completely when TEFM levels are simultaneously reduced as is indicated by the data of the POLRMT + TEFM double knockdown. Hence, the reduction of TEFM stimulates replication of nucleoids in a POLRMT knockdown background. A loss of TEFM alone reveals only a slight shift towards mitochondrial replication. However, the general activity in the TEFM knockdown as well as in the double knockdown is decreased. For the first time, these data reveal on single nucleoid level, the nucleoids are triggered towards replication or transcription by nuclear factors and that these factors also mediate nucleoids general level of activity.

During the analysis of the STED images, it was apparent that nucleoids in TEFM knockdown cells appear larger and tend to form cluster resulting in enlarged structures which cannot be further resolved. These enlarged structures are always EdU positive. As a result, the slightly decreased fraction of replicating nucleoids in TEFM knockdown cells could partially be a result of the clustering of EdU positive nucleoids that are recognized only as a single structure instead of several nucleoids. To quantify this observation, the average size of nucleoids in the different knockdown cell lines were estimated. These enlarged nucleoid structures are not formed in the POLRMT + TEFM double knockdown.

Since replication is clearly reduced in POLRMT knockdowns, the density and size of single nucleoids within mitochondria were measured with STED nanoscopy and analyzed.

3.5.3 Nucleoids are smaller in size upon POLRMT reduction and bigger upon TEFM decrease

In the previous analysis of mitochondrial transcription and replication, it became apparent that siPools have different influences in replication. Therefore, it was tested if this effect can be detected by an analysis of nucleoids density within mitochondria, as well. Furthermore, nucleoids appear to be different in size in the different knockdowns. The most distinct alteration of the size of single nucleoids is observed in the TEFM knockdown (Fig 3.18). A comparison of nucleoids in U-2 OS cells treated with an unspecific siPool (A) and siRNA against TEFM (B) reveals the appearance of enlarged structures upon TEFM reduction.

To quantify the influence of the reduced protein levels on nucleoid density and size, U-2 OS cells were incubated with the siPools for 36 h or 72 h. Wild type cells, control cells treated with unspecific siRNAs as well as the POLRMT knockdown, the TEFM knockdown and the POLRMT + TEFM double knockdown were incubated with antibodies against Mic60 to determine the area of the mitochondrial network for each cell and dsDNA to identify single nucleoids with STED nanoscopy. A ratio of the area covered by the mitochondrial network and the number of nucleoids was calculated for each cell line (Fig 3.18 C). Significance was again determined with an ANOVA test and only significant differences between knockdown cells and the respective control and the wild type cells are indicated. Both controls, 36 h and 72 h after transfection with an unspecific siPool reveal a slightly increased density of nucleoids compared to the wild type (all three bars are displayed in green). This difference is not significant but some values of the analyzed knockdowns (orange) show an alteration that is different compared to the control cells but not to the wild type. Four samples show a significant reduced density of nucleoids compared to the respective control cells. The density of nucleoids in the POLRMT knockdown is reduced after 36 h as well as after 72 h of siPool treatment. The TEFM knockdown and the POLRMT + TEFM double knockdown also reveal a reduced density at both incubation periods. However, only the TEFM knockdown after 36 h of siRNA treatment and the double knockdown after 72 h of protein reduction display a significant decrease of nucleoids density.

The size of single nucleoids identified in the STED measurements were determined at the full width at half maximum (FWHM) of the signal (Fig 3.18 D). As the achieved resolution is higher than the size of single nucleoids, differences in the size of nucleoids between different samples do not a result from different resolutions of the images. Cells were treated as described above. Only significant differences between knockdown cells and the respective control and wild type cells are indicated. 36 h after transfection,

nucleoids of the POLRMT knockdown were significantly smaller than nucleoids in the remaining samples. This reduction appears not to be significant after 72 h of siPool treatment, but can still be detected. Nucleoids in the TEFM knockdown are significantly enlarged after 72 h.

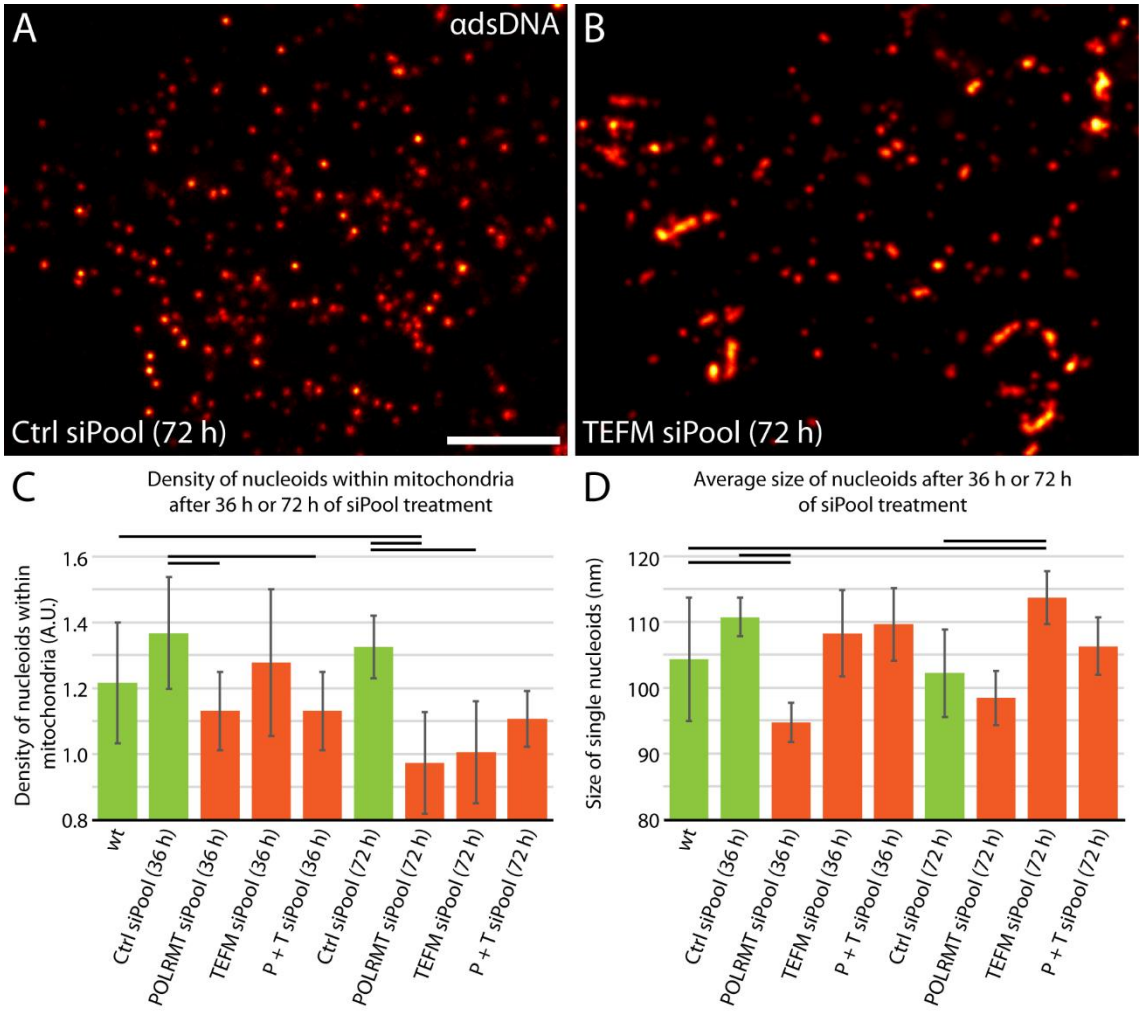

Figure 3.18 Density and size of nucleoids upon reduction of POLRMT or TEFM: U-2 OS cells were incubated with siPools for 36 h or 72 h, respectively. An unspecific siPool as a control as well as siPools against POLRMT, TEFM and a combination of both siRNAs (P+T) were used. Cells were labeled with antisera against Mic60 to mark the mitochondria and dsDNA to visualize the nucleoids and afterwards measured with STED nanoscopy. About 80 cells with over 50,000 nucleoids were analyzed. **A and B)** Nucleoids treated with a control siPool (A) or a siPool against TEFM (B) for 72 h. STED images reveal the occurrence of large aggregations of nucleoids upon TEFM knockdown. **C and D)** Density and size of nucleoids upon siPool treatment for 36 h and 72 h. Wild type and control siRNA incubations are shown as green bars. The POLRMT and TEFM knockdown as well as the POLRMT and TEFM double knockdown (P + T) are shown in orange. Density of nucleoids (C) was calculated by quantifying the area of the mitochondrial network in µm² and dividing it by the number of single nucleoids in STED. The resulting values were then multiplied by 1000. The density of nucleoids is significantly reduced after 36 h of siPool treatment in the POLRMT knockdown and P+T double knockdown in relation to the control cells. After 72 h of siPool treatment, the density of nucleoids is reduced in the POLRMT and TEFM knockdown compared to the control. Size of nucleoids was estimated at the full width at half maximum (FWHM; D). Nucleoids in cells after a 36 h treatment with a siPool against POLRMT reveal significantly smaller

nucleoids compared to the wild type cells und the control. After 72 h of siRNA incubation, nucleoids within the TEFM knockdown appear significantly enlarged compared to the control and the wild type. Scale bar: 2 µm, error bars indicate the standard deviation, indicated significance was calculated with an OneWay ANOVA using α=0.05.

This analysis reveals that especially the knockdown of POLRMT but also the TEFM knockdown and the POLRMT + TEFM double knockdown show a decreased density of nucleoids. Simultaneously, nucleoids upon POLRMT reduction appear smaller, whereas nucleoids upon TEFM decrease appear enlarged. This coincides with the occurrence of strongly enlarged nucleoid structures that can be identified within the TEFM knockdown cells. Therefore, the low detected density of nucleoids in the TEFM knockdown is most likely a result of an increased clustering of these structures. Since these large structures are always positive for EdU, the reduced amount of detected replication in Fig 3.17 in TEFM knockdown cells, could also be a result of clustered replicating nucleoids that are detected as a single structure. In contrast, the reduced density upon POLRMT decrease is a result of a lower mitochondrial DNA content as the size of single nucleoids is not increased but reduced.

Tab 3.3 summarizes the different parameters that are changed in the different knockdown cell lines.

Table 3.3 Summary of all detected changes in the POLRMT knockdown, the TEFM knockdown and the POLRMT+TEFM double knockdown: Asterisk label differences that were apparent, but not significant in every sample.

Knockdown	**Replication**	**Transcription**	**Nucleoid activity**
POLRMT	reduced	increased	Triggered towards transcription
TEFM	reduced*	reduced	Less active
POLRMT+TEFM	reduced	reduced*	Less active
	Nucleoid density	**Nucleoid size**	**Comment**
POLRMT	reduced	reduced*	-
TEFM	reduced	increased	Highly enlarged EdU-positive nucleoid cluster
POLRMT+TEFM	reduced*	normal	-

f

4.Discussion

A large and growing body of literature deals with the function and regulation of mitochondrial DNA since it is essential for the maintenance of the respiratory chain (Larsson et al., 1998, Gustafsson et al., 2016). Besides, the influence of mtDNA on a variety of diseases is discussed intensively as mutation of mtDNA can be associated with an impairment of skeletal muscles, brain, heart and malfunctions within any tissue with high energy demand (Holt et al., 1988; Lin et al., 2002; Johnson et al., 2006).

Single cells do not contain only a single nucleoid but hundreds to thousands of copies, which provide the basis for mitochondrial gene expression. Recently, the distinct number of nucleoids was determined by STED nanoscopy (Kukat and Wurm et al., 2011). It was shown, that the clinical expression of an mtDNA mutation depends on the fraction of mutated molecules within a single cell. Each mutation has to reach a specific threshold before it causes a biochemical effect (Taylor and Turnbull, 2005, Wallace et al. 2005; Stefano et al., 2017). This in turn strongly depends on the involvement of mtDNA in transcription and replication (Wallace, 1989; Wallace, 1992; Yoneda et al., 1992; Taylor et al., 1997). Therefore the need to understand the regulatory mechanisms behind mitochondrial transcription and replication is indicated.

4.1 Methods to visualize single nucleoids engaged in the process of transcription and regulation

Mitochondrial transcription and replication are investigated using a wide range of different methods. In recent years, many important findings were based on the probing of ensembles of cells by analyzing nucleoid activity with Western, Northern or Southern Blots (Agaronyan et al., 2015; Kühl et al., 2016). Studies analyzing mitochondrial replication and transcription often have to consider that the majority of mitochondrial transcription and replication is prematurely terminated (Hallberg 1974, Bogenhagen and Clayton, 1978; Wanjooij et al., 2010; Kornblum et al., 2013). In the study, presented here in this thesis, it was not of interest if both processes are completed, but only, whether the nucleoid shows current activity. An initial objective of this study was the visualization of all mitochondrial transcription and replication on a single nucleoid level within the whole cell using multicolor STED nanoscopy. In the current work, a fluorescence microscopy based imaging approach was developed that enabled one to identify single nucleoids that are engaged in replication, transcription or both processes simultaneously (Fig. 3.8).

4.1.1 Nucleoside analogues as specific labels the active nucleoids

In this study, synthetic nucleosides, namely EdU and BrU, were used to visualize mitochondrial transcription and replication. The specificity of synthetic nucleoside incorporation for the respective process was tested within cells using additional EtBr treatment. EtBr blocks the melting of the mtDNA and as a result inhibits both, transcription and replication (Holt and Reyes, 2012). When cells were incubated with EtBr, no incorporation of EdU and BrU could be observed anymore (Fig 3.6).

Most published reports so far labelled specific proteins of the mitochondrial transcription or replication machinery to recognize the respective process. Interestingly, this study shows that antisera against proteins involved in mitochondrial transcription and replication do not specifically label active nucleoids (Fig 3.2, Fig 3.3, Supplement Fig. 9.2 and 9.3). Indirect immunofluorescence labeled only a subset of the nucleoids within the cell. However, upon inactivation of the nucleoids with EtBr treatment of the cells, components of the transcription and replication machinery were still associated with nucleoids and labeled a subset of those structures (Fig 3.2, Fig 3.3, Supplement Fig. 9.2 and 9.3). This means, the replication or transcription machinery can be associated to the nucleoids without replication or transcription being active.

In support with this finding, a number of previous studies have found that the replication and transcription machinery can arrest on the mtDNA (Bowmaker, 2003; Brambati et al., 2015; Shi et al., 2016; Cline et al., 2010).

To date some fluorescence microscopy based methods have been developed to label mitochondrial replication and transcription (Chatre et al., 2013 (1); Legros et al. 2004 Lewis et al., 2016; Sasaki et al. 2017). Surprisingly, only a minority of the studies characterized the specificity of the staining method used in these studies with EtBr or a comparable control.

In conclusion, specific labeling of mitochondrial transcription and replication cannot be achieved by labeling the involved proteins. In contrast, nucleoside analogues revealed specific visualization of the mitochondrial transcription and replication.

4.1.2 Analysis of the incorporation of nucleoside analogues into mtDNA

Nucleoside analogues are incorporated into nascent RNA during transcription and into freshly synthesized DNA during replication. The incubation time had to be set to a minimum compared to those in previous publications to ensure a good temporal resolution (Kukat and Wurm et al., 2011 Lewis et al., 2016; Legros et al., 2004; Iborra et

al., 2004; Jourdain et al. 2013). Very long incubation times with nucleoside analogues lead to a brighter signal with improved contrast but misses the improved temporal resolution. Therefore long incubation times were omitted. Initial experiments based on the analysis of the signal intensity of EdU signals suggested that only very few EdU molecules are incorporated into the mtDNA during these short incubation times (not shown). This ensured that good temporal resolution was achieved with this method.

Nanoscopy revealed that the BrU signal is slightly shifted to the nucleoid signal whereas EdU shows a better colocalization to the mtDNA (Fig 3.8, Fig 3.9 (images) and Fig 3.10 (evaluation)). This was true for a majority of the BrU signals, indicating that these signals rise from RNAs starting to diffuse away from the transcribing nucleoids. Only a minority of the BrU signal was in very close proximity to the mtDNA. However, since 2D-STED imaging was performed, a potential shift of the BrU signal in the Z axis could have not been recognized.

Since replication initiation starts with a RNA primer, BrU incorporation could, in theory, also label the replication primer instead of functional transcription only. Both mitochondrial primers are very short (H-strand replication primer: 194 nt and L-strand replication primer: 20-30 nt; Uhler and Falkenberg et al., 2015) and feature only a very short lifetime (Crews et al., 1979; Holmes et al., 2015). However, the incorporation of BrU into the replication primers cannot be ruled out definitely. Overall, the demonstrated differences in the signal patterns between BrU and EdU prove that both nucleosides label different structures. This shift was not detectable when diffraction limited confocal images were analyzed (Fig. 3.8 and 3.9).

4.1.3 Importance of super resolution STED nanoscopy

Diffraction limited light microscopy lacks the resolution to uncover features with a distance below the size of 200 nm in the lateral axis. The development of nanoscopy in recent years enables one to analyze smaller structures with light microscopy (Hell and Wichmann, 1994; Hell, 2007; Hell, 2009). Since mitochondria have a diameter below 200 nm, nanoscopy is the essential method to analyze the size and shape of single nucleoids (Kukat and Wurm et al., 2011). STED microscopy revealed that a single nucleoid has an average diameter of 99 nm when labeled with antibodies. A combination of STED nanoscopy and quantitative real time PCR (qrtPCR) revealed that the majority of single nucleoids contain only a single mtDNA (Kukat and Wurm et al., 2011; Kukat et al., 2015). In the majority of studies published before 2011 it was hypothesized that nucleoids contain a large amount of different mtDNAs. So, when single nucleoids identified with

nanoscopy contain only a single mtDNA, then the analysis of single mtDNA molecules and their respective function is possible (Fig 4.1).

On condition of a nucleoid containing only a single mtDNA, it can be determined if an mtDNA is engaged in transcription or replication when STED nanoscopy is used. That analysis would not be possible when the different transcription and replication signals, would overlay, thereby hiding this information, either by a large amount of mtDNA within a single nucleoid, or when several adjacent nucleoids are classified as one single nucleoid using diffraction limited confocal microscopy (Fig 4.1).

In the current study presented here, multicolor STED nanoscopy was used to visualize single nucleoids. Throughout the different experiments, single nucleoids revealed an average diameter between 94 nm and 120 nm when decorated with primary and secondary antibodies (Tab 3.2). Differences in the average size of nucleoids in the different experiments are a result of the different achievable resolution caused by the different used fluorophores and the imaging parameters necessary for different multicolor approaches (see section 3.3.1). In none of the images, nucleoids with a significant enlarged diameter potentially originating from two single nucleoids are apparent. This provides strong evidence that in every experiment indeed single nucleoids are analyzed.

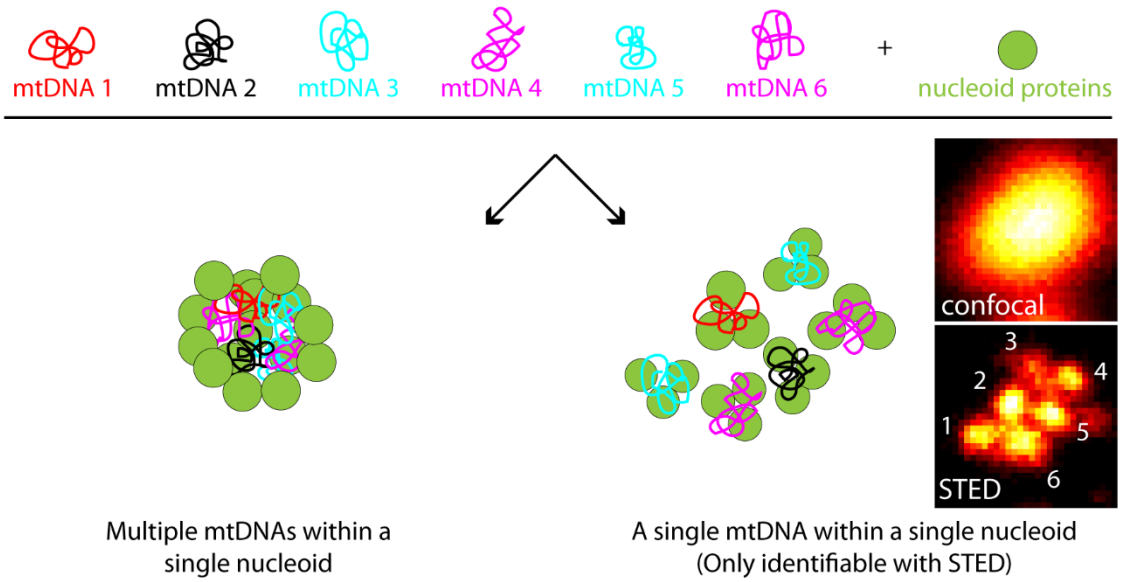

Figure 4.1 The majority of nucleoids identified in STED contain a single mtDNA: STED analysis and quantitative real time PCR revealed that most single nucleoid visualized with STED nanoscopy contain only one copy of mtDNA. As a result, an analysis of single nucleoids with STED correspond to an analysis of single mtDNA. Confocal microscopy cannot provide this information.

As to be expected, the signal intensity of nucleoid clusters was higher than the intensity of isolated nucleoids recorded with diffraction limited confocal microscopy on average. Most nucleoid clusters that appeared brighter in the confocal-mode revealed several nucleoids when STED nanoscopy was used (Tab 4.1). However, because of a high intensity variation the number of detected counts in confocal images could not be used to determine the precise amount of nucleoids that hide within a confocal cluster. Reasons for this variance could be for instance differences in the size of different nucleoids, nucleoids located slightly outside the focal plane, or different levels of background signal within a single cell.

Table 4.1 Comparison between the signal intensity of a confocal nucleoid signal and the amount of nucleoids resolved in the STED mode: Data originate from the records shown in Fig 3.1.

Amount of nucleoids in STED	Counts of the confocal cluster	Counts of the confocal cluster (normalized)
1	34165	1
2	20653	0.6
3	52785	1.5
4	68063	2
5	115545	3.4
6	211688	6.2

In conclusion, super-resolution nanoscopy is essential to identify the activity of single mtDNA molecules in this study. The same analysis with conventional confocal microscopy would not be possible since the signal intensity in confocal images does not strictly correlate with the number of single nucleoids.

4.2 Functional heterogeneity of nucleoids

Mitochondrial heterogeneity is striking not only in different tissues, but also in different regions of a single cell mitochondria can reveal different (sub-)populations (Kuznetsov et al., 2009). So, mitochondria within single cells can show different functional and structural properties. This functional heterogeneity of mitochondria is not only apparent for different mitochondria in different parts of a cell, but even different subdomains of a single mitochondrion can reveal different functions (Kuznetsov et al., 2004; Kuznetsov et al., 2006). The organelles can vary for instance in their redox state and in their different level of ROS (Romashko et al., 1998; Collins et al., 2002; Bruce et al., 2004; Kuznetsov et al., 2004). Especially different membrane potentials within mitochondria

in a single cell and within subdomains of single mitochondria are well documented (Bernard et al., 2008). Numerous studies suggest that the functional heterogeneity of mitochondria is connected to the energy demand in different regions of the cell (reviewed: Kuznetsov et al., 2009). Although many reports discuss the functional heterogeneity of mitochondria, no study existed which show evidence of different functional subpopulations of nucleoids.

In the present study, mitochondrial transcription and replication were visualized simultaneously. It could be demonstrated that single nucleoids can be engaged in transcription and replication at the same time (Fig 3.9). Interestingly, an analysis of over 18,000 nucleoids revealed that the majority of nucleoids within a cell are inactive (Fig. 3.10). Quantification of the data showed that nucleoids are organized in at least two functional subpopulations within cells. Nucleoids can appear active with the tendency to be involved in transcription and replication as well or remain inactive. Furthermore, an analysis of nucleoid replication over a longer time period revealed that not all nucleoids are equally engaged in replication. This further supports the existence of at least two functionally different subpopulation of nucleoids.

Nucleoid gene expression is necessary for the activity of OXPHOS (Larsson et al., 1998, Gustafsson et al., 2016). Different activity level of mtDNA would as a result cause a different functionality of the respiratory chain which would result in a different membrane potential, a different production of ROS and a different redox state of the mitochondria (Appleby et al., 1999; Gustafsson et al., 2016)

4.2.1 Active nucleoids are evenly distributed within the cell

Some reports indicate that the previously mentioned functional heterogeneity of mitochondria is linked to their distance to the nucleus (Park et al 2001; Bruce et al., 2004; Kuznetsov et al., 2009). Also it was suggested that perinuclear mitochondria are triggered towards ATP generation (Dzeja et al., 2002). This could play an important role in the mechanisms that drive nuclear import as well as further functions of the nucleus that need ATP (Dzeja et al., 2002).

In contrast, in the present study active and inactive nucleoids are evenly distributed within the cell if the distance to the nucleus is taken as a reference (Fig 3.13). Neither single nucleoids that are only engaged in transcription, nor nucleoids involved in replication, nor nucleoids engaged in both processes simultaneously show an enrichment in perinuclear regions (Fig 3.13). Hence, the findings of the current study do not explain the increased ATP production of perinuclear mitochondria. This effect could

be a result of a general increased density of nucleoids in perinuclear areas (Kukat and Wurm et al., 2011)

4.2.2 Activity and inactivity of nucleoids

So far, only a few reports show hints for inactivity of nucleoids in cells (Davis and Clayton, 1996; Piko and Taylor, 1987). Previous studies that used the nucleoside analogue BrdU to label mitochondrial replication achieved contradictory results. On the one hand it was published that nucleoids are equally engaged in replication (Iborra et al., 2004), on the other hand it was reported that a subset of nucleoids within cells show an increased replication rate compared to the remaining nucleoids (Davis and Clayton, 1996). Nevertheless, in both studies, diffraction limited microscopy was used, thereby lacking the resolution to observe single nucleoids. Furthermore, studies performed in early mouse embryos suggest that a large population of the mtDNA molecules remains inactive (Piko and Taylor, 1987). However, until now, there has been no reliable evidence that nucleoids reveal different activity levels.

The analysis of mitochondrial transcription and replication in this study finally shows that not all nucleoids are active within a cell at a given time point. That gives rise to the question why mitochondria contain such a high amount of nucleoids while not all of them are active. An explanation could be that the high copy number works as a pool to react to environmental stress. In situations with low glucose, respiration becomes more important since the energy need cannot be fulfilled with glycolysis (Auger et al., 2011). In the future, it has to be tested if this fraction of inactive nucleoids can be stimulated by a reduction of glucose and thereby, the triggering of OXPHOS activity. Experiments with cells growing in media with high glucose concentration or with low glucose but high galactose concentration could reveal if inactive nucleoids work as a pool for potential OXPHOS activity when needed. That could show if cells can regulate the activity of respiration by activation or inactivation of mtDNAs.

4.2.3 Outlook: TFAM as a regulator for nucleoid activity?

A question that remains unanswered is the mechanism that controls the activity and inactivity of nucleoids. This is an important issue for further research.

A molecular switch that triggers nucleoids towards activity or inactivity could be the packaging level of mtDNA by TFAM (Farge et al., 2014; Gustafsson et al. 2016). TFAM is not only essential to initiate mitochondrial transcription but also represents the most abundant nucleoid protein important for the nucleoid maintenance (Bogenhagen,

2012). At the physiological level of TFAM, an inhomogeneous compaction level was observed *in vitro* (Farge et al., 2014). It has been proposed in previous reports that the compaction level of mtDNA with TFAM could regulate if a nucleoid is engaged in replication, transcription or both processes together (Gustafsson et al., 2016). A lower compaction level could open the regulatory non coding region (NCR) of the mtDNA and by this grant access to both promotors for the mitochondrial RNA polymerase POLRMT and the second mitochondrial transcription factor TFB2M (Gustafsson et al., 2016). An analysis of nucleoids' activity upon varying TFAM level should enhance the understanding of TFAM's influence on nucleoids' activity.

4.3 Regulation of mitochondrial transcription and regulation by POLRMT and TEFM

Functional transcription and primer synthesis for replication is mediated by a single RNA polymerase in mitochondria (POLRMT; Agaronyan et al., 2015; Kühl et al., 2016; Gustafsson et al., 2016). Transcription occurs at two distinct regions in the mtDNA, the light strand promotor (LSP) and the heavy strand promotor (HSP). Transcription initiated at LSP can result in the production of a polycistronic RNA or a primer for replication (Agaronyan et al., 2015; Kühl et al., 2016). This primer can afterwards be used as a substrate by POLγ to initiate replication. The decision if transcription initiated at LSP results in functional transcription or replication is made at a sequence about 100 bp upstream of LSP termed CSBII (Posse et al., 2015; Agaronyan et al., 2015). Transcription by POLRMT can be prematurely terminated at CSBII, resulting in primer synthesis. Whether mitochondrial transcription occurs throughout CSBII or is terminated depends on the presence of the mitochondrial transcription elongation factor TEFM (Posse et al., 2015; Agaronyan et al., 2015).

When TEFM is present, the elongation complex is stable and functional transcription is favored. If TEFM is missing, a termination structure forms and POLRMT dissociates from the mtDNA (Agaronyan et al., 2015; Hillen et al., 2017 (2)). Although previous data indicate that TEFM presence triggers nucleoids towards transcription at CSBII, no negative influence of TEFM on replication has been demonstrated so far.

The presence of TEFM influences not only transcription initiated at LSP, but is also important to enhance the processivity of POLRMT at the heavy strand (Minczuk et al., 2011; Posse et al., 2015). It was shown in mice that the protein level of POLRMT affects the level of TEFM, as more TEFM could be detected in a heterozygous POLRMT knockout (Kühl et al., 2016). Hence, in the current study it was assumed that POLRMT and TEFM

together regulate if a nucleoid is engaged in transcription or replication. In this study, a fluorescence microscopy based approach was used to analyze the role of POLRMT and TEFM on single nucleoid level.

4.3.1 POLRMT level influences nucleoid activity

The analysis of mitochondrial transcription and replication in POLRMT knockdown cells revealed that lower POLRMT level trigger nucleoids towards transcription. The fraction of nucleoids engaged in transcription is increased and the number of replicating nucleoids significantly reduced in POLRMT knockdown cells (Fig 3.17). This reduction of replication is reflected in a decreased density of nucleoids (Fig 3.18). Furthermore, nucleoids upon POLRMT reduction appear significantly smaller in size (Fig 3.18), which could be a result of less ongoing replication as this would reduce the average amount of DNA per nucleoid. Since POLRMT is responsible for initiating both transcription and replication, POLRMT reduction alone cannot explain the different influence of the decreased protein level in both processes. Fig 3.14 revealed that the TEFM level is increased upon POLRMT reduction, this was also shown before in a heterozygous POLRMT knockout in mice (Kühl et al., 2016). This could be a cellular mechanism to ensure proper transcription upon POLRMT reduction and could explain the different effects observed in POLRMT knockdown cells (Fig 4.2).

When POLRMT is reduced, less transcription is initiated (Kühl et al., 2016). Hence, less elongation complexes reach CSBII. The increased level of TEFM in the POLRMT knockdown could represent a mechanism to ensure that the majority of elongation complexes are active throughout CSBII and the complex is not prematurely terminated. In conclusion, the amount of initiated transcription is reduced upon POLRMT decrease, but is more processive in comparison (Fig 4.2).

If the limited transcription initiation is counterbalanced by increased processivity, it would result in reduced events of transcription termination at CSBII and therefore lead to impaired synthesis of a replication primer. This would explain the reduction of replicating nucleoids within the POLRMT knockdown (Fig 4.2). Not only transcription initiated at LSP is stabilized by TEFM, but also HSP transcription (Posse et al., 2015). Again, the decreased initiation of transcription at HSP because of reduced POLRMT level could result in a more processive transcription due to increased TEFM level. An increased processivity of HSP transcription would not affect mitochondrial replication.

In conclusion, the cell limits its ability to replicate the mitochondrial DNA to ensure its ability to generate functional transcripts and therefore maintain the respiratory chain upon POLRMT reduction.

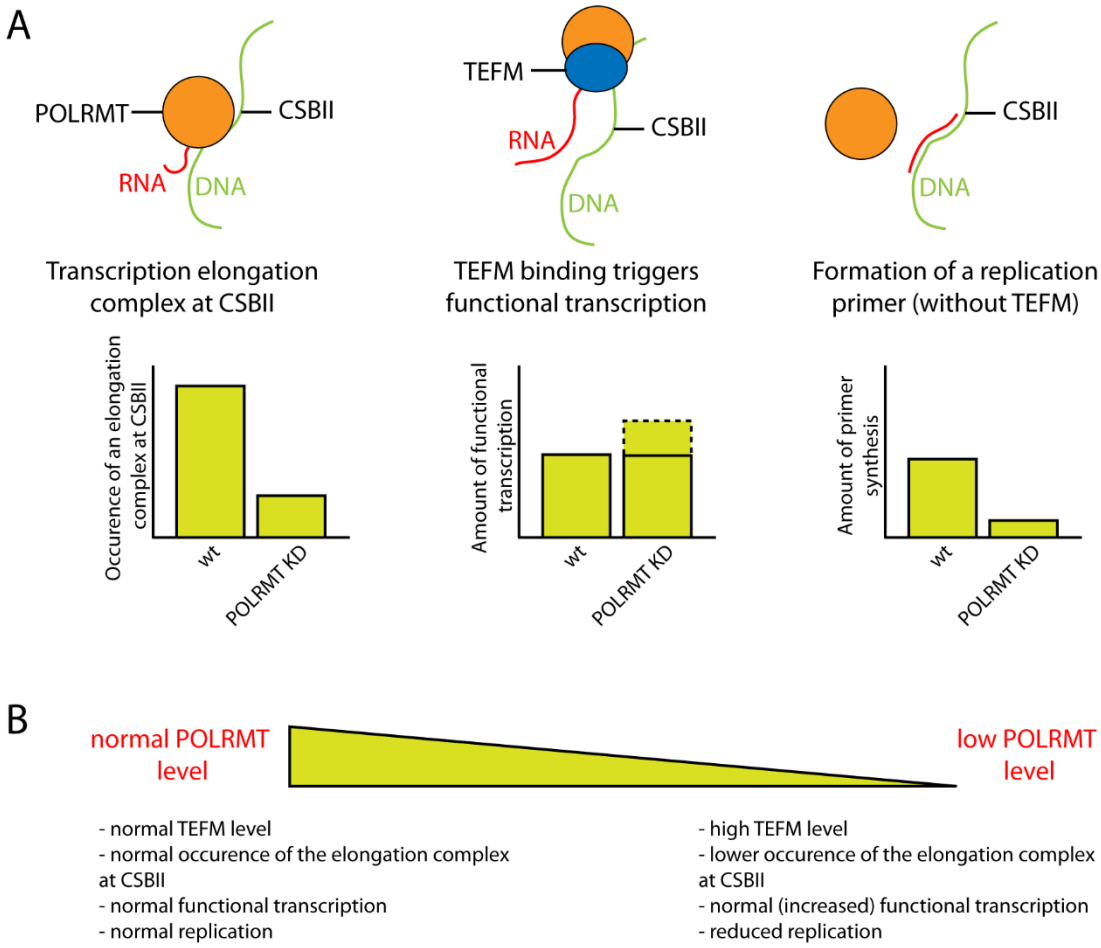

Figure 4.2 Transcription is favored under low POLRMT level: A) In the POLRMT knockdown (POLRMT KD) transcription initiation is reduced and therefore also the occurrence of a transcription elongation complex at CSBII. Due to the increased level of TEFM, the transcription complex provides enhanced stability and functional transcription is ensured. Replication is impaired in POLRMT KD cells, less replication primer is synthesized. **B)** Summary of the changes that might occur upon POLRMT reduction that ensures mitochondrial transcription.

In contrast to the outcome of the present study, a previous work stated that upon low POLRMT level replication is favored over transcription in mice (Kühl et al., 2016).

It was also observed in the previous study that POLRMT reduction leads to an increased amount of LSP transcription compared to HSP transcription. Since LSP transcription is essential for replication, it was concluded that POLRMT reduction triggers nucleoids towards replication. Also in this previous work, an increased TEFM level could be observed. However, its positive influence on transcription was barely discussed.

Furthermore, this previous analysis of reduced POLRMT level in mice revealed a reduced amount of mtDNA (Kühl et al., 2016). Discussing this previous study, I come to another conclusion. An increased level of TEFM and a reduced amount of mtDNA are hints for favored transcription.

The presented data of the current study reveal that mitochondrial transcription is favored upon low POLRMT level. The observed higher initiation rate at LSP (Kühl et al., 2016) could secure a minimal level of replication.

4.3.2 Additional reduction of TEFM in the POLRMT knockdown triggers nucleoids towards replication

In the current study, the effect of TEFM reduction was analyzed in a POLRMT knockdown background. It was demonstrated that an additional loss of TEFM in a POLRMT knockdown suppresses the phenotypes of lower POLRMT level (3.17 and 3.18). Even though the protein level has not been quantified yet, immunofluorescence data reveal that the POLRMT reduction in the double knockdown is comparable to the single knockdown (3.14 and 3.16). The shift of nucleoid activity towards transcription observed in POLRMT knockdown cells vanishes partially when the TEFM level is additionally reduced. The overall fraction of nucleoids engaged in transcription and replication is reduced in the double knockdown compared to the wild type (Fig 3.17). It appears that nucleoids in the double knockout are less active, but nucleoids are no longer triggered towards transcription as is observed in the POLRMT single knockdown (Tab 4.2). Moreover, the nucleoid density and the nucleoid diameter in POLRMT knockout cells are less reduced when TEFM is additionally decreased (Fig 3.18). Hence, additional TEFM reduction suppresses the POLRMT knockdown phenotypes.

Mechanistically, these results fit into the model of nucleoids activity upon POLRMT reduction presented in the previous section (Fig 4.2). In vitro data of TEFM reduction revealed that its presence prevents termination of the transcription elongation at CSBII (Agaronyan et al., 2015). The reduced initiation of transcription at LSP results in a lower occurrence of transcription elongation complex at CSBII, which cannot be counterbalanced by increased TEFM level any more. As a result, the ratio between mitochondrial transcription and replication is no longer shifted towards transcription and the ratio is unchanged in the double knockdown compared to the wild type. The lower initiation rates at both promotors result only in reduced overall activity.

In conclusion, a comparison between the POLRMT knockdown and the POLRMT + TEFM double knockdown reveals how TEFM influences mitochondrial transcription and

replication. The decrease of TEFM level upon POLRMT reduction leads to a reduction of transcription and an increase of replication (Fig 3.17 and Tab 4.2). Hence, this data reveal that TEFM is a positive regulator of transcription, at least in a POLRMT reduced background. The previously described *in vitro* function of TEFM as a molecular switch between mitochondrial transcription and replication as well as a general stimulator of mitochondrial transcription (Minczuk et al., 2011; Posse et al., 2015; Agaronyan et al., 2016) could be demonstrated on a single nucleoid level.

Table 4.2 Proportion of mitochondrial transcription and replication in wild type cells, the POLRMT knockdown (POLRMT KD) and the POLRMT + TEFM double knockdown (POLRMT + TEFM dKD): A ratio between transcription and replication higher than 1 indicates that nucleoids tend to be more often engaged in transcription compared to wild type cells. A ratio lower than 1 indicates that nucleoids tend to be engaged more often in replication compared to the wild type.

	Wild type	POLRMT KD	POLRMT + TEFM dKD
Transcription	8%	11%	6%
Replication	7%	2%	4%
Relation of transcription and replication	1	4.6	1.1

4.3.3 Single TEFM knockdown reveals only weak phenotypes.

In a POLRMT reduced background, an additional loss of TEFM stimulated replication. Surprisingly, treatment of wild type cells with the used siPools against TEFM did only cause a slight shift of the nucleoids towards replication (Fig 3.17).

Although the fraction of nucleoids engaged in transcription is significantly reduced upon TEFM reduction, no enhancing effects on the proportion of replicating were observed. Compared to the wild type, nucleoids in the TEFM knockdown cells are only slightly shifted towards replication (Fig 3.17; Tab 4.3). Hence, TEFM appears as a stimulator of transcription but only as a weak repressor of replication. Previous experiments with conventional siRNAs revealed an incomplete reduction of TEFM after 72 h of treatment (Minczuk et al., 2011). The incubation time with the siPool against TEFM has to be increased in future experiments. Potential mechanisms that could compensate low TEFM levels and repress an increase of replication are discussed later.

The different strength of the phenotype of TEFM loss in wild type background and in the POLRMT knockdown background could be explained by the different steady state levels

of TEFM in both situations. TEFM appears to be reduced to a similar level in the TEFM single knockdown as in the POLRMT and TEFM double knockdown according to the immunofluorescence data (Fig 3.14 and 3.15). However, POLRMT knockdown cells reveal an increased level of TEFM compared to the wild type (Fig 3.14). Hence, the overall reduction of TEFM is higher in the POLRMT knockdown background than in the wild type.

Furthermore, upon reduction of TEFM, an increased level of POLRMT could be observed (Fig 3.14). This increased POLRMT level could display a regulatory mechanism to ensure that functional transcription still occurs. A high level of POLRMT should lead to a higher number of transcription elongation complexes at CSBII. This could enable an efficient usage of the limited amount of TEFM proteins as it is saturated by enough active POLRMT. This would be in line with the previous observation that cells seem to ensure proper transcription upon low POLRMT level to maintain the respiratory chain.

Table 4.3 Proportion of mitochondrial transcription and replication in wild type cells and TEFM knockdown cells (TEFM KD): If the ratio between transcription and replication is higher than 1, nucleoids tend to be engaged in transcription compared to wild type cells. A ratio lower than 1 indicates nucleoids tend to be engaged in replication.

	Wild type	TEFM KD
Transcription	8%	11%
Replication	7%	2%
Relation of transcription and replication	1	4.6

One observed phenotype in TEFM knockdown cells is the occurrence of increased EdU positive nucleoid structures, which result in an increased average diameter of nucleoids in these cells. This might be a result of nucleoid clustering (Fig 3.18). It was shown that the morphology of the mitochondrial network appears normal in TEFM knockdown cells (Fig 3.14). Therefore, this clustering of nucleoids is not a secondary effect of an altered morphology of the mitochondrial network.

Such clustering of replicating nucleoids could influence the analysis as only single replicating nucleoids could be detected as separate single structures. That error in the evaluation would reduce the determined fraction of replicating nucleoids. Moreover, as this clustering affects the total amount of nucleoids, this error would also affect the calculated proportion of nucleoids engaged in transcription. A higher number of total nucleoids would decrease the determined fraction of nucleoids engaged in transcription (Fig 4.3).

These enlarged nucleoid structures, are not found in the POLRMT + TEFM double knockdown. Hence, the additional reduction of POLRMT suppressed the appearance of large nucleoid cluster in a TEFM reduced background. If the enlarged EdU positive clusters are indeed a result of increased replication, it remains unclear why replication is restricted to only a few nucleoid cluster and not equally distributed like observed in the wild type or the other knock down cell lines.

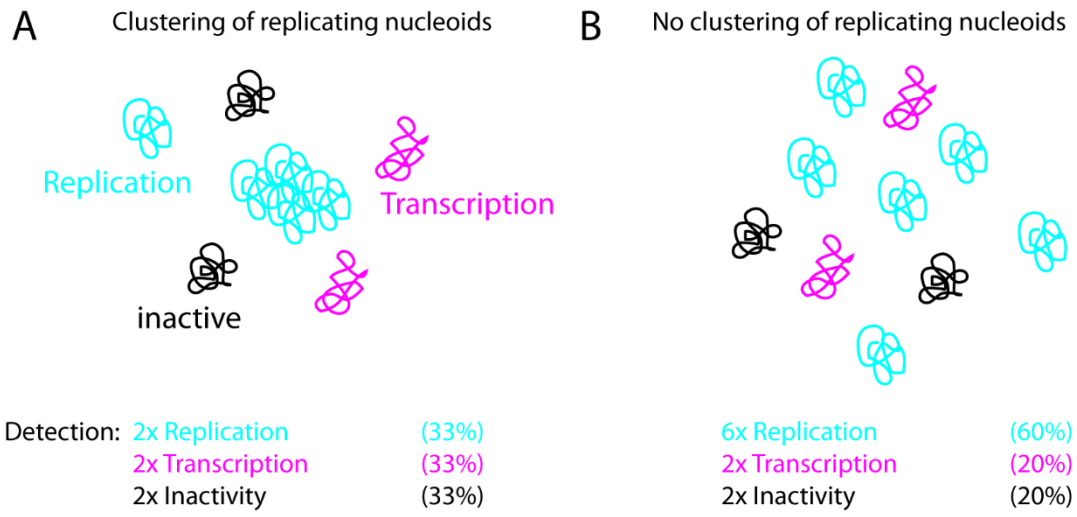

Figure 4.3 Effect of nucleoid clustering on the evaluation of nucleoids activity: A) Clustering of replicating nucleoids leads to a reduced amount of these nucleoids being detected. **B)** If replicating nucleoids do not form cluster, the detected fraction of these structures is higher. Furthermore, as the total amount of detected nucleoids increases, the proportion of detected nucleoids engaged in transcription is reduced.

4.3.4 Outlook: Analysis of the protein level of TWINKLE as well as the amounts of the 7S DNA.

The mitochondrial helicase TWINKLE is essential for mitochondrial replication (Tyynismaa et al., 2004; Hance et al., 2005). Northern, Southern and Western Blots revealed that a reduction of the TWINKLE level causes a decreased amount of ongoing replication along with a reduced amount of nucleoids, less transcripts and a decrease of OXPHOS proteins (Milenkovic et al., 2011; Rajala et al., 2014). Initiated replication can lead to a complete round of replication or it can be prematurely terminated at the TAS region, resulting in the 7S DNA and the formation of the D-loop (Robberson and Clayton, 1972; Doda et al., 1981). When TWINKLE levels are high at the TAS region, nucleoids favor complete replication over prematurely termination. Hence, TWINKLE is a stimulator of functional replication (Milenkovic et al., 2013). Furthermore, it was demonstrated that TWINKLE levels are increased in homozygous but not heterozygous

POLRMT knockout mice (Kühl et al., 2016). In conclusion, there is evidence that TWINKLE is involved in the regulatory mechanism of mitochondrial transcription and replication.

In POLRMT knockdown cells, the amount of primer synthesis could be limited due to favored elongation of transcription at CSBII (Fig 4.2). It has to be ensured that the limited amount of initiation of replication leads to complete replication and not to the formation of the D-loop. The amount of 7S DNA could be directly used as an indicator of D-loop formation as it can be detected by radioactive labeling of the DNA (Doda et al., 1981). The ratio between single replicating nucleoids and the amount of 7S DNA should provide information about the completion rate of replication upon low POLRMT level compared to the wild type and therefore whether the regulatory mechanisms in mitochondria react to the limited amount of replication primers. In homozygous POLRMT knockout mice, the amount of 7S DNA is reduced. However, the level of 7S DNA is not influenced in homozygous POLRMT knockout mice.

As mentioned, the level of TWINKLE influences the amount of D-loop formations. It has to be analyzed if POLRMT knockdown cells have an increased level of TWINKLE to ensure functional replication. The level of TWINKLE and the amount of D-loop formation should also enhance the understanding of the TEFM knockdown phenotype and the general influence of TEFM on mitochondrial replication. In this study, it was shown that low TEFM level trigger nucleoids towards replication in a POLRMT reduced background and cause the formation of large cluster of replicating nucleoids in wild type cells (section 4.3.2 and 4.3.3). Low TEFM level, should favor termination of transcription at CSBII and, as a result, the synthesis of a replication primer.

Since, in theory, more replication can be initiated upon TEFM reduction, an analysis of the amounts of 7S DNA and the TWINKLE level could uncover regulatory mechanisms of mitochondria to limit replication in situations in which primer synthesis is favored at CSBII. Such a mechanism is expected since the reduction of TEFM in the wild type background does not lead to a clear increase of replicating nucleoids but decreased transcription (Fig 3.17). A reduction of TWINKLE level would represent that mechanism. The increased offer of replication primer would then be counterbalanced by a lower completion rate of replication and a higher number of D-loop formation. It could not only explain the normal replication rates upon TEFM reduction but also explain the occurrence of the detected enlarged EdU positive nucleoid structures (Fig 3.18).

More nucleoids could be involved in replication, but low TWINKLE level would reduce the fraction of complete replication. Only in regions with a normal level of TWINKLE are nucleoids engaged in functional replication, leading to cluster of replicating nucleoids.

The fraction of nucleoids containing a D-loop have not been determined upon lower TEFM level so far.

4.3.5 Outlook: Analysis of mitochondrial transcription and replication upon reduced levels of TFAM and TWINKLE

The analysis of the POLRMT and TEFM knockdowns revealed that the regulation of mitochondrial replication is a highly dynamic process but not only POLRMT and TEFM are involved in that regulation but also other factors. The involvement of the helicase TWINKLE for instance was discussed above.

The transcription activator TFAM is the main structural protein of nucleoids revealing an uneven compaction rate of mitochondrial DNA. It is discussed in several reports that this uneven distribution of TFAM could regulate nucleoid activity by making the regulatory elements of the mtDNA accessible or not. (Bogenhagen, 2012; Farge et al., 2014; Gustafsson et al., 2016). There is indication that high TFAM level block nucleoid activity (Farge et al., 2014). However, this suggestion has not been confirmed so far. An influence of POLRMT reduction on TFAM level could not be observed and it has not been tested if low TEFM level influence TFAM (Kühl et al., 2016). During the current study, siPools against TFAM were used to generate a TFAM knockdown and then the activity of nucleoids was analyzed. Unfortunately, siPools seem not to work properly as no effects on the TFAM protein level or vitality of the cells could be observed upon siRNA treatment. However, this experiment will be repeated in the future with another siPool.

POLγ consists of two subunits POLγA and POLγB in mammals and is the only DNA polymerase in mitochondria (Ropp and Copeland, 1996; Korhonen et al., 2004). POLγA level is unchanged at low POLRMT level (Kühl et al., 2016). The protein level of the POLγB subunit has not been analyzed so far. Although a direct connection between the POLRMT-TEFM mechanism and POLγB has not been observed, it was shown that POLγB is necessary for proper TWINKLE function (Farge et al., 2007).

In conclusion, reports indicate that TFAM regulates the overall activity of nucleoids (Bogenhagen et al., 2012; Farge et al., 2014; Gustafsson et al., 2016). POLRMT and TEFM regulate the switch between mitochondrial transcription and replication at CSBII (Minczuk et al., 2011; Posse et al., 2015; Agaronyan et al. 2016: Kühl et al., 2016; this study). Regulatory mechanisms at CSBII influence the amount of TWINKLE that influence the fraction of complete replication (Milenkovoc et al., 2013; Kühl et al., 2016). Finally, POLγ is essential for proper TWINKLE function (Farge et al., 2014). A summary of these regulatory mechanisms is shown in Fig 4.4. Further analysis of the transcription and

replication of nucleoids in different knockdown cell lines and the influence of the protein level, as well as the analysis of the fraction of D-loops should help to uncover the regulatory mechanisms of mitochondrial nucleoids.

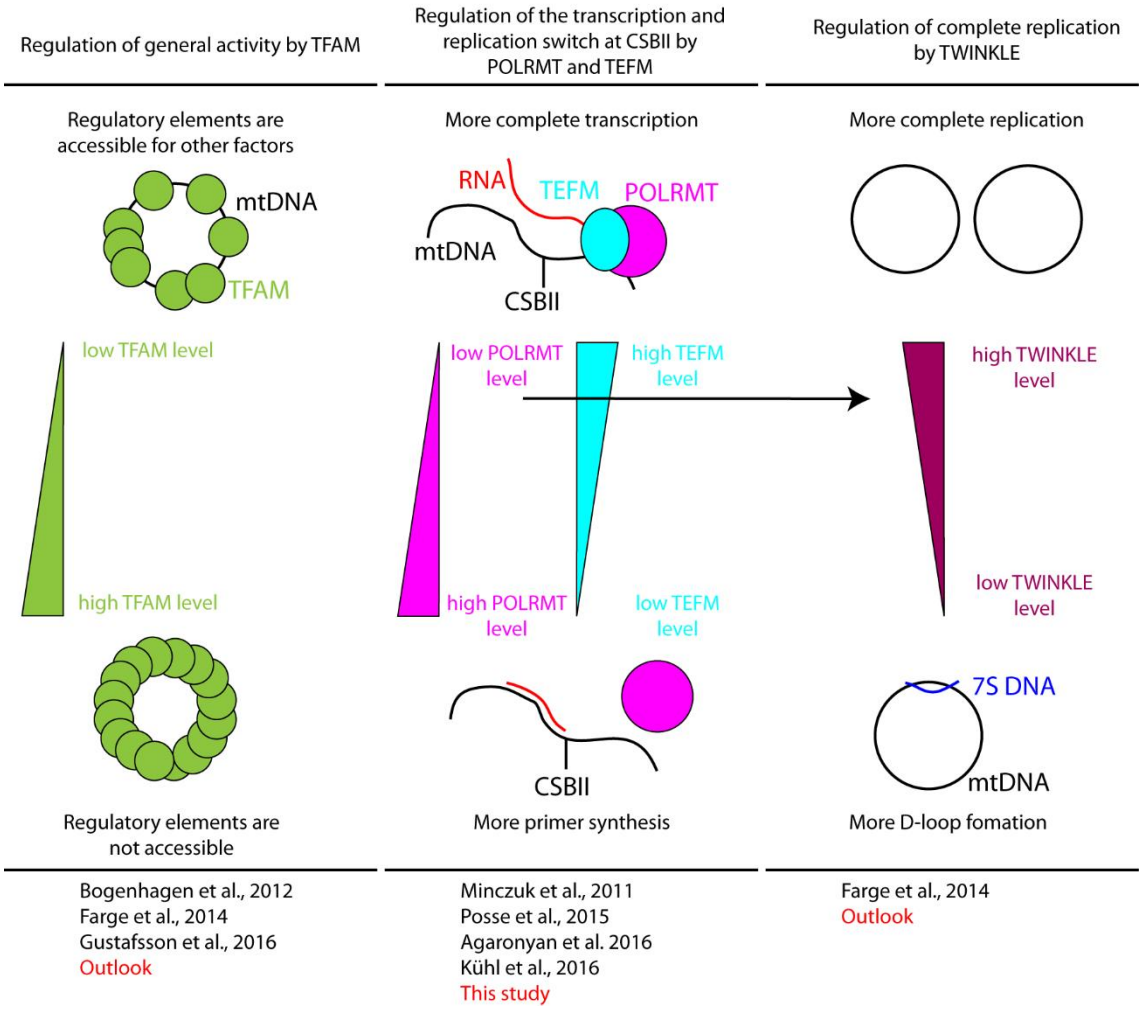

Figure 4.4 Regulatory mechanisms of mitochondrial transcription and replication: Reports indicate that the compaction level of the mtDNA regulates the overall activity. A lower compaction level could make regulatory sequences accessible for other factors and therefore trigger nucleoids towards activity. The level of POLRMT and TEFM trigger nucleoids towards replication or transcription, respectively. The TWINKLE level is influenced by the POLRMT level and could represent the switch between complete replication and D-loop formation.

5. List of Figures

6. List of Tables

7. Abbreviations

ANOVA	Analysis of variance
ATP	Adenosine triphosphate
ATPB	β-subunit of the ATP synthase
BrdU	5'-Bromo-2'-desoxyuridine
BrU	5'-Bromouridine
CTD	C-terminal domain
CSB	Conserved sequence block
CuAA	Copper(I)-catalyzed alkyne-azide cycloaddition
dsDNA	Double strand deoxyribonucleic acid
EdU	5'-Ethynyl-2'-desoxyuridine
EtBr	Ethidium Bromide
FWHM	Full width at half maximum
h	Hour
HSP	Heavy strand promotor
IC	Initiation complex
LSP	Light strand promotor
Mic60	MICOS complex subunit Mic60
min	Minute
NCR	Noncoding region
NTD	N-terminal domain
nm	Nanometer
NTE	N-terminal extension
mtDNA	Mitochondrial deoxyribonucleic acid
MTERF	Mitochondrial transcription termination factor
mtSSBP	Mitochondrial single strand binding protein
O_H	Origin of heavy strand replication
O_L	Origin of light strand replication
OXPHOS	Oxidative phosphorylation
PBS	Phosphate-buffered saline
POLRMT	Mitochondrial RNA polymerase
POLγ	DNA polymerase gamma
qPCR	Quantitative polymerase chain reaction
RITOLS	Ribonucleotide incorporation throughout the lagging strand
SDM	Strand displacement model

siRNA	Small interfering ribonucleic acid
STED	Stimulated emission depletion
T7RNAP	Bacteriophage T7 RNA polymerase
TAS	Termination associated sequence
TBS	Tris-buffered saline
TEFM	Mitochondrial transcription elongation factor
TFAM	Mitochondrial transcription factor A
TFB2M	Mitochondrial transcription factor B2
TIM	Translocase of the inner membrane
TOM	Translocase of the outer membrane
µm	Micrometer
µM	Micromolar
v/v	volume/volume
w/v	weight/volume

8. References

Agaronyan, K., Morozov, Y.I., Anikin, M., Temiakov, D. (2015). Mitochondrial biology: replication-transcription switch in human mitochondria. Science, 347, 548–51

Albring, M., Griffith, J., G. Attardi, G., (1977). Association of a protein structure of probable membrane derivation with HeLa cell mitochondrial DNA near its origin of replication. Proc Natl Aca. Sci U S A, 74(4), 1348-1352

Ambika Bumb, A., Sarkar, S.K., Wu, X.S., Brechbiel, M.W., Neuman, K.C. (2011). Quantitative characterization of fluorophores in multi-component nanoprobes by single-molecule fluorescence. Biomed Opt Express, 2(10), 2761–2769

Amiott, E.A., Jaehning, J.A. (2006). Sensitivity of the yeast mitochondrial RNA polymerase to + 1 and + 2 initiating nucleotides. J Biol Chem, 281 (2006), 34982–34988

Antes, A., Tappin, I., Chung, S., Lim, R., Lu, B. Parrott, A.M., Hill, H.Z., Suzuki, C.K., Lee, C.G. (2010). Differential regulation of full-length genome and a single-stranded 7S DNA along the cell cycle in human mitochondria. Nucleic Acids Res, 38(19), 6466-76

Appleby, R.D., Porteous, W.K., Hughes, G., James, A.M., Shannon, D., Wei, Y.H., Murphy, M.P. (1999). Quantitation and origin of the mitochondrial membrane potential in human cells lacking mitochondrial DNA. , 262(1), 108-16

Arnberg, A., Van Bruggen, E.F.J., Ter Schegget, J., Borst, P. (1971). The presence of DNA molecules with a displacement loop in standard mitochondrial DNA preparations. Biochim Biophys Acta, 246, 353-357

Aguer, C., Gambarotta, D., Mailloux, R.J., Moffat, C., Dent, R., McPherson, R., Harper, M.E. (2011). Galactose Enhances Oxidative Metabolism and Reveals Mitochondrial Dysfunction in Human Primary Muscle Cells. PLoS One, 6(12), e28536

Bailey, L.J., Doherty A.J. (2017), Mitochondrial DNA replication: a PrimPol perspective. Biochem Soc Trans, 45(2), 513-529

Beese, L.S., Derbyshire, V., Steitz, T.A. (1993). Structure of DNA polymerase I Klenow fragment bound to duplex DNA. Science, 260, 352–55

Behar, D.M., Villems, R., Soodyall, H., Blue-Smith, J., Pereira, L., Metspalu, E., Scozzari, R., Makkan, H., Tzur, S., Comas, D., Bertranpetit, J., Quintana-Murci, L., Tyler-Smith, C., Wells, R.S., Rosset, S., Genographic Consortium (2008). The dawn of human matrilineal diversity. Am J Hum Genet, 82(5), 1130-40

Benard, G., Rossignol, R. (2008). Ultrastructure of the mitochondrion and its bearing on function and bioenergetics. Antioxid Redox Signal, 10(8), 1313-42

Berk, A.J., Clayton, D.A. (1974). Mechanism of mitochondrial DNA replication in mouse L-cells: asynchronous replication of strands, segregation of circular daughter molecules, aspects of topology and turnover of an initiation sequence. J Mol Biol, 86, 801–24

Berk, A.J., Clayton, D.A. (1976). Mechanism of mitochondrial DNA replication in mouse L-cells: topology of circular daughter molecules and dynamics of catenated oligomer formation. J Mol Biol, 100, 85–92

Bibb, M.J., Van Etten, R.A., Wright, C.T., Walberg, M.W., Clayton, D.A. (1981). Sequence and gene organization of mouse mitochondrial DNA. Cell, 26, 167–80

Blachly-Dyson, E., Forte, M. (2001). VDA channels. IUBMB Life, 52(3-5), 113-8.

Bogenhagen, D., Clayton, D.A. (1978). Mechanism of mitochondrial DNA replication in mouse L-cells: kinetics of synthesis and turnover of the initiation sequence. J Mol Biol, 119, 49-68

Bogenhagen, D.F., Rousseau, D., Burke, S. (2008). The layered structure of human mitochondrial DNA nucleoids. J Biol Chem, 283(6), 3665-75

Bogenhagen, D.F. (2012). Mitochondrial DNA nucleoid structure. Biochim Biophys Acta, 1819, 914–20

Bowmaker, M., Yang, M.Y., Yasukawa, T., Reyes, A., Jacobs, H.T., Huberman, J.A., Holt, I.J. (2003). Mammalian mitochondrial DNA replicates bidirectionally from an initiation zone. J Biol Chem, 278(51), 50961-9

Brambati, A., Colosio, A., Zardoni, L., Galanti, L., Liberi, G. (2015). Replication and transcription on a collision course: eukaryotic regulation mechanisms and implications for DNA stability. Front Genet, 6, 166

Bron, S., Holsappel, S., Venema, G., Peeters, B.P. (1991). Plasmid deletion formation between short direct repeats in Bacillus subtilis is stimulated by single-stranded rolling-circle replication intermediates. Mol Gen Genet, 226(1-2), 88-96

Brown, W.M., George, M. Jr., Wilson, A.C. (1979). Rapid evolution of animal mitochondrial DNA. Proc Natl Acad Sci U S A, 76(4), 1967-71

Brown, W.M., Prager, E.M., Wang, A., Wilson, A.C. (1982). Mitochondrial DNA sequences of primates: tempo and mode of evolution. J Mol Evol, 18(4), 225-39

Brown, T.A. , Tkachuk, A.N., Shtengel, G., Kopek, B.G., Bogenhagen, D.F., Hess, H.F., Clayton, D.A. (2011) Superresolution fluorescence imaging of mitochondrial nucleoids reveals their spatial range, limits, and membrane interaction. Mol Cell Biol, 31(24), 4994-5010

Bruce, J.I., Giovannucci, D.R., Blinder, G., Shuttleworth, T.J., Yule, D.I. (2004). Modulation of $[Ca^{2+}]i$ signaling dynamics and metabolism by perinuclear mitochondria in mouse parotid acinar cells. J.Biol Chem, 279, 12909–12917

Bua, E., Johnson, J., Herbst, A., Delong, B., McKenzie, D., Salamat, S., Aiken, J.M. (2006). Mitochondrial DNA-deletion mutations accumulate intracellularly to detrimental levels in aged human skeletal muscle fibers. Am J Hum Genet, 79(3), 469-80

Carthew, R.W., Sontheimer, E.J. (2009). Origins and Mechanisms of miRNAs and siRNAs. Cell, 136(4), 642–655

Carrodeguas, J.A., Pinz, K.G., Bogenhagen, D.F. (2002). DNA binding properties of human pol γB. J Biol Chem, 277, 50008–14

Chan, D.C. (2006). Mitochondrial fusion and fission in mammals. Annu Rev Cell Dev Biol, 22, 79-99

Chatre, L., Ricchetti, M. (2013 (1)). Large heterogeneity of mitochondrial DNA transcription and initiation of replication exposed by single-cell imaging. J Cell Sci, 126, 914-926

Chatre, L., Ricchetti, M. (2013 (2)). Prevalent coordination of mitochondrial DNA transcription and initiation of replication with the cell cycle. Nucleic Acids Res, 241(5), 3068-78

Chen, H., Detmer, S.A., Ewald, A.J., Griffin, E.E., Fraser, S.E., Chan, D.C. (2003). Mitofusins Mfn1 and Mfn2 coordinately regulate mitochondrial fusion and are essential for embryonic development. J Cell Biol, 160(2), 189-200

Chinnery, P.F., DiMauro, S., Shanske, S., Schon, E.A., Zeviani, M., Mariotti, C., Carrara, F. Lombes, A., Laforet, P., Ogier, H., Jaksch, M., Lochmüller, H., Horvath, R., Deschauer, M., Thorburn, D.R., Bindoff, L.A., Poulton, J., Taylor, R.W., Matthews, J.N., Turnbull, D.M. (2004). Risk of developing a mitochondrial DNA deletion disorder. Lancet, 364(9434), 592-6

Clayton, D.A. (1991). Replication and transcription of vertebrate mitochondrial DNA Annu Rev Cell Biol, 7, 453–78

Cline, S.D., Lodeiro, F.M., Marnett, L.J., Cameron, C.E., Arnold, J.J. (2010). Arrest of human mitochondrial RNA polymerase transcription by the biological aldehyde adduct of DNA, M_1dG. Nucleic Acids Res, 38(21), 7546–7557

Collins, T.J., Berridge, M.J., Lipp, P., Bootman, M.D. (2002). Mitochondria are morphologically and functionally heterogeneous within cells. EMBO J, 21(7), 1616-27

Corral-Debrinski, M., Shoffner, J.M., Lott, M.T., Wallace, D.C. (1992). Association of mitochondrial DNA damage with aging and coronary atherosclerotic heart disease. Mutat Res, 275(3-6), 169-80

Cotterill, M., Harris, S.E., Fernandez, E.C., Lu, J., Huntriss, J.D., Campbell, B.K., Picton, H.M. (1987). The activity and copy number of mitochondrial DNA in ovine oocytes throughout oogenesis in vivo and during oocyte maturation in vitro. Mol Hum Reprod, 19(7), 444–450

Cree, L,M., Samuels, D.C., de Sousa Lopes, S.C., Rajasimha, H.K., Wonnapinij ,P., Mann, J.R., Dahl, H.H., Chinnery, P.F. (2008). A reduction of mitochondrial DNA molecules during embryogenesis explains the rapid segregation of genotypes. Nat Genet, 40(2), 249-54

Crews, S., Ojala, D., Posakony, J., Nishiguchi, J., Attardi, G. (1979). Nucleotide sequence of a region of human mitochondrial DNA containing the precisely identified origin of replication. Nature, 277(5693), 192-8

Dairaghi, D.J., Shadel, G.S., Clayton, D.A. (1995). Addition of a 29 residue carboxyl-terminal tail converts a simple HMG box-containing protein into a transcriptional activator. J Mol Biol, 249, 11–28

Davis, A.F., Clayton, D.A. (1996). In situ localization of mitochondrial DNA replication in intact mammalian cells. JCB Home, 135(4), 883

De Silva, D., Tu, Y.T., Amunts, A., Fontanesi, F., Barrientos, A. (2015). Mitochondrial ribosome assembly in health and disease. Cell Cycle, 14(14), 2226-50

Doda, N., Wright, C.T., Clayton, D.A. (1981). Elongation of displacement-loop strands in human and mouse mitochondrial DNA is arrested near specific template sequences. Proc Natl Acad Sci U S A, 78(10), 6116-6120

Dolezal, P., Likic, V., Tachezy, J., Lithgow, T. (2006). Evolution of the molecular machines for protein import into mitochondria. Science, 313(5785), 314-8

Duxin, J.P., Dao, B., Martinsson, .P, Rajala, N., Guittat, L., Campbell, J.L., Spelbrink, J.N., Stewart, S.A. (2009). Human Dna2 is a nuclear and mitochondrial DNA maintenance protein. Mol Cell Biol, 29(15), 4274-82

Dzeja, P.P., Bortolon, R., Perez-Terzic, C., Holmuhamedov, E.L., Terzic, A. Energetic communication between mitochondria and nucleus directed by catalyzed phosphotransfer. Proc Natl Acad Sci U S A, 2002 Jul 23, 99(15), 10156-61

Eidinoff, M.L., Cheong, L., Rich, M.A. (1959). Incorporation of unnatural pyrimidine bases into deoxyribonucleic acid of mammalian cells. Science, 129(3362), 1550-1

Ekstrand, M.I., Falkenberg, M., Rantanen, A., Park, C.B., Gaspari, M., Hultenby, K., Rustin, P., Gustafsson, C.M., Larsson, N.G. (2004). Mitochondrial transcription factor A regulates mtDNA copy number in mammals. Hum Mol Genet, 13(9), 935-44

Elson, J.L., Samuels, D.C., Turnbull, D.M., Chinnery, P.F. (2001). Random intracellular drift explains the clonal expansion of mitochondrial DNA mutations with age. Am J Hum Genet, 68(3), 802-6

Embley, T.M., Martin, W. (2006). Eukaryotic evolution, changes and challenges. Nature, 440, 623–630

Ernster, L., Schatz, G. (1981). Mitochondria: a historical review. J Cell Biol, 91(3 Pt 2), 227s-255s

Falkenberg, M., Gaspari, M., Rantanen, A., Trifunovic, A., Larsson, N.G., Gustafsson, C.M. (2002). Mitochondrial transcription factors B1 and B2 activate transcription of human mtDNA. Nat Genet, 31, 289–94

Falkenberg, M., Larsson, N.G., Gustafsson, C.M. (2007). DNA replication and transcription in mammalian mitochondria. Annu Rev Biochem, 76, 679-99.

Farge, G., Pham, X.H., Holmlund, T., Khorostov, I., Falkenberg, M. (2007). The accessory subunit B of DNA polymerase γ is required for mitochondrial replisome function. Nucleic Acids Res, 35, 902–11

Farge, G., Mehmedovic, M., Baclayon, M., van den Wildenberg, S.M., Roos, W.H., Gustafsson, C.M., Wuite, G.J., Falkenberg, M. (2014). In vitro-reconstituted nucleoids can block mitochondrial DNA replication and transcription. Cell Rep, 8(1), 66-74

Fernandez-Silva, P., Martinez-Azorin, F., Micol, V., Attardi, G. (1997). The human mitochondrial transcription termination factor (mTERF) is a multizipper protein but binds to DNA as a monomer, with evidence pointing to intramolecular leucine zipper interactions. EMBO J, 16, 1066–79

Fisher, R.P., Clayton, D.A., (1988). Purification and characterization of human mitochondrial transcription factor 1. Mol Cell Biol, 8(8), 3496-509

Frey, T.G., Mannella, C.A. (2000). The internal structure of mitochondria. Trends Biochem Sci, 225(7), 319-24

Fuste, J.M., Wanrooij, S., Jemt, E., Granycome, C.E., Cluett, T.J., Shi, Y., Atanassova, N., Holt, I.J., Gustafsson, C.M, Falkenberg, M. (2010). Mitochondrial RNA polymerase is needed for activation of the origin of light-strand DNA replication, Mol Cell, 37, 67–78

Futami, K., Shimamoto, A., Furuichi, Y. (2007). Mitochondrial and nuclear localization of human Pif1 helicase. Biol Pharm Bull, 30, 1685–1692

Garcia-Gomez, S., Reyes, A., Martinez-Jimenez, M.I., Chocron, E.S., Mouron, S. (2013). PrimPol, an archaic primase/polymerase operating in human cells. Mol. Cell, 52, 541–53

Garrido, N., Griparic, L., Jokitalo, E., Wartiovaara, J., van der Bliek, A.M., Spelbrink, J.N. (2003). Composition and dynamics of human mitochondrial nucleoids. Mol Biol Cell, 14(4), 1583-96

Gaspari, M., Larsson, N.G., Gustafsson, C.M. (2004 (1)). The transcription machinery in mammalian mitochondria. Biochim Biophys Acta, 1659, 148–152

Gaspari, M., Falkenberg, M., Larsson, N.G., Gustafsson, C.M. (2004 (2)). The mitochondrial RNA polymerase contributes critically to promoter specificity in mammalian cells. EMBO J, 23(23), 4606-14

Gerber, J.K., Gogel, E., Berger, C., Wallisch, M., Muller, F., Grummt, F. (1997). Termination of mammalian rDNA replication: polar arrest of replication fork movement by transcription termination factor TTF-I. Cell, 90, 559–567

Gilkerson, R.W., Schon, E.A., Hernandez, E., Davidson, M.M. (2008). Mitochondrial nucleoids maintain genetic autonomy but allow for functional complementation. J Cell Biol, 181(7), 1117-28

Gilkerson, R., Bravo, L., Garcia, I., Gaytan, N., Herrera, A., Maldonado, A., Quintanilla, B. (2013). The mitochondrial nucleoid: integrating mitochondrial DNA into cellular homeostasis. Cold Spring Harb Perspect Biol, 5(5)

Goto, Y., Hayashi, R., Kang, D., Yoshida, K. (2006) Acute loss of transcription factor E2F1 induces mitochondrial biogenesis in HeLa cells. J Cell Physiol, 209, 923-934

Gratzner, H.G. (1982). Monoclonal antibody to 5-bromo- and 5-iododeoxyuridine: A new reagent for detection of DNA replication. Science, 218(4571), 474-5

Gray, M.W., Burger, G., Lang, B.F. (1999). Mitochondrial evolution. Science, 283, 1476–81

Gray, M.W. (2012). Mitochondrial Evolution. Cold Spring Harb Perspect Biol, 4(9)

Anderson, S., Bankier, A.T., Barrell, B.G., de Bruijn, M.H., Coulson AR (1981). Sequence and organization of the human mitochondrial genome. Nature, 290, 457–65

Guja, K.E., Venkataraman, K., Yakubovskaya, E., Shi, H., Mejia, E., Hambardjieva, E., Karzai, A.W., Garcia-Diaz, M. (2013). Structural basis for S-adenosylmethionine binding and methyltransferase activity by mitochondrial transcription factor B1. Nucleic Acids Res, 41, 7947–7959

Gustafsson, C.M., Falkenberg, M., Larsson, N.G. (2016). Maintenance and Expression of Mammalian Mitochondrial DNA. Annu Rev Biochem, 85, 133-60

Hallberg R.L (1974). DNA in *Xenopus laevis* oocytes I. Displacement loop occurrence. Dev Biol, 38, 346-355

Hallberg, B.M., Larsson, N.G. (2014). Making proteins in the powerhouse. Cell Metab, 20, 226–40

Hance, N., Ekstrand, M.I., Trifunovic, A., (2005). Mitochondrial DNA polymerase γ is essential for mammalian embryogenesis. Hum Mol Genet, 14, 1775–83

Hannus, M., Beitzinger. M., Engelmann, J.C., Weickert, M.-T., Spang, R., Hannus, S., Meister, G. (2014). siPools: highly complex but accurately defined siRNA pools eliminate off-target effects. Nucleic Acids Research, 42(12), 8049-61

Hauswirth, W.W, Laipis, P.J. (1982). Mitochondrial DNA polymorphism in a maternal lineage of Holstein cows. Proc Natl Acad Sci U S A, 79(15), 4686–4690

Hayakawa, T., Noda, M., Yasuda, K., Yorifuji, H., Taniguchii, S,, Miwai, I., Sakura, H., Terauchi, Y., Hayashi, J.-I., Sharp, G.W.G., Kanazawa, Y., Akanuma, Y., Yazaki, Y., Kadowaki, T. (1998). Ethidium Bromide-induced Inhibition of Mitochondrial Gene Transcription Suppresses Glucose-stimulated Insulin Release in the Mouse Pancreatic β-Cell Line βHC9. The Journal of Biological Chemistry, 273, 20300-20307

He, J., Mao, C.-C., Reyes, A., Sembongi, H., Di Re, M., Granycome, C., Clippingdale, A.B., Fearnley, I.M., Harbour, M., Robinson, A.J., Reichelt, S., Spelbrink, J.N, Walker, J.E., Holt,

I.J. (2007). The AAA + protein ATAD3 has displacement loop binding properties and is involved in mitochondrial nucleoid organization. J Cell Biol, 176(2), 141-6

Hedtke, B., Börner, T., Weihe, A. (1997). Mitochondrial and Chloroplast Phage-Type RNA Polymerases in Arabidopsis. Science, 277(5327), 809-811

Hell, S.W., Wichmann, J. (1994). Breaking the diffraction resolution limit by stimulated emission: stimulated-emission-depletion fluorescence microscopy. Opt Lett, 19(11), 780-782

Hell, S.W. (2007). Far-field optical nanoscopy. Science, 316(5828), 1153-1158

Hell, S.W. (2009). Microscopy and its focal switch. Nat Methods, 6(1), 24-32

Hillen, H.S., Morozov, Y.I., Sarfallah, A., Temiakov. D, Cramer, P. (2017 (1)). Structural Basis of Mitochondrial Transcription Initiation. Cell, 171(5), 1072-1081

Hillen, H.S., Parshin, A.V., Agaronyan, K., Morozov, K.I., Graber, J.J., Chernev, A., Schwinghammer, K., Urlaub, H., Anikin, M., Cramer, P., Temiakov, D. (2017 (2)). Mechanism of Transcription Anti-termination in Human Mitochondria. Cell, 171(5), 1082-1093

Holmes, J.B., Akman, G., Wood, S.R., Sakhuja, K., Cerritelli, S.M. (2015). Primer retention owing to the absence of RNase H1 is catastrophic for mitochondrial DNA replication. PNAS, 112, 9334–39

Holt, I.J., He, J., Mao, C-C., Boyd-Kirkup, J.D., Martinsson, P.,Sembongi, H., Reyes, A.,Spelbrink, J.N. (2007). Mammalian mitochondrial nucleoids: organizing an independently minded genome. Mitochondrion, 7(5), 311-321

Holt, I.J., Harding, A.E., Morgan-Hughes, J.A. (1988). Deletions of muscle mitochondrial DNA in patients with mitochondrial myopathies. Nature, 331, 717–719

Holt, I.J., Lorimer, H.E., Jacobs, H.T. (2000). Coupled leading- and lagging-strand synthesis of mammalian mitochondrial DNA. Cell, 100, 515–24

Holt, I.J. (2009). Mitochondrial DNA replication and repair: All a flap. Trends Biochem Sci, 34, 358–365

Holt, I.J., Reyes, A. (2012). Human mitochondrial DNA replication. Cold Spring Harb Perspect Biol, 4(12).

Holt, I.J., Jacobs, H.T. (2014). Unique features of DNA replication in mitochondria: a functional and evolutionary perspective. BioEssays, 36, 1024–31

Hyvärinen, A.K., Pohjoismäki, J.L., Reyes, A., Wanrooij, S., Yasukawa, T., Karhunen, P.J., Spelbrink, J.N., Holt, I.J., Jacobs, H.T. (2007). The mitochondrial transcription termination factor mTERF modulates replication pausing in human mitochondrial DNA. Nucleic Acids Res, 35(19), 6458-74

Hyvärinen, A.K., Pohjoismäki, J.L., Holt, I.J., Jacobs, H.T. (2011). Overexpression of MTERFD1 or MTERFD3 impairs the completion of mitochondrial DNA replication. Mol Biol Rep, 38(2), 1321-8

Iborra, F.J., Kimura, H., Cook, P.R. (2004). The functional organization of mitochondrial genomes in human cells. BMC Biol, 2, 9

Ingman, M., Kaessmann, H., Pääbo, S., Gyllensten, U. (2000). Mitochondrial genome variation and the origin of modern humans. Nature, 408(6813), 708-13

Ikeda, M., Ide, T., Fujino, T., Arai, S., Saku, K., Kakino, T., Tyynismaa, H., Yamasaki, T., Yamada, K.-I., Kang, D., Suomalainen, A., Sunagawa, K. (2015). Overexpression of TFAM or Twinkle Increases mtDNA Copy Number and Facilitates Cardioprotection Associated with Limited Mitochondrial Oxidative Stress. PLoS One, 10(3), e0119687

Istiaq Alam, T., Kanki, T., Muta, T., Ukaji, k., Abe, Y., Nakayama, H., Takio, K., Hamasaki, n., Kang, D. (2003). Human mitochondrial DNA is packaged with TFAM. Nucleic Acids Res, 31(6), 1640–1645

Jans, D.C., Wurm, C.A., Riedel , D., Wenzel, D., Stagge, F., Deckers, M., Rehling, P., Jakobs, S. (2013). STED super-resolution microscopy reveals an array of MINOS clusters along human mitochondria. Proc Natl Acad Sci U S A, 110(22), 8936–8941

Jemt, E., Persson, Ö., Shi, Y., Mehmedovic, M., Uhler, J.P., Dávila López, M., Freyer, C., Gustafsson, C.M., Samuelsson, T., Falkenberg, M. (2015). Regulation of DNA replication at the end of the mitochondrial D-loop involves the helicase TWINKLE and a conserved sequence element. Nucleic Acids Res, 43(19), 9262-75

Jeruzalmi, D., Steitz, T.A. (1998). Structure of T7 RNA polymerase complexed to the transcriptional inhibitor T7 lysozyme. EMBO J, 17(14), 4101-13

Kaguni, L.S. (2004). DNA polymerase γ, the mitochondrial replicase. Annu Rev Bioche. 73, 293–320

Jourdain, A.A., Koppen, M., Wydro, M., Rodley, C.D., Lightowlers, R.N., Chrzanowska-Lightowlers, Z.M., Martinou, J.C. (2013). GRSF1 regulates RNA processing in mitochondrial RNA granules. Cell Metab, 17(3), 399-410

Kasamatsu, H., Robberson, D.L., Vinograd, J. (1971). A novel closed-circular mitochondrial DNA with properties of a replicating intermediate. Proc Natl Acad Sci U S A, 68(9), 2252-225

Kasamatsu, H., Vinograd, J. (1973). Unidirectionality of replication in mouse mitochondrial DNA. Nat New Biol, 241(108), 103-5.

Kaufman, B.A., Durisic, N., Mativetsky, J.M., Costantino, S., Hancock, M.A., Grutter, P., Shoubridge, E.A. (2007). The mitochondrial transcription factor TFAM coordinates the assembly of multiple DNA molecules into nucleoid-like structures. Mol Biol Cell, 18(9), 3225-36

Kerner, J., Hoppel, C. (2000). Fatty acid import into mitochondria. Biochimica et Biophysica Acta (BBA) - Molecular and Cell Biology of Lipids,1486(1), 1-17

Klingbeil, M.M., Motyka, S.A., Englund, P.T. (2002). Multiple mitochondrial DNA polymerases in *Trypanosoma brucei*. Mol Cell, 10, 175–186

Kobayashi, T., Horiuchi, T. (1996). A yeast gene product, Fob1 protein, required for both replication fork blocking and recombinational hotspot activities. Genes Cells, 1, 465–474

Korhonen, J.A., Gaspari, M., Falkenberg, M. (2003). TWINKLE has 5′ → 3′ DNA helicase activity and is specifically stimulated by mitochondrial single-stranded DNA-binding protein. J Biol Chem, 278, 48627–32

Korhonen, J.A., Pham, X.H., Pellegrini, M., Falkenberg, M. (2004). Reconstitution of a minimal mtDNA replisome in vitro. EMBO J, 23, 2423–29

Kornblum, C., Nicholls, T.J., Haack, T.B., Schöler, S., Peeva, V., Danhauser, K., Hallmann, K., Zsurka, G., Rorbach, J., Iuso, A., Wieland, T., Sciacco, M., Ronchi, D., Comi, G.P., Moggio, M., Quinzii, C.M., Dimauro, S., Calvo, S.E.,Mootha, V.K., Klopstock, T., Strom, T.M.,Meitinger, T., Minczuk, M., Kunz, W.S., Prokisch, H. (2013). Loss-of-function mutations in MGME1 impair mtDNA replication and cause multisystemic mitochondrial disease. Nat Genet, 45(2), 214-219

Kruse, B., Narasimhan, N., Attardi, G. (1989). Termination of transcription in human mitochondria: identification and purification of a DNA binding protein factor that promotes termination. Cell, 58, 391–97

Kühl, I., Miranda, M., Posse, V., Milenkovic, D., Mourier, A., Siira, J., Bonekamp, N.A. (2016). POLRMT regulates the switch between replication primer formation and gene expression of mammalian mtDNA. Science Advances, 2(8), e1600963

Kühlbrandt, W. (2015). Structure and function of mitochondrial membrane protein complexes. BMC Biol, 13, 89

Kukat, C., Wurm, C.A., Spahr, H., Falkenberg, M., Larsson, N.G., Jakobs, S. (2011) Super-resolution microscopy reveals that mammalian mitochondrial nucleoids have a uniform size and frequently contain a single copy of mtDNA. PNAS, 108, 13534–39

Kukat, C., Larsson, N.G. (2013). mtDNA makes a U-turn for the mitochondrial nucleoid. Trends Cell Biol, 23, 457–63

Kukat, C., Davies, K.M., Wurm, C.A., Spåhr, H., Bonekamp, N.A., Kühl, I., Joos, F., Polosa, P.L., Park, C.B., Posse, V., Falkenberg, M., Jakobs, S., Kühlbrandt, W., Larsson, N.G. (2015) Cross-strand binding of TFAM to a single mtDNA molecule forms the mitochondrial nucleoid." PNAS, 112(36), 11288-93,

Kuznetsov, A.V., Mayboroda, O., Kunz, D., Winkler, K., Schubert, W., Kunz, W.S. (1998). Functional imaging of mitochondria in saponin-permeabilized mice muscle fibers. J Cell Biol, 140(5), 1091-9

Kuznetsov, A.V., Usson, Y., Leverve, X., Margreiter, R. (2004). Subcellular heterogeneity of mitochondrial function and dysfunction: evidence obtained by confocal imaging. Mol Cell Biochem, 256–257, 359–365

Kuznetsov, A.V., Troppmair, J., Sucher, R., Hermann, M., Saks, V., Margreiter, R. (2006). Mitochondrial subpopulations and heterogeneity revealed by confocal imaging: possible physiological role? Biochim Biophys Acta, 1757(5-6), 686-91

Kuznetsov, A.V., Margreiter, R. (2009). Heterogeneity of Mitochondria and Mitochondrial Function within Cells as Another Level of Mitochondrial Complexity. Int J Mol Sci, 10(4), 1911–1929

Kwong, L.K., Sohal, R.S. (2000). Age-related changes in activities of mitochondrial electron transport complexes in various tissues of the mouse. Arch Biochem Biophys, 373(1), 16-22

Laemmli, U.K. (1970). Cleavage of Structural Proteins During the Assembly Bacteriophage T4. Nature, 227(5259), 680-5

Lakshmipathy, U., Campbell, C. (1999). The human DNA ligase III gene encodes nuclear and mitochondrial proteins. Mol Cel. Biol, 19, 3869–76

Larsson, N.G., Clayton, D.A. (1995). Molecular genetic aspects of human mitochondrial disorders. Annu Rev Genet, 29, 151-78

Larsson, N.G., Garman, J.D., Oldfors, A., Barsh, G.S., Clayton, D.A. (1996). A single mouse gene encodes the mitochondrial transcription factor A and a testis-specific nuclear HMG-box protein. Nat Genet, 13, 296–302

Larsson, N.G., Wang, J., Wilhelmsson, H., Oldfors, A., Rustin, P., (1998). Mitochondrial transcription factor A is necessary for mtDNA maintenance and embryogenesis in mice. Nat Genet, 18, 231–36

Lee, S.R., Han J. (2017). Mitochondrial Mutations in Cardiac Disorders. Adv Exp Med Biol, 982, 81-111

Legros, F., Malka, F., Frachon, P., Lombès, A., Rojo, M. (2004). Organization and dynamics of human mitochondrial DNA. Journal of Cell Science, 117, 2653-2662

Lewis, S.C., Uchiyama, L.F., Nunnari, J. (2016). ER-mitochondria contacts couple mtDNA synthesis with mitochondrial division in human cells. Science, 353, 6296

Li, F., Wang, Y., Zeller, K.I., Potter, J.J., Wonsey, D.R., O'Donnell, k.A., Kim, J.-W., Yustein, J.T., Lee, L.A., Dang, C.V. (2005). Myc Stimulates Nuclearly Encoded Mitochondrial Genes and Mitochondrial Biogenesis. Mol Cell Biol, 25(14), 6225–6234

Li, H., Ruan, Y., Zhang, K., Jian, F., Hu, C., Miao, L., Gong, L., Sun, L., Zhang, X., Chen, S., Chen, H., Liu, D., Zong, S. (2016). Mic60/Mitofilin determines MICOS assembly essential for mitochondrial dynamics and mtDNA nucleoid organization. Cell Death Differ, 23(3), 380–392

Liang, L., Astruc, D. (2011). The copper(I)-catalyzed alkyne-azide cycloaddition (CuAAC) “click” reaction and its applications. An overview. Volume 255, 23–24, 2933-2945

Ligasová, A., Strunin, D., Friedecký, D., Adam, T., Koberna, K. (2015). A Fatal Combination: A Thymidylate Synthase Inhibitor with DNA Damaging Activity. PLoS One, 10(2), e0117459

Lill, R., Fekete, Z., Sipos, K. and Rotte, C. (2005). Is there an answer? Why are mitochondria essential for life? IUBMB Life, 57(10), 701-70.

Lin, M.T., Simon, D.K., Ahn, C.H., Kim, L.M., Beal, M.F. (2002). High aggregate burden of somatic mtDNA point mutations in aging and Alzheimer's disease brain. Hum Mol Genet, 11(2), 133-45

Liu, P., Qian, L., Sung, J.S., de Souza-Pinto, N.C., Zheng, L., Bogenhagen, D.F., Bohr, V.A., Wilson, D.M. 3rd, Shen, B., Demple, B. (2008). Removal of oxidative DNA damage via FEN1-dependent long-patch base excision repair in human cell mitochondria. Mol Cell Biol, 28(16), 4975-87

Lodeiro, M.F., Uchida, A., Bestwick, M., Moustafa, I.M., Arnold, J.J., Shadel, G.S., Cameron, C.E. (2012). Transcription from the second heavy-strand promoter of human mtDNA is repressed by transcription factor A *in vitro*. Proc Natl Acad Sci U S A, 109, 6513–6518

Longley, M.J., Nguyen, D., Kunkel, T.A., Copeland, W.C. (2001). The fidelity of human DNA polymerase γ with and without exonucleolytic proofreading and the p55 accessory subunit. J Biol Chem, 276, 38555–62

Low, R.L., Orton, S., Friedman, D.B. (2003). A truncated form of DNA topoisomerase IIbeta associates with the mtDNA genome in mammalian mitochondria. Eur J Biochem, 270(20), 4173-86

Lu, B., Lee, J., Nie, X., Li, M., Morozov, Y.I., Venkatesh, S., Bogenhagen, D.F., Temiakov, D., Suzuki, C.K. (2013). Phosphorylation of human TFAM in mitochondria impairs DNA binding and promotes degradation by the AAA+ Lon protease. Mol Cell, 49(1), 121-32

Macao, B., Uhler, J.P., Siibak, T., Zhu. X., Shi, Y. (2015). The exonuclease activity of DNA polymerase γ is required for ligation during mitochondrial DNA replication. Nat Commun, 6, 7303

Madsen, C.S., Ghicizzani, S.C., Hauswirth, W.W. (1993). Binding to a Single Termination-Associated Sequence in the Mitochondrial DNA D-Loop Region. Mol Cell Biol, 13(4), 2162-71.

Maniura-Weber, K., Goffart, S., Garstka, H.L., Montoya, J., Wiesner, R.J. (2004). Transient overexpression of mitochondrial transcription factor A (TFAM) is sufficient to stimulate mitochondrial DNA transcription, but not sufficient to increase mtDNA copy number in cultured cells. Nucleic Acids Res, 32(20), 6015-27

Martin, W., Garg, S., Zimorski, V. (2015). Endosymbiotic theories for eukaryote origin. Philos Trans R Soc Lond B, 370, 20140330

Mello, C.C., Conte, D., Jr. (2004). Revealing the world of RNA interference. Nature, 431, 338–342

Minczuk, M., He, J., Duch, A.M., Ettema, T.J., Chlebowski, A., Dzionek, K., Nijtmans, L.G., Huynen, M.A., Holt, I.J. (2011). TEFM (c17orf42) is necessary for transcription of human mtDNA. Nucleic Acids Res, 39, 4284–4299

Milenkovic, D., Matic, S., Kühl, I., Ruzzenente, B., Freyer, C., Jemt, E., Park, C.B., Falkenberg, M., Larsson, N.-G. (2013). TWINKLE is an essential mitochondrial helicase

required for synthesis of nascent D-loop strands and complete mtDNA replication. Human Molecular Genetics, 22(10), 1983–1993

Milner, D.J., Mavroidis, M., Weisleder, N., Capetanaki, Y. (2000) Desmin cytoskeleton linked to muscle mitochondrial distribution and respiratory function. J Cell Biol, 150, 1283–1298

Montoya, J., Christianson, T., Leven,s D., Rabinowitz, M., Attardi, G. (1982). Identification of initiation sites for heavy-strand and light-strand transcription in human mitochondrial DNA. PNAS, 79, 7195–99

Montoya. J., López-Pérez, M.J., Ruiz-Pesini, E. (2006). Mitochondrial DNA transcription and diseases: past, present and future. Biochim Biophys Acta, 1757(9-10), 1179-89

Morozov, Y.I., Agaronyan, K., Cheung, A.C.M., Anikin, M., Cramer, P., Temiakov, D. (2014). A novel intermediate in transcription initiation by human mitochondrial RNA polymerase. Nucleic Acids Res, 42(6), 3884–3893

Morozov, Y.I., Parshin, A.V., Agaronyan, K., Cheung, A.C.M., Anikin, M., Cramer, P., Temiakov, D. (2015) A model for transcription initiation in human mitochondria. Nucleic Acids Res, 43(7), 3726–3735

Morozov, Y.I., Temiakov, D. (2016). Human Mitochondrial Transcription Initiation Complexes Have Similar Topology on the Light and Heavy Strand Promoters. J Biol Chem, 291(26), 13432-5

Mourón, S., Rodriguez-Acebes, S., Martínez-Jiménez, M.I., García-Gómez. S., Chocrón, S., Blanco, L., Méndez, J. (2013). Repriming of DNA synthesis at stalled replication forks by human PrimPol. Nat Struct Mol Biol, 20(12), 1383-9

Narasimhan, N., Attardi, G. (1987). Specific requirement for ATP at an early step of in vitro transcription of human mitochondrial DNA. Proc Natl Acad Sci U S A, 84 (1987), 4078–4082

Nass, S., Nass, M.M.K. (1963). Intramitochondrial fibers with DNA characteristics. J Cell Biol, 19, 613-629

Neckelmann, N., Li, K., Wade, R.P., Shuster, R., Wallace, D.C. (1987). cDNA sequence of a human skeletal muscle ADP/ATP translocator: lack of a leader peptide, divergence from a fibroblast translocator cDNA, and coevolution with mitochondrial DNA genes. Proc Natl Acad Sci U S A, 84(21), 7580-4

Neupert, W, Herrmann, J.M. (2007). Translocation of Proteins into Mitochondria. Annual Review of Biochemistry, 76, 723-749

Nicholls, T.J., Minczuk, M. (2014). D-loop: 40 years of mitochondrial 7S DNA. Exp Gerontol, 56, 175-81

Nowakowski, R.S., Lewin, S.B., Miller, M.W. (1989). Bromodeoxyuridine immunohistochemical determination of the lengths of the cell cycle and the DNA-synthetic phase for an anatomically defined population. J Neurocytol, 8(3), 311-8

Nunnari, J., Suomalainen, A. (2012). Mitochondria: in sickness and in health. Cell, 148(6), 1145-59

Ojala, D., Montoya, J., Attardi, G. (1981). tRNA punctuation model of RNA processing in human mitochondria. Nature, 290, 470–74

Park, M.K., Ashby, M.C., Erdemli, G., Petersen, O.H., Tepikin, A.V. (2001). Perinuclear, perigranular and sub-plasmalemmal mitochondria have distinct functions in the regulation of cellular calcium transport. EMBO J; 20(8), 1863-74

Pikó, L., Taylor K.D. (1987). Amounts of mitochondrial DNA and abundance of some mitochondrial gene transcripts in early mouse embryos. Dev Biol, 123(2), 364-74

Pinz, K.G., Bogenhagen, D.F. (2000). Characterization of a catalytically slow AP lyase activity in DNA polymerase γ and other family A DNA polymerases. J Biol Chem, 275, 12509–14

Posse, V., Shahzad, S., Falkenberg, M., Hallberg, B.M., Gustafsson, C.M. (2015). TEFM is a potent stimulator of mitochondrial transcription elongation in vitro. Nucleic Acids Res, 43, 2615–24

Pohjoismäki, J.L.O., Wanrooij, S., Hyvärinen, A.K., Goffart, S., Holt, J.I., Spelbrink, J.N., Jacobs, H.T. (2006). Alterations to the expression level of mitochondrial transcription factor A, TFAM, modify the mode of mitochondrial DNA replication in cultured human cells. Nucleic Acids Res, 34(20), 5815–5828

Pohjoismaki, J.L.O., Holmes, J.B., Wood, S.R., Yang, M.Y., Yasukawa, T., Reyes, A., Bailey, L.J., Cluett, T.J., Goffart, S., Willcox, S., (2010). Mammalian mitochondrial DNA replication intermediates are essentially duplex but contain extensive tracts of RNA/DNA hybrid. J Mol Biol, 397, 1144–1155

Pyle, A., Anugrha, H., Kurzawa-Akanbi, M. , Burn, D., Hudson, G., (2016). Reduced mitochondrial DNA copy number is a biomarker of Parkinson's disease. Neurobiology of Aging, 216.e7-216.e10

Ravichandran, V., Vasquez, G.B., Srivastava, S., Verma, M., Petricoin, E., (2004). Data standards for proteomics: mitochondrial two-dimensional polyacrylamide gel electrophoresis data as a model system. Mitochondrion, 3, 327–36

Ringel, R., Sologub. M, Morozov, Y.I., Litonin, D., Cramer, P., Temiakov, D. (2011). Structure of human mitochondrial RNA polymerase. , 478(7368), 269-73

Cheetham, G.M, Steitz TA. (1999). Structure of a transcribing T7 RNA polymerase initiation complex. Science, 286, 2305–2309

Robberson, D.L., Clayton, D.A. (1972). Replication of mitochondrial DNA in mouse L cells and their thymidine kinase - derivatives: displacement replication on a covalently-closed circular template. Proc Natl Acad Sci U S A, 69(12), 3810-4

Robberson, D.L., Kasamatsu, H., Vinograd, J. (1972). Replication of mitochondrial DNA. Circular replicative intermediates in mouse L cells. Proc Natl Acad Sci U S A, 69(3), 737-741

Romashko, D.N., Marban, E., O'Rourke, B. (1998). Subcellular metabolic transients and mitochondrial redox waves in heart cells. Proc Natl Acad Sci U S A, 95(4), 1618-23

Ropp, P.A., Copeland, W.C. (2013). Cloning and characterization of the human mitochondrial DNA polymerase, DNA polymerase gamma. Genomics, 36(3), 449-58

Rostovtsev, V.V., Green, L.G., Fokin, V.V., Sharpless, K.B. (2002). A stepwise huisgen cycloaddition process: copper(I)-catalyzed regioselective "ligation" of azides and terminal alkynes. Angew Chem Int Ed Engl, 41(14), 2596-9

Saccone, C., Pesole, G., Sbisa, E. (1991). The main regulatory region of mammalian mitochondrial DNA: structure–function model and evolutionary pattern. J Mol Evol, 33, 83-91

Sagan, L. (1976). On the origin of mitosing cells. J Theor Biol, 14(3), 255-74

Saks VA, Kaambre T, Sikk P, Eimre M, Orlova E, Paju K, Piirsoo A, Appaix F, Kay L, Regitz-Zagrosek V, Fleck E, Seppet E. Intracellular energetic units in red muscle cells. Biochem. J, 356, 643–657.

Salic, A., Mitchison, T. J. (2008). A chemical method for fast and sensitive detection of DNA synthesis in vivo. Proceedings of the National Academy of Sciences of the United States of America, 105(7), 2415-2420

Salinovich, O., Montelaro, R.C. (1986). Reversible Staining and Peptide Mapping of

Proteins Transferred to Nitrocellulose after Separation by Sodium Dodecylsulfate-Polyacrylamide Gel Electrophoresis. Anal Biochem, 156(2), 341-7

Sasaki, T., Sato, Y., Higashiyama, T., Sasaki, N. (2017). Live imaging reveals the dynamics and regulation of mitochondrial nucleoids during the cell cycle in Fucci2-HeLa cells. Sci Rep, 7, 11257

Sbisà, E., Tanzariello, F., Reyes, A., Pesole, G., Saccone, C. (1997). Mammalian mitochondrial D-loop region structural analysis: identification of new conserved sequences and their functional and evolutionary implications. Gene, 205, 125-140

Schwinghammer, K., Cheung, A.C.M., Morozov, Y.I., Agaronyan, K., Temiakov, D., Cramer, P. (2013). Structure of human mitochondrial RNA polymerase elongation complex. Nat Struct Mol Biol, 20(11), 1298–1303

Scott, I., Youle. R.J. (2010). Mitochondrial fission and fusion. Essays Biochem, 47, 85-98

Seppet, E.K., Kaambre, T., Sikk, P., Tiivel, T., Vija, H., Tonkonogi, M., Sahlin, K., Kay, L., Appaix, F., Braun, U., Eimre, M., Saks, V.A. (2001). Functional complexes of mitochondria with Ca, MgATPases of myofibrils and sarcoplasmic reticulum in Muscle Cells Biochim Biophys Acta, 1504, 379–395

Shi, Y., Dierckx, A., Wanrooij, P.H., Wanrooij, S., Larsson, N.G., (2012). Mammalian transcription factor A is a core component of the mitochondrial transcription machinery. PNAS, 109, 16510–15

Shi, Y., Posse, V., Zhu, X., Hyvärinen, A.K., Jacobs, H.T., Falkenberg, M., Gustafsson, C.M. (2016). Mitochondrial transcription termination factor 1 directs polar replication fork pausing. Nucleic Acids Res, 44(12), 5732–5742

Shutt, T.E., Gray, M.W. (2006). Bacteriophage origins of mitochondrial replication and transcription proteins. Trends Genet, 22, 90–95

Shutt, T.E., Shadel, G.S. (2011). A compendium of human mitochondrial gene expression machinery with links to disease. Environ Mol Mutagen, 51, 360–379

Sickmann, A., Reinders, J., Wagner, Y., Joppich, C., Zahedi, R. (2003). The proteome of *Saccharomyces cerevisiae* mitochondria. PNAS, 100, 13207–12

Sidenstein, S.C., D'Este, E., Böhm, M.J., Danzl, J.G., Belov, V.N., Hell, S.W. (2016). Multicolour Multilevel STED nanoscopy of Actin/Spectrin Organization at Synapses. Sci Rep, 6, 26725

Smirnova, E., Griparic, L., Shurland, D.L., van der Bliek A.M. (2001). Dynamin-related protein Drp1 is required for mitochondrial division in mammalian cells. Mol Biol Cell, 12(8), 2245-56

Sobek, S., Dalla Rosa, I., Pommier, Y., Bornholz, B., Kalfalah, F., Zhang, H., Wiesner, R.J., von Kleist-Retzow, J.-C., Hillebrand, F., Schaal, H., Mielke, C., Christensen, M.O., Boege, F. (2013). Negative regulation of mitochondrial transcription by mitochondrial topoisomerase I. Nucleic Acids Res, 41(21), 9848–9857

Sologub, M., Litonin, D., Anikin, M., Mustaev, A., Temiakov, D. (2009), TFB2 is a transient component of the catalytic site of the human mitochondrial RNA polymerase. Cell, 139, 934–944

Spelbrink, J.N., Li, F.Y., Tiranti, V., Nikali, K., Yuan, Q.P., (2001). Human mitochondrial DNA deletions associated with mutations in the gene encoding Twinkle, a phage T7 gene 4-like protein localized in mitochondria. Nat Genet, 28, 223–31

Stefano, G.B., Bjenning, C., Wang, F., Wang, N., Kream, R.M. (2017). Mitochondrial Heteroplasmy. Adv Exp Med Biol, 982, 577-594

Stewart, J.B., Freyer, C., Elson, J.L., Larsson, N.G. (2008). Purifying selection of mtDNA and its implications for understanding evolution and mitochondrial disease. Nat Rev Genet, 9(9), 657-62

Taanman, J.-W. (1999). The mitochondrial genome: structure, transcription, translation and replication. Biochimica et Biophysica Acta (BBA) - Bioenergetics, 1410(9), 103-123

Tani, H., Akimitsu, N. Genome-wide technology for determining RNA stability in mammalian cells: Historical perspective and recent advantages based on modified nucleotide labeling. RNA Biol, 9(10), 1233-8

Taupin, P. (2007). BrdU immunohistochemistry for studying adult neurogenesis: paradigms, pitfalls, limitations, and validation. Brain Res Rev, 53, 198–214

Taylor, R.W., Chinnery, P.F., Turnbull, D.M., Lightowlers, R.N. (1997). Selective inhibition of mutant human mitochondrial DNA replication in vitro by peptide nucleic acids. Nat Genet, 15(2), 212-5

Taylor, R.W., Turnbull, D.M. (2005). Mitochondrial DNA mutations in human disease. Nat Rev Genet, 6(5), 389-402

Temiakov, D., Patlan, V., Anikin, M., McAllister, W.T., Yokoyama, S., Vassylyev, D.G. (2004). Structural basis for substrate selection by t7 RNA polymerase. Cell. 116, 381–391

Terzioglu, M., Ruzzenente, B., Harmel, J., Mourier, A., Jemt, E., Lopez, M.D., Kukat, C., Stewart, J.B., Wibom, R., Meharg, C. (2013). MTERF1 binds mtDNA to prevent transcriptional interference at the light-strand promoter but is dispensable for rRNA gene transcription regulation. Cell Metab, 17, 618–626

Tornøe, C.W., Christensen, C., Meldal, M. (2002). Peptidotriazoles on Solid Phase: [1,2,3]-Triazoles by Regiospecific Copper(I)-Catalyzed 1,3-Dipolar Cycloadditions of Terminal Alkynes to Azides. J Org Chem, 67(9), 3057–3064

Trifunovic, A., Wredenberg, A., Falkenberg, M., Spelbrink, J.N., Rovio, A.T. (2004). Premature ageing in mice expressing defective mitochondrial DNA polymerase. Nature, 429, 417–23

Tuppen, H.A., Blakely, E.L., Turnbull, D.M., Taylor, R.W. (2010). Mitochondrial DNA mutations and human disease. Biochim Biophys Acta, 1797(2), 113-28

Tyynismaa, H., Sembongi, H., Bokori-Brown, M., Granycome, C., Ashley, N. (2004). Twinkle helicase is essential for mtDNA maintenance and regulates mtDNA copy number. Hum. Mol. Genet, 13, 3219–27

Uhler, J.P., Falkenberg, M. (2015). Primer removal during mammalian mitochondrial DNA replication. DNA Repair, 34, 28-38

van den Ouweland, J.M., Lemkes, H.H., Trembath, R,C,, Ross, R., Velho, G., Cohen, D., Froguel, P., Maassen, J.A. (1994). Maternally inherited diabetes and deafness is a distinct subtype of diabetes and associates with a single point mutation in the mitochondrial tRNA(Leu(UUR)) gene. Diabetes, 43(6), 746-51

Vanderlaan, M., Thomas, C.B. (1985). Characterization of monoclonal antibodies to bromodeoxyuridine. Cytometry, 6(6), 501-5

Walberg, M.W., Clayton, D.A. (1981). Sequence and properties of the human KB cell and mouse L cell D-loop regions of mitochondrial DNA. Nucleic Acids Res, 9(20), 5411-5421

Wanrooij, S., Falkenberg, M. (2010(1)). The human mitochondrial replication fork in health and disease. Biochim Biophys Acta, 1797, 1378–1388

Wanrooij, P.H., Uhler, J.P., Simonsson, T., Falkenberg, M. Gustafsson, C.M. (2010(2)). G-quadruplex structures in RNA stimulate mitochondrial transcription termination and primer formation. Proc Natl Acad Sci U S A, 107(37), 16072–16077

Wanrooij, S., Miralles Fuste, J., Stewart, J.B., Wanrooij, P.H., Samuelsson, T. (2012 (1)). In vivo mutagenesis reveals that OriL is essential for mitochondrial DNA replication. EMBO Rep, 13, 1130–37

Wanrooij, P.H., Uhler, J.P., Shi, Y., Westerlund, F., Falkenberg, M., Gustafsson, C.M. (2012 (2)). A hybrid G-quadruplex structure formed between RNA and DNA explains the extraordinary stability of the mitochondrial R-loop. Nucleic Acids Res, 40(20), 10334-44

Wallace, D.C., Ye, J.H., Neckelmann, S.N., Singh, G., Webster, K.A., Greenberg, B.D. (1987). Sequence analysis of cDNAs for the human and bovine ATP synthase beta subunit: mitochondrial DNA genes sustain seventeen times more mutations. Curr Genet, 12(2), 81-90

Wallace, D.C., Singh, G., Lott, M.T., Hodge, J.A., Schurr, T.G., Lezza, A.M., Elsas, L.J. Jr., Nikoskelainen, E.K. (1988). Mitochondrial DNA mutation associated with Leber's hereditary optic neuropathy. Science, 242(4884), 1427-30

Wallace, D.C. (2005). A mitochondrial paradigm of metabolic and degenerative diseases, aging, and cancer: a dawn for evolutionary medicine. Annu Rev Genet, 39, 359-407

Wallace, D.C., Chalkia, D, (2013). Mitochondrial DNA Genetics and the Heteroplasmy Conundrum in Evolution and Disease. Cold Spring Harb Perspect Biol, 5(11), a021220

Wang, Y., Lyu, Y.L., Wang, J.C. (2002). Dual localization of human DNA topoisomerase IIIalpha to mitochondria and nucleus. Proc Natl Acad Sci U S A, 99(19), 12114-9

Williams, K.P., Sobra,l B.W., Dickerman, A.W. (2007). A robust species tree for the Alphaproteobacteria. J Bacteriol 189, 4578–4586

Wurm, C.A., Neumann, D., Lauterbach, M.A., Harke, B., Egner, A., Hell, S.W. and Jakobs, S. (2011). Nanoscale distribution of mitochondrial import receptor Tom20 is adjusted to cellular conditions and exhibits an inner-cellular gradient. Proc Natl Acad Sci U S A, 108(33), 13546-13551

Yakubovskaya, E., Guja, K.E., Eng, E.T., Choi, W.S., Mejia, E., Beglov, D., Lukin, M., Kozakov, D., Garcia-Diaz, M. (2014) Organization of the human mitochondrial transcription initiation complex. Nucleic Acids Res, 42, 4100–4112

Yang, D., Oyaizu, Y., Oyaizu, H., Olsen, G.J., Woese, C.R. (1985). Mitochondrial origins. Proc Natl Acad Sci U S A, 82(13), 4443–4447

Yang, M.Y., Bowmaker, M., Reyes, A., Vergani, L., Angeli, P., Gringeri, E., Jacobs, H.T., Holt, I.J. (2002). Biased incorporation of ribonucleotides on the mitochondrial L-strand accounts for apparent strand-asymmetric DNA replication. Cell, 111(4), 495-505.

Yasukawa, T., Reyes, A., Cluett, T.J., Yang, M.Y., Bowmaker, M., Jacobs, H.T., Holt, I.J. (2006). Replication of vertebrate mitochondrial DNA entails transient ribonucleotide incorporation throughout the lagging strand. EMBO J, 25, 5358–5371

Yen, T.C., Su, J.H., King, K.L., Wei, Y.H. (1991). Ageing-associated 5 kb deletion in human liver mitochondrial DNA. Biochem Biophys Res Commun, 178(1), 124-31

Yoneda, M., Chomyn, A., Martinuzzi, A., Hurko, O., Attardi, G. (1992). Marked replicative advantage of human mtDNA carrying a point mutation that causes the MELAS encephalomyopathy. Proc Natl Acad Sci U S A, 89(23), 11164-8

Young, M.J., Copeland W.C. (2015). Mitochondrial POLG2 disease mutations impair cellular energy supply. Atlas of Science

Zarsky, V., Tachezy, J., Dolezal, P. (2012). Tom40 is likely common to all mitochondria. Curr Biol, 22(12), 479-81

Zhang. H., Barceló. J.M., Lee. B., Kohlhagen, G., Zimonjic, D.B., Popescu, N.C., Pommier, Y. (2001). Human mitochondrial topoisomerase I. Proc Natl Acad Sci U S A, 98(19), 10608-13

Zhang, H., Pommier, Y. (2008). Mitochondrial topoisomerase I sites in the regulatory D-loop region of mitochondrial DNA. Biochemistry, 47, 11196-11203

Zheng, W., Khrapko, K., Coller, H.A., Thilly, W.G., Copeland, W.C. (2006). Origins of human mitochondrial point mutations as DNA polymerase gamma-mediated errors. Mutat Res, 599(1-2), 11-20

9. Supplementary information

Supplement figure 9.1: PicoGreen dissociates from mtDNA

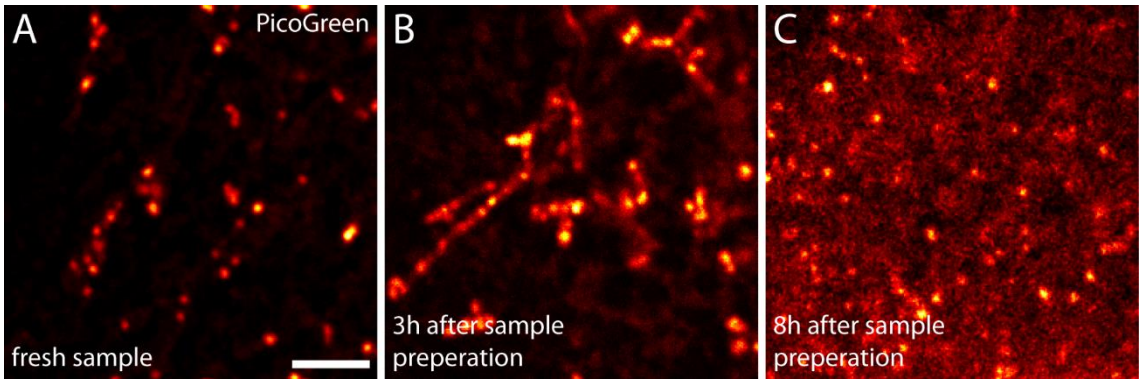

Figure 9.1 PicoGreen dissociates from the mtDNA: U-2 OS cells were incubated with PicoGreen according to the protocol shown in the material and method section. **A)** A confocal record directly after the sample preparation. Single nucleoid signals can be identified and the signal reveals a good contrast. **B)** 3 h after the sample preparation single nucleoid signals can still be identified. However, the background signal is increased, especially in the mitochondrial network as tubular structures can be identified. C) 8 h after the sample preparation single nucleoid signals are very dim. The sample reveals a high level of background and a poor contrast. Scale bar: 3 µm

Supplement figure 9.2: Antibodies against proteins involved in mitochondrial replication do not label active nucleoids

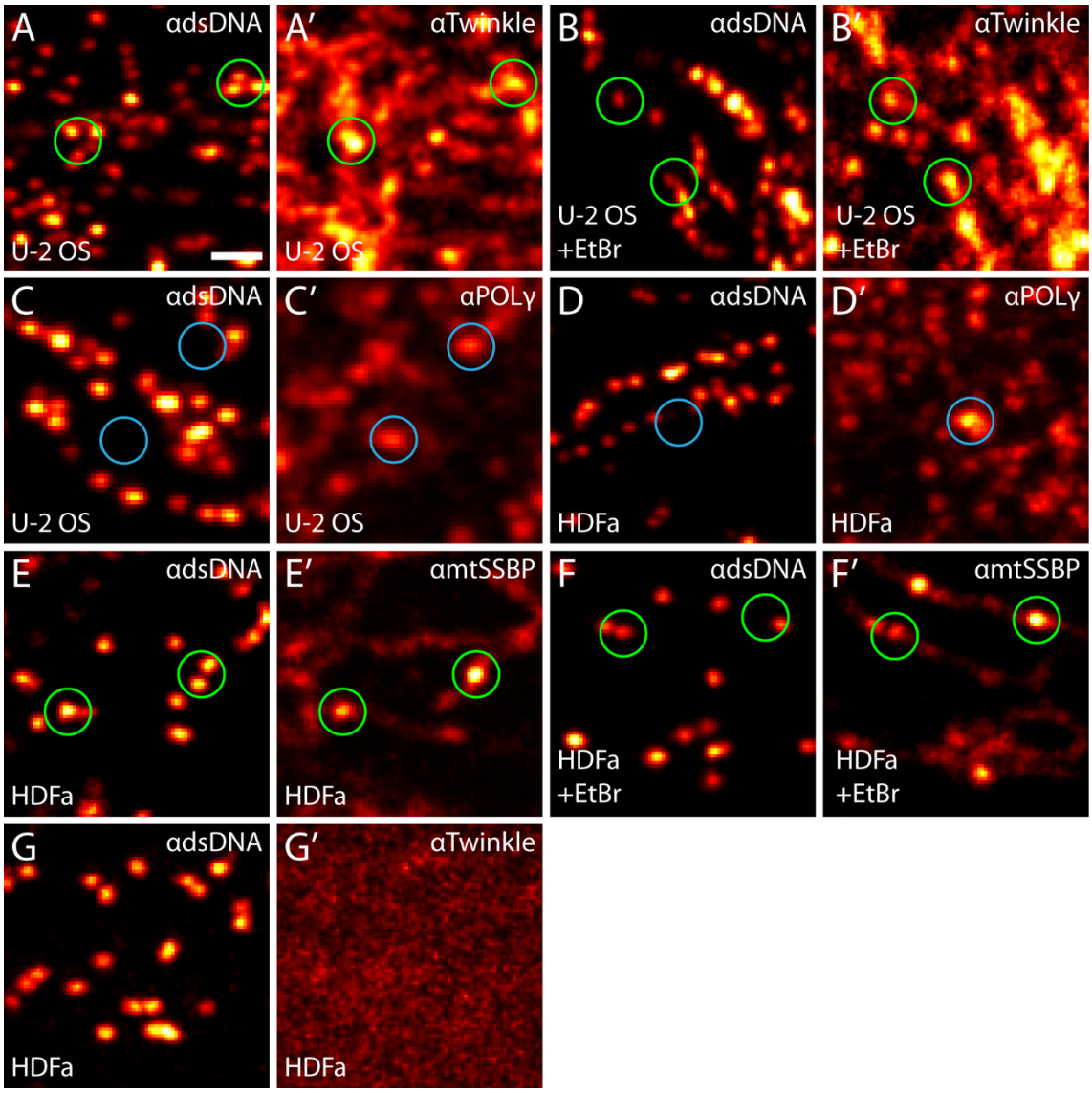

Figure 9.2 Antibodies against proteins involved in mitochondrial replication do not label active nucleoids: U-2 OS cells and HDFa cells were incubated with antisera against dsDNA to label nucleoids and different proteins involved in mitochondrial transcription. **A-B'')** Un U-2 OS cells TWINKLE signal is located in the cytoplasm and the mitochondria (A-A'). The signal reveals an enrichment in dots that partially colocalize with nucleoids (green circles). Upon EtBr treatment (B-B'), this colocalization can still be observed (green circles). **C-D'')** The used antibodies against POLγ showed a weak enrichment in some dots in U-2 OS and HDFa cells (blue circles) that do not colocalize with nucleoids. **E-F')** In HDFa cells antibodies against mtSSBP show a signal that is enriched at nucleoids (E-E'; green circles). This colocalization of mtSSBP and nucleoids is not impaired by EtBr treatment (F-F'). **G-G')** In HDFa cells, TWINKLE antibodies show no signal. Scale bar: 1 µm

Supplement figure 9.3: Antibodies against proteins involved in mitochondrial transcription do not label active nucleoids

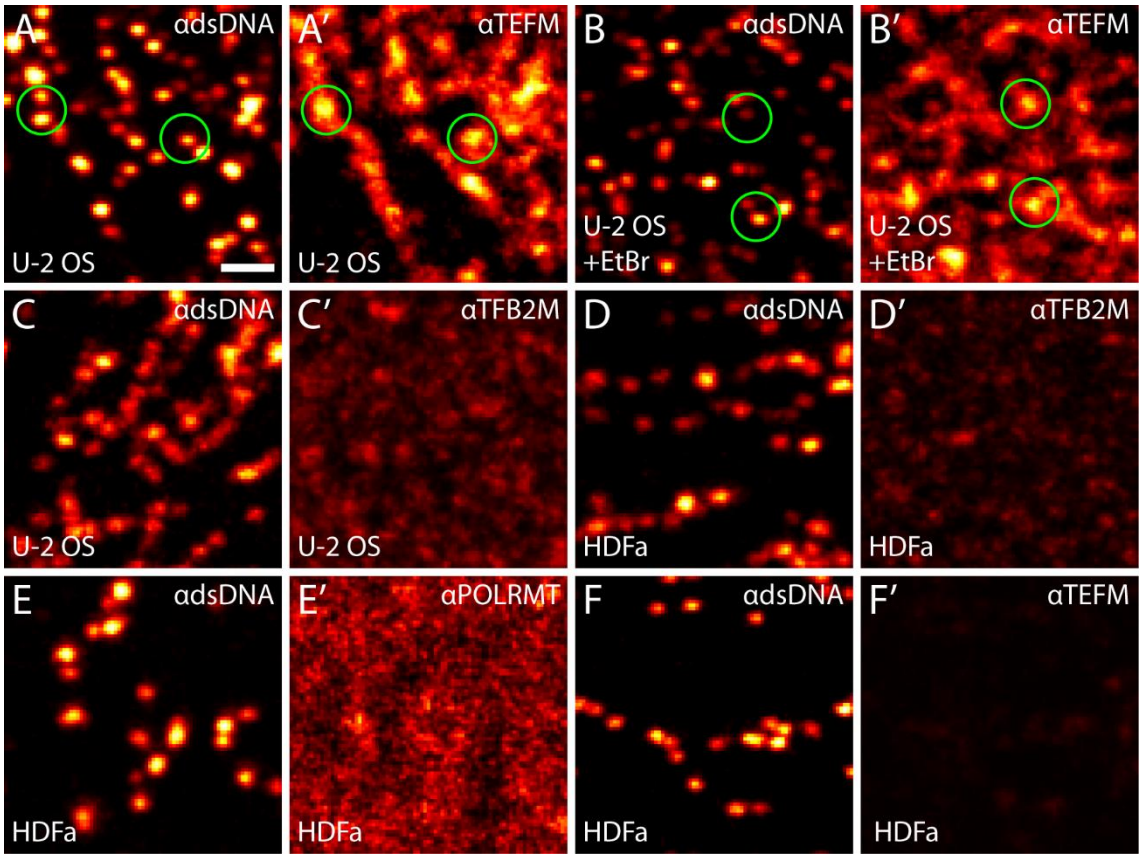

Figure 9.3 Antibodies against proteins involved in mitochondrial transcription do not label active nucleoids: U-2 OS cells and HDFa cells were incubated with antisera against dsDNA to label nucleoids and different proteins involved in mitochondrial transcription. **A-B')** In U-2 OS cells, TEFM signal is enriched in defined dots within mitochondria that partially colocalize with nucleoids (A-A'; green circles). This colocalization is not disturbed by EtBr treatment (B-B'). **C-D')** Neither in U-2 OS cells nor in HDFa cells, the used antibodies against TFB2M revealed a specific signal. **E-F')** In HDFa cells, the used antibodies against POLRMT and TEFM show no specific signal. Scale bar 1 µm

Supplement figure 9.4: Optimized concentration and incubation time for EdU and BrU

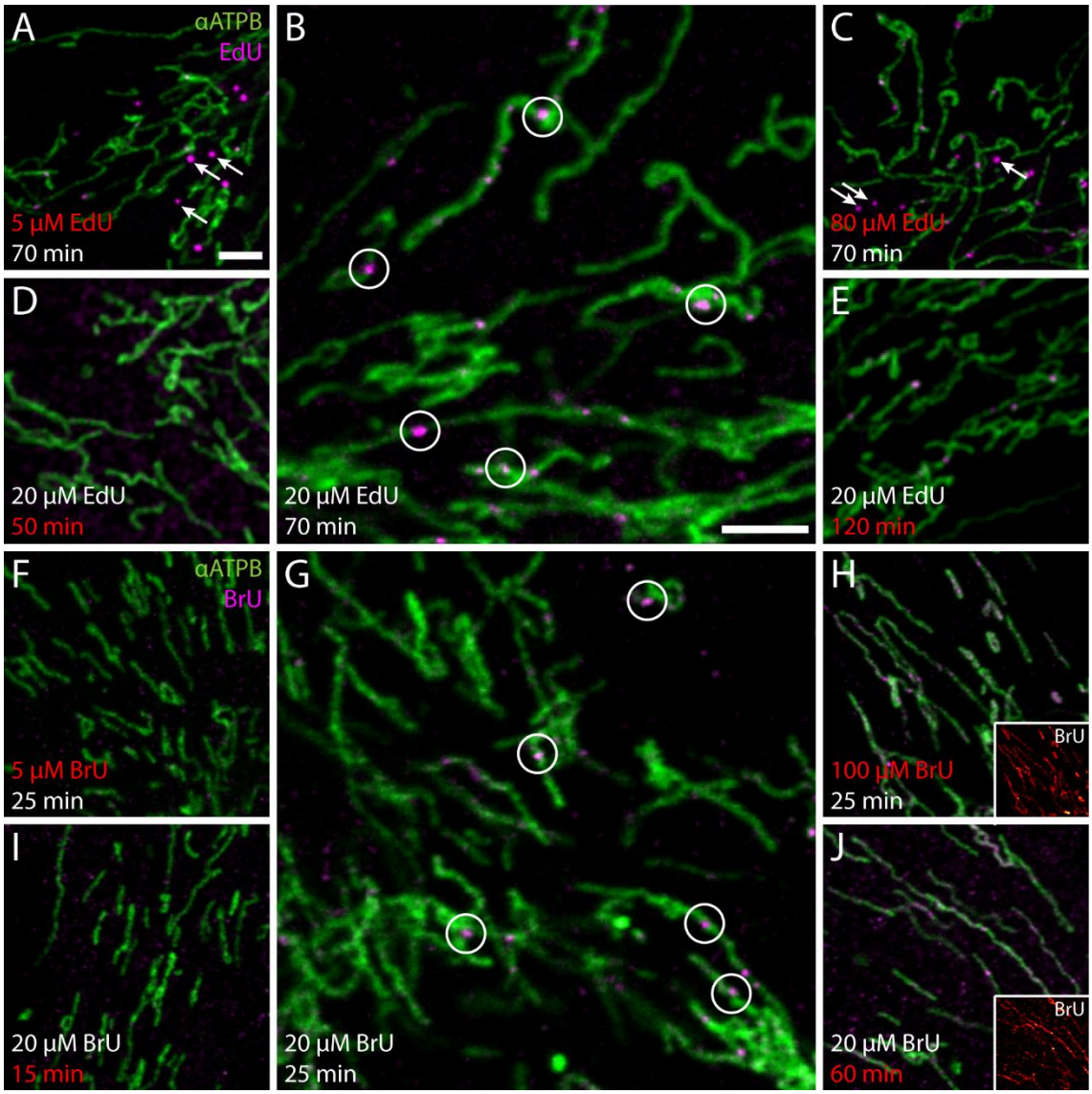

Figure 9.4 Optimized concentration and incubation time for EdU and BrU: HDFa cells were incubated with EdU and BrU for different incubation periods and with different concentration. EdU und BrU (magenta) were labeled afterwards. Furthermore antibodies against the β-subunit of the ATP synthase (green) were used to label the mitochondria. **A-E) EdU staining:** The best results could be obtained with an incubation time of 70 min and a concentration of 20 µM (C). EdU signal is located within the mitochondria. If a lower concentration is used (A) the specific EdU signal disappears and only bright unspecific spots in the cytoplasm are detected (arrowheads). If the concentration of EdU it too high (C), specific signal within the mitochondria is detectable, but additionally bright signal outside the mitochondria appear (arrowheads). When lower incubation times than 70 minutes and a concentration of 20 µM were used (D), no signal was detected. If incubation times were above 70 minutes (E) the signal within the mitochondria appears brighter and more dots were detected. **F-J) BrU staining:** The best were achieved with an incubation time of 25 min and a concentration of 20 µM (G). Upon a reduced concentration of BrU (F) or a lower incubation time (I) no BrU signal was detected. When either the concentration of BrU (H) or the incubation time (J) were increased, dots within the mitochondria were detectable but an increased labeling of the complete mitochondrial network could be observed. Scale bar: 3 µm

Supplement figure 9.5: STED nanoscopy of BrdU labeled nucleoids

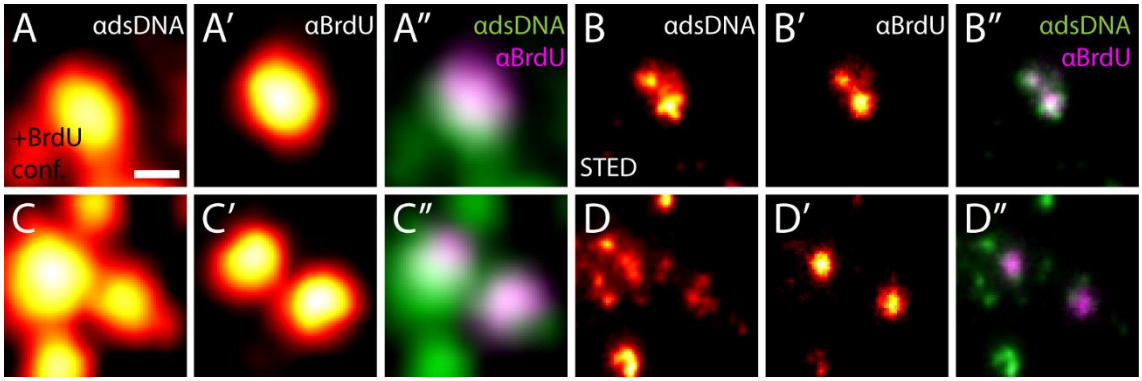

Figure 9.5 STED nanoscopy of BrdU labeled nucleoids: HDFa cells were incubated with 20 µM BrdU for 2 h. Sample was incubated with HCl and nucleases to enable a BrdU staining. Afterwards, BrdU (magenta) and dsDNA (green) were labeled with antisera. **A-A'')** A single confocal nucleoid signal that is positive for BrdU. **B-B'')** Record of the same section like in A-A'' applying STED nanoscopy. Two single nucleoids are apparent and both of them are positive for BrdU. The nucleoids in the DNA cannel reveal an irregular shape. **C-C'')** multiple confocal nucleoid signals. Only some of the nucleoids are labeled with BrdU. **D-D'')** The section shown in C-C'' was recorded with the STED mode. The nucleoids appear fragmented and single structures can barely be identified. The BrdU channel could be recorded with a good contrast. Scale bar: 200 nm.

Supplement figure 9.6: Models for the fitting of the data of the increasing EdU incubation times:

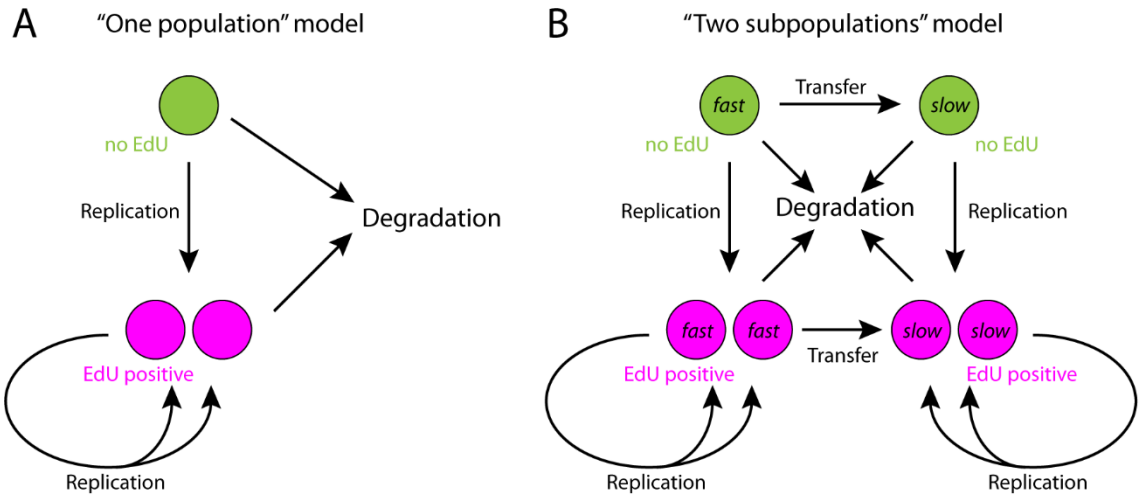

Figure 9.6 Models for the fitting of the data of the increasing EdU incubation times: In Fig 3.12 HDFa cells were treated with EdU for different periods of incubation. Both presented models were fitted to the data points. **A) The "one population" model:** In this model it is assumed that all nucleoids are equally involved in mitochondrial replication and reveal an equal replication rate. When an EdU negative nucleoid finished replication, two EdU positive nucleoids appear. If a nucleoid is already EdU positive it can still be involved in replication. It is furthermore assumed that all nucleoids reveals the same chance to be degraded. **B) The "two subpopulations" model:** In this model it is assumed that nucleoids reveal two different subpopulations with two different replication rates termed "active / fast" and "inactive / slow" nucleoids. Previous incorporation of EdU has no influence on nucleoid replication. It is assumed that the fraction of "active / fast" and "inactive / slow" nucleoids is constant during the experiments. Therefore it was assumed that a transfer from "active / fast" to "inactive / slow" nucleoids occur. In the mitochondria this transfer could be realized by a limitation of the involved factors. Limitation of the responsible factors could ensure that only a constant subpopulation is "active / fast". It is furthermore assumed that all nucleoids reveals the same chance to be degraded.

Supplement Table 9.1: Single measures of the toxicity tests of EdU, BrU and BrU (see Tab 3.1)

Table 9.1 Single measures of the toxicity tests of EdU, BrU and BrU (see Tab 3.1)

	untreated	Aphidicholin	EdU	BrdU	BrU
1st Round					
Cells in G1-Phase (2 h)	**86.2%**	86.8%	84.5%	85.7%	86%
Cells in S-Phase (2 h)	**5.1%**	5.1%	5.9%	5.3%	5.2%
Cells in G2-Phase (2 h)	**7.3%**	6.1%	7.4%	7.4%	7.3%
Viability (2 h)	**95.4**	87.5%	89.6%	96.1%	91%
Cells in G1-Phase (48 h)	**91.3%**	82.9%	83.6%	89%	87.6%
Cells in S-Phase (48 h)	**2.1%**	7.4%	2.9%	2.3%	3%
Cells in G2-Phase (48 h)	**5.7%**	8.7%	12.7%	7.4%	8.5%
Viability (48 h)	**91.7%**	69.2%	88.4%	82.3%	86.8%
2nd Round					
Cells in G1-Phase (2 h)	**88.2%**	91%	91.5%	90.5%	90.6%
Cells in S-Phase (2 h)	**3.4%**	3.2%	2.5%	3.3%	2.6%
Cells in G2-Phase (2 h)	**6.9%**	6.3%	6.5%	6.4%	6.1%
Viability (2 h)	**76%**	81.1%	82.3%	82.2%	79.2%
Cells in G1-Phase (48 h)	**90.6%**	87.9%	86.4%	93.2%	90%
Cells in S-Phase (48 h)	**2.5%**	4.9%	2.1%	1.5%	2.4%
Cells in G2-Phase (48 h)	**6.6%**	6.6%	10.7%	4.6%	6.8%
Viability (48 h)	**94.9%**	90%	94.2%	97%	94.1%
3rd Round					
Cells in G1-Phase (2 h)	**84.5%**	86.4%	81%	81.5%	84.6%
Cells in S-Phase (2 h)	**4.6%**	4.6%	6.9%	6%	5.2%
Cells in G2-Phase (2 h)	**10%**	8.4%	11.6%	11.5%	9.7%
Viability (2 h)	**95.3%**	95.7%	96.5%	95.5%	95.3%
Cells in G1-Phase (48 h)	**89.9%**	79.2%	77.4%	88.1%	90.9%
Cells in S-Phase (48 h)	**3%**	10.2%	3.3%	2.2%	3.3%
Cells in G2-Phase (48 h)	**5.8%**	9%	17.6%	8.1%	4.5%
Viability (48 h)	**96.2%**	84.1%	91.2%	82.5%	94.9%

Affidavit

I declare, that I prepared the PhD thesis entitled

“Analysis of mitochondrial transcription and replication on the single nucleoid level”

submitted on 30th March, 2018 is the result of my own work and prepared with no other sources than quoted.

Göttingen, 30th March, 2018

Christian Brüser

Acknowledgements

Es ist vollbracht! Alle Experimente sind abgeschlossen, alle Proben gemessen, jede Erkenntnis niedergeschrieben. Nun fehlt es den Leuten zu danken die mir direkt oder indirekt dabei halfen.

Ich danke Herrn Prof. Dr. Stefan Jakobs für die Möglichkeit an diesem interessanten Thema zu arbeiten und für seine fortwährende Unterstützung die einen wichtigen Beitrag zum Gelingen dieser Arbeit darstellte.

Darüber hinaus möchte ich Herrn Prof. Dr. Peter Rehling für die Übernahme des Koreferats danken. Besonders für die konstruktiven Diskussionen und das Interesse an dieser Arbeit möchte ich mich bedanken.

Zudem bedanke ich mich bei Herrn Prof. Dr. Ahmed Mansouri für die hilfreichen Ratschläge, Besprechungen und die freundliche Begleitung dieser Arbeit.

Herrn Prof. Dr. Patrick Cramer, Herrn PD Dr. Wilfried Kramer und Herrn Prof. Dr. Thomas Teichmann danke ich für ihre Teilnahme an meiner Disputation.

Ein großer Dank gebührt Tanja Gilat, Sylvia Löbermann, Rita Schmitz-Salue und Ellen Rothermel für alle Hilfestellungen und die perfekte Organisation des Labors. Auch möchte ich bei Jan Keller-Findeisen bedanken, da er mir eine enorme Hilfe bei der Auswertung der Daten war. Zudem möchte ich mich bei Jaydev Jethwa, Stefan Stoldt, und Nickels Jensen für die Korrektur meiner Arbeit bedanken.

Ein besonderer Dank geht an alle Mitglieder der Abteilung für NanoBiophotonics. Viele Aufgaben lösen sich, wenn man den Kopf frei bekommt und man die Probleme für einen Moment vergisst. Deshalb: Danke für das Film-gucken, das Pokern, das Trinken, das Essen, das Laufen, das Schwimmen, das Ausflüge machen, das Feiern, das Pumpen, das Kaffeepause machen, das Reden, das Lachen, das Zug fahren, das Spielen, das Rätseln und den Fußball. Danke für alle Hilfestellungen, jeden guten Rat und jedes nette Wort. Danke dafür, dass es für jede Frage eine Antwort gab.

Der folgende Satz steht so bereits in meiner vorigen Arbeit: Die letzten Worte gehören Isabelle, meiner Mutter und meinem Vater. Danke für alles.

Manches ändert sich nie.